University of Cyprus
Department of Biological Sciences

Adherens Junctions spatially guide ECM deposition by stimulating integrin activation and clustering

Maria Zheltkova

A Research-Based Master's Thesis
for the
Degree of Magister Scientiae in Biomedical Sciences

May 30, 2022

ABSTRACT

The extracellular matrix (ECM) plays an essential role in all multicellular organisms as a substrate for cell anchorage and tissue scaffolding. It is involved in diverse processes such as cell proliferation and survival, tissue morphogenesis, cell fate determination, and wound healing. Given the critical role of the ECM, the mechanisms regulating its formation have been studied extensively both *in vitro* and *in vivo*. Tissue tension and cadherin-based interactions were early on identified as critical factors through which ECM deposition was regulated. However, the mechanism through which adherens junctions influence ECM deposition was unclear and believed to be indirect, through the establishment of tissue-level tension. Unpublished data from our group however revealed that AJs can stimulate and spatially guide integrin activation creating spatially restricted pools of high ligand affinity receptors at cell-cell junctions. In this study we addressed the possibility that these AJ-driven pools of high ligand affinity integrins can a) spatially influence ligand binding on the cell surface and b) impact ECM deposition. To address these questions, we initially developed a protocol to allow monitoring fibronectin assembly both during live imaging as well as in fixed samples. Specifically, we generated fluorescently labelled fibronectin – YPET FN conditioned media using HEK293 cells. We showed that these conditioned media allow labelling of FN fibrils in different cell lines and used this assay to select appropriate cells for our experiments. Subsequently, HeLa and NIH 3T3 fibroblasts were used to show selective accumulation of FN on cell-cell contacts in various contexts. These data conclusively confirm our hypothesis that the AJ-driven active integrin pools in fact spatially influence ligand binding on the cell surface. Interestingly, use of a number of conformational specific integrin antibodies showed that at early time points only integrins with an extended closed headpiece conformation are recruited at cell-cell junctions, while accumulation of FN, leads to headpiece opening. We propose that the selective recruitment of ligands at cell-cell junctions is due to the recruitment and stabilization of extended conformation integrins at these sites. Given the fact that AJ-driven integrin activation is believed to be driven by PM tension and subsequent topological adaptation of the transmembrane domains we then asked if Talin is necessary for this process. Using Talin null cells we show that ligand accumulation on cell-cell contacts is strictly dependent on Talin

raising the possibility that additional mechanisms may contribute to the process of integrin activation at AJs. Finally, to directly examine the role of AJs in ECM formation and FN fibrillogenesis we modulated AJs using various approaches including pharmacological agents and function-blocking cadherin mutants. These data show that AJs have a profound influence not only on ligand binding on the cell surface but also on the 3D architecture of the ECM generated by cells in culture. Collectively our data demonstrate that the impact of AJs on ECM formation and remodeling goes well beyond the establishment of tissue-level tension and provides mechanistic insight into the critical integrin cadherin cross talk.

ACKNOWLEDGEMENTS

First and foremost, I would like to sincerely thank my advisor, Dr. Paris A. Skourides, for his guidance and patience during the completion of this thesis, as well as his constant support and help. Additionally, I would like to thank all my fellow lab members, and especially a PhD candidate Rania Hadjisavva for not only being an invaluable thesis advisor during these two years but being my friend and always supporting me. Finally, I thank my family and friends for their patience and unconditional support.

COMPOSITION OF THE EXAMINATION COMMITTEE

Thesis Supervisor (Examination Committee coordinator): Assoc.Prof. Paris A. Skourides, Dept. of Biological Sciences, UCY

Committee Member: Assoc.Prof. Antonis Kirmizis, Dept. of Biological Sciences, UCY

Committee Member: Prof. Leondios G. Kostrikis, Dept. of Biological Sciences, UCY

SEMINAR ANNOUNCEMENT

University of Cyprus
Department of Biological Sciences

Master Research Dissertation in Biomedical Sciences (BIO 830/600)

Student Presentation

Monday, 30 May 2022 10:00
Building Learning Resource Centre UCY Library 'Stelios Ioannou', Room Amphitheatre LRC 019, Panepistimioupoli Campus

This seminar is open to the public

Maria Zheltkova

Thesis Supervisor: Assoc. Prof. Paris Skourides

"Adherens Junctions spatially guide ECM deposition by stimulating integrin activation and clustering"

The extracellular matrix (ECM) plays an essential role in all multicellular organisms as a substrate for cell anchorage and tissue scaffolding. It is involved in diverse processes such as cell proliferation and survival, tissue morphogenesis, cell fate determination, and wound healing. Given the critical role of the ECM, the mechanisms regulating its formation have been studied extensively both *in vitro* and *in vivo*. Tissue tension and cadherin-based interactions were early on identified as critical factors through which ECM deposition was regulated. However, the mechanism through which adherens junctions influence ECM deposition was unclear and believed to be indirect, through the establishment of tissue-level tension. Unpublished data from our group however revealed that AJs can stimulate and spatially guide integrin activation creating spatially restricted pools of high ligand affinity receptors at cell-cell junctions. In this study we addressed the possibility that these AJ driven pools of high ligand affinity integrins can a) spatially influence ligand binding on the cell surface and b) impact ECM deposition. To address these questions, we initially developed a protocol to allow monitoring fibronectin assembly both during live imaging as well as in fixed samples. Specifically, we generated fluorescently labelled fibronectin – YPET FN conditioned media using HEK293 cells. We showed that these conditioned media allow labelling of FN fibrils in different cell lines and used this assay to select appropriate cells for our experiments. Subsequently, HeLa and NIH 3T3 fibroblasts were used to show selective accumulation of FN on cell-cell contacts in various contexts. These data conclusively confirm our hypothesis that the AJ driven active integrin pools in fact spatially influence ligand binding on the cell surface. Interestingly, use of a number of conformational specific integrin antibodies showed that at early time points only integrins with an extended closed headpiece conformation are recruited at cell-cell junctions, while accumulation of FN, leads to headpiece opening. We propose that the selective recruitment of ligands at cell-cell junctions is due to the recruitment and stabilisation of extended conformation integrins at these sites. Given the fact that AJ driven integrin activation is believed to be driven by PM tension and subsequent topological adaptation of the transmembrane domains we then asked if Talin is necessary for this process. Using Talin null cells we show that ligand accumulation on cell-cell contacts is strictly dependent on Talin raising the possibility that additional mechanisms may contribute to the process of integrin activation at AJs. Finally, to directly examine the role of AJs in ECM formation and FN fibrillogenesis we modulated AJs using various approaches including pharmacological agents and function-blocking cadherin mutants. These data show that AJs have a profound influence not only on ligand binding on the cell surface but also on the 3D architecture of the ECM generated by cells in culture. Collectively our data demonstrate that the impact of AJs on ECM formation and remodelling goes well beyond the establishment of tissue-level tension and provides mechanistic insight into the critical integrin cadherin cross talk.

TABLE OF CONTENTS

INTRODUCTION

1. Adherens Junctions

Adherens junctions (AJs) are multi-protein complexes required for the development and survival of multicellular organisms (Meng and Takeichi, 2009). Cell-cell adhesions are initiated, mediated, and stabilized by the formation of AJs at the lateral membrane of cells, rendering the AJs essential for morphogenesis and tissue remodeling. In addition, these complexes are involved in the remodeling of the actin cytoskeleton, intracellular signaling, and transcriptional regulation (Hartsock and Nelson, 2008).

The core of AJs includes interactions between the transmembrane glycoprotein Cadherins and the cytoplasmic catenin family members, including p120 catenin, β-catenin, and α-catenin (**Figure 1**). Cadherins of adjacent cells form calcium-dependent homophilic interactions resulting in the recruitment of intracellular catenins, which in turn can bind to the actin cytoskeleton (Gumbiner, 2005; Hartsock and Nelson, 2008; Meng and Takeichi, 2009).

Interestingly, AJs are highly dynamic structures, able to alter their assembly or disassembly in association with the epithelial to mesenchymal transition (EMT) of cells, a process known to occur during development and carcinogenesis. Specifically, tightly adherent, and polarized cells dissociate from each other, after AJ disassembly, followed by the increased migration of those cells (Berx and Van Roy, 2001, Conacci-Sorrell et al., 2002).

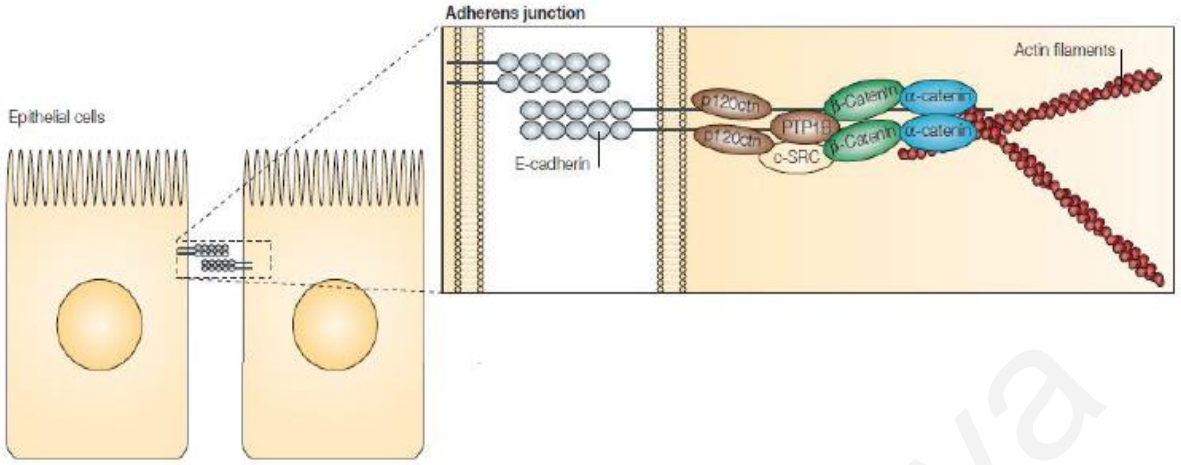

Figure 1: Adherens Junction structure. Adherens junctions are cadherin-based structures formed at the lateral membrane of adjacent cells. They consist of the transmembrane Cadherins and the cytoplasmic components, including p120 catenin, α-catenin, and β-catenin.

Courtesy of: Yeatman, 2004

1.1 Cadherins

Cadherins constitute a large superfamily of transmembrane glycoproteins involved in cell-cell adhesion. The cadherin-superfamily consists of the type I cadherins (E-, N-, P-, R-), known as the classic cadherins, the type II (cadherin-6 and VE-cadherin), the desmosomal cadherins (desmocollin and desmoglein) and a subfamily of cadherin-like molecules (Gumbiner,2005).

Cadherins have been linked to a variety of developmental processes, such as the regulation of the embryonic layer separation and tissue boundary formation. Additionally, cadherins are essential for cell signaling, homeostasis maintenance, and nervous system formation (Paladi and Tepass, 2004; Nishimura and Takeichi, 2009).

Cadherins consist of three main domains: the extracellular domain, the transmembrane domain, and the cytoplasmic domain. Classic cadherins mentioned above, appear to have extracellular domains divided into five repetitive ectodomain modules, known as EC domains (EC1-5), each containing three calcium-binding sites (Paladi and Tepass, 2004; Shapiro and Weis, 2009) (**Figure 2**). These EC domains have a β-fold structure, like the immunoglobulin domains. Upon association

with calcium, the extracellular domain undergoes a conformational change required for the trans-cadherin homophilic interaction between adjacent cells (Gumbiner, 1986; Patel et al.,2006). The heterodimerization of Cadherins of opposing cells is achieved by interaction of their EC1 domains, while clustering within the AJ is established through the homodimerization of two cadherin molecules via EC1-EC2 domain binding (Boggon et al., 2002). The anchoring of cadherins on the plasma membrane is achieved via their transmembrane domain. The short cytoplasmic domain of cadherins can mediate direct or indirect intracellular interactions with molecules of the catenin family, which are essential for adherens junction strength by promoting cadherin clustering and lateral spreading (Adams et al., 1998). These binding sites within the cytoplasmic domain are known as catenin binding domains (CBD). Specifically, p120 catenin associates with the juxtamembrane domain (JMD) of the cytoplasmic region (Yap et al., 1998), while the carboxy-terminal domain of the cytoplasmic region binds β-catenin (Aberle et al., 1994). α-catenin cannot interact with Cadherins directly, but through the interaction with β-catenin (Tominaga et al., 2008). Catenins, in turn, can associate with the actin cytoskeleton, either by directly binding actin filaments or indirectly, via actin-binding molecules, such as Vinculin (Rimm et al., 1995).

1.1.1 N-Cadherin

N-Cadherin (Neural Cadherin) is a 130kDa glycoprotein involved in the formation of small AJs at synapses and regulation of axonal growth (Doherty and Walsh, 1996). It is widely expressed in the neural cells, although it can be found as well in several non-epithelial types of cells, such as endothelial and stroma cells (Loh et al., 2019). During neurulation, N-Cadherin replaces E-Cadherin in neural tissue, forming strong adherens junctions to maintain tissue architecture and regulate the proliferation and differentiation of neural progenitor cells (Miyamoto et al.,2015). Interestingly, the expression of N-Cadherin has been correlated with various types of carcinomas (Islam et al., 1996; Hui et al., 2013; Wang et al., 2016).

1.2 Catenins

Catenins are cytoplasmic proteins, linking cadherins with the actin cytoskeleton (**Figure 2**). Many studies identified the role of catenins in the formation, clustering, and disassembly of AJs, as well as in several signaling pathways (Yamada and Nelson, 2007; Capaldo and Macara, 2007; Nishimura and Takeichi, 2009). Specifically, p120 catenin, β-catenin, and α-catenin can be found at AJs.

1.2.1 p120 catenin

p120 catenin interacts with the cytoplasmic domain of cadherins via the juxtamembrane domain (JMD), stabilizing the cadherins at the plasma membrane during the formation of cell junctions. Interestingly, phosphorylation of p120 catenin can increase the binding affinity to E-Cadherin (Piedra et al., 2003). Moreover, it has been proposed that the p120catenin-cadherin interaction prevents the degradation and internalization of cadherins, thus enhancing their surface abundance. siRNA-mediated knock-down studies suggested that degradation sequences within the JMD domain were exposed leading to the decreased retention of cadherins at the plasma membrane (Davis et al., 2003; Xiao et al., 2003). Furthermore, p120 catenin is implicated in the surface transport of cadherins by connecting them to microtubules via motor proteins, such as kinesin (Ishiyama et al.,2010). Hence, p120 catenin has a major regulatory role rather than a structural role in the cadherin function.

1.2.2 β catenin

β catenin, known also as armadillo-repeat protein, contains thirteen repeats of the armadillo domain that form a triple α-helix, serving as a docking site for several proteins, and the N- and C-terminal regulatory domains that are essential for its degradation and signaling. β-catenin interacts with the α-catenin through the tyrosine residue Y142, while it binds the distal region of the C-terminal cytoplasmic domain of Cadherins in a phospho-regulated manner (Aberle et al., 1994). Three serine residues, S684, S686, and S692, are phosphorylated by the CKII and GSK-3β kinases resulting in enhanced interaction affinity (Lickert et al., 2000). This interaction is essential for the stabilization of the newly formed protein in the Endoplasmic Reticulum (ER) and its transportation to the plasma membrane (Chen et al., 1999). Conversely, cadherin endocytosis and degradation

are promoted by the phosphorylation of β-catenin at the tyrosine residues Y489 or Y654, since it decreases the affinity for cadherin binding and disrupts the catenin-cadherin interaction (Huber and Weis, 2001; Lilien et al., 2002). In addition, β catenin appears to act as an intracellular signal transduction molecule in the Wnt signaling pathway. In the absence of an external Wnt ligand, β catenin levels in the cytosol are low since it is targeted for degradation. Wnt signaling via Frizzled-LRP receptors prevents the degradation of β catenin, resulting in increased cytosolic β catenin levels, followed by the nucleus translocation and enhanced gene expression via the interaction with TCF (T-cell factor) or LEF (leukocyte enhancing factor) (Nelson and Nusse, 2004). However, it is unclear how the adhesive and transcriptional functions of β catenin are distinguished, although it is possible that the transcription factor BCL9-2 facilitates the switch between the two functions. Phosphorylation of β-catenin at Y142 favors BCL9-2 binding, inhibiting other protein interactions and enhancing the nucleus translocation (Brembeck et al., 2004).

1.2.3 α catenin

α catenin is a cytoskeletal protein composed of four functional domains: an N-terminal β-catenin binding domain, a Vinculin and α-actinin binding domain, an l-afadin binding motif that lies within the dimerization domain, and a C-terminal domain essential for the interaction with F-actin (Rimm et al., 1995). α catenin is involved in the formation and function of AJs, as well as in the actin cytoskeleton regulation and cell proliferation (Gumbiner, 2005). α-catenin exists in two different states, a monomeric and a homo-dimeric state. The β-catenin binding domain overlaps with the homodimerization domain on α-catenin, although it does not with the actin-binding domain (Pokutta and Weis, 2000). Monomeric α-catenin can interact with the Cadherin/β-catenin complex but not with actin, while a homo-dimeric α-catenin can bind actin and not the β-catenin (Yamada et al., 2005). Thus, simultaneous binding of α-catenin to both β-catenin and actin filaments cannot happen, and it is still unclear how exactly α-catenin can directly link the adherens junctions to the actin cytoskeleton. Several studies have suggested a model where the connection happens through the dynamic crosstalk between the monomeric and homo-dimeric states of α-catenin. Specifically, it is suggested that the increase in the local concentration of α-catenin at the membrane during cadherin-catenin clustering at cell-cell junctions provides a significant increase in the α-catenin concentration to induce cytosolic dimerization of α-catenin. These dimers can compete with the

actin-related protein 2/3 (ARP2/3) complex, for actin interaction, and convert actin networks found in lamellipodia of migrating cells into actin bundles associated with AJs (Yamada et al., 2005). Moreover, α-catenin can interact and recruit several proteins to AJs that are able to bind directly to actin filaments, including Vinculin and Zyxin.

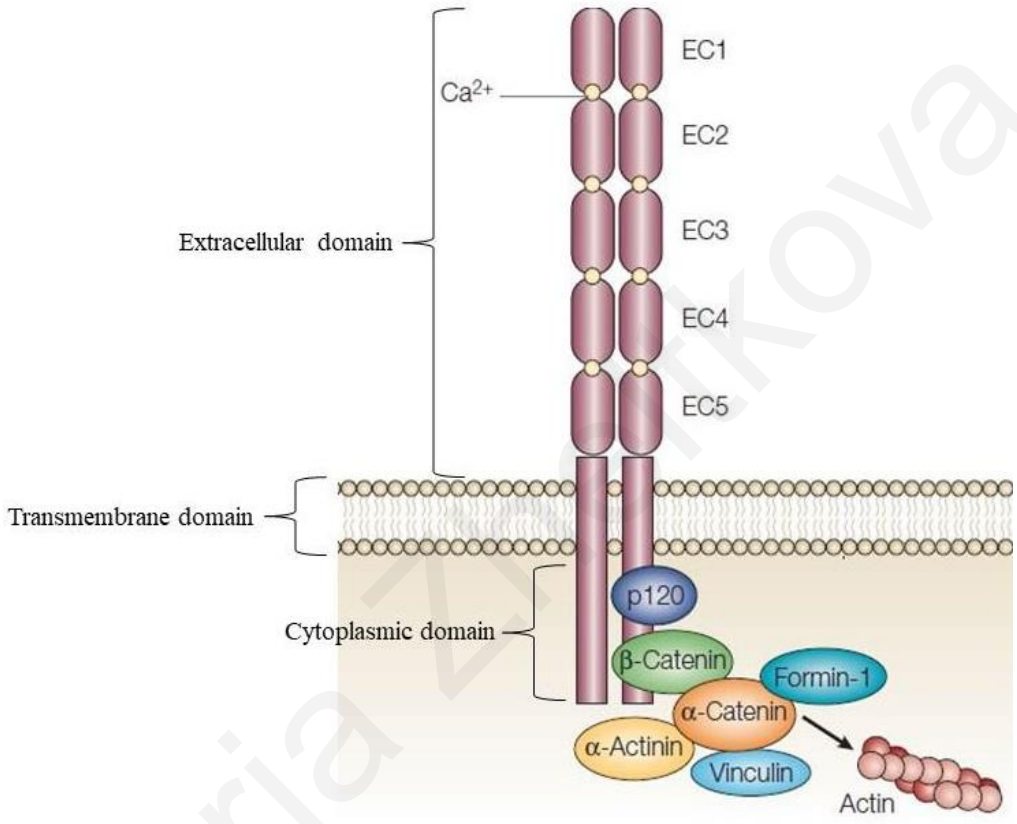

Figure 2: Classical cadherin-catenin complex structure. Cadherins are composed of an extracellular domain, a transmembrane domain, and a cytoplasmic domain. The extracellular domain of classical cadherins consists of five EC domains (EC1-5), each containing 3 calcium-binding sites. The transmembrane domain is responsible for the anchoring of the receptor to the plasma membrane. The cytoplasmic domain contains numerous catenin-binding domains (CBD) for interaction with catenins, including α-catenin, β-catenin, and p120 catenin, as shown in the above scheme.

Courtesy of: Gumbiner, 2005

2. Focal Adhesions

Focal Adhesions (FAs) are multiprotein complexes where transmembrane integrin receptors link the actin cytoskeleton with the extracellular matrix (ECM), mediating interactions of the cell with its extracellular environment (Shemesh et al, 2005). These highly dynamic structures are formed at the cell periphery after the interaction of integrins with ECM ligands, such as collagen, fibronectin, and vitronectin. This interaction leads to integrin clustering and activation, which is followed by the hierarchical recruitment of numerous structural and signal transduction proteins, including Talin, Vinculin, paxillin, and Focal Adhesion Kinase (FAK), among others (**Figure 3**, Miyamoto et al., 1995).

Several studies suggested that there are three forms of integrin-mediated adhesions that can be distinguished molecularly and/or functionally (Zamir and Geiger, 2001). The main precursors of FAs are known as Focal Complexes (FXs), which are formed under the lamellipodia of migrating cells (Zaidel-Bar et al., 2003, Zaidel-Bar et al., 2004). These small short-lived adhesions are implicated in tethering the actin cytoskeleton to the membrane and are controlled by Rac (Rac Family Small GTPase 2) and Cdc42 (Cell division cycle 42 protein) (Hotchin and Hall, 1995; Petit and Thiery, 2000). Maturation of FXs into more stable and large structures at the cell periphery, known as FAs, is promoted by Rho-A activity (Ballestrem et al., 2001), followed by the recruitment of Zyxin that leads to the mechanical force generation required for the transformation of FXs into FAs (Hotchin and Hall, 1995). The stabilization of FAs is controlled by Tensin recruitment (Zaidel-Bar et al., 2003), while the dynamics and turnover are controlled by tyrosine kinases targeted at the sites, two of the major ones being FAK and Src. However, the continuous application of mechanical force has been shown to be involved in the turnover of FAs as well, and in the generation of Fibrillar Adhesions (FBs). Fibrillar Adhesions are formed more centrally in the cell and are implicated in the reorganization of the ECM (Pankov et al., 2000; Zaidel-Bar et al., 2004).

Interaction of cells with the extracellular matrix is essential for many biological processes including cell migration, tissue formation, cell survival, and embryogenesis (Petit and Thiery, 2000; Zaidel-Bar et al. 2004). Disruption of the FA complex has been shown to be associated with several human diseases, such as malignant diseases and Kindler syndrome (Wu, 2007).

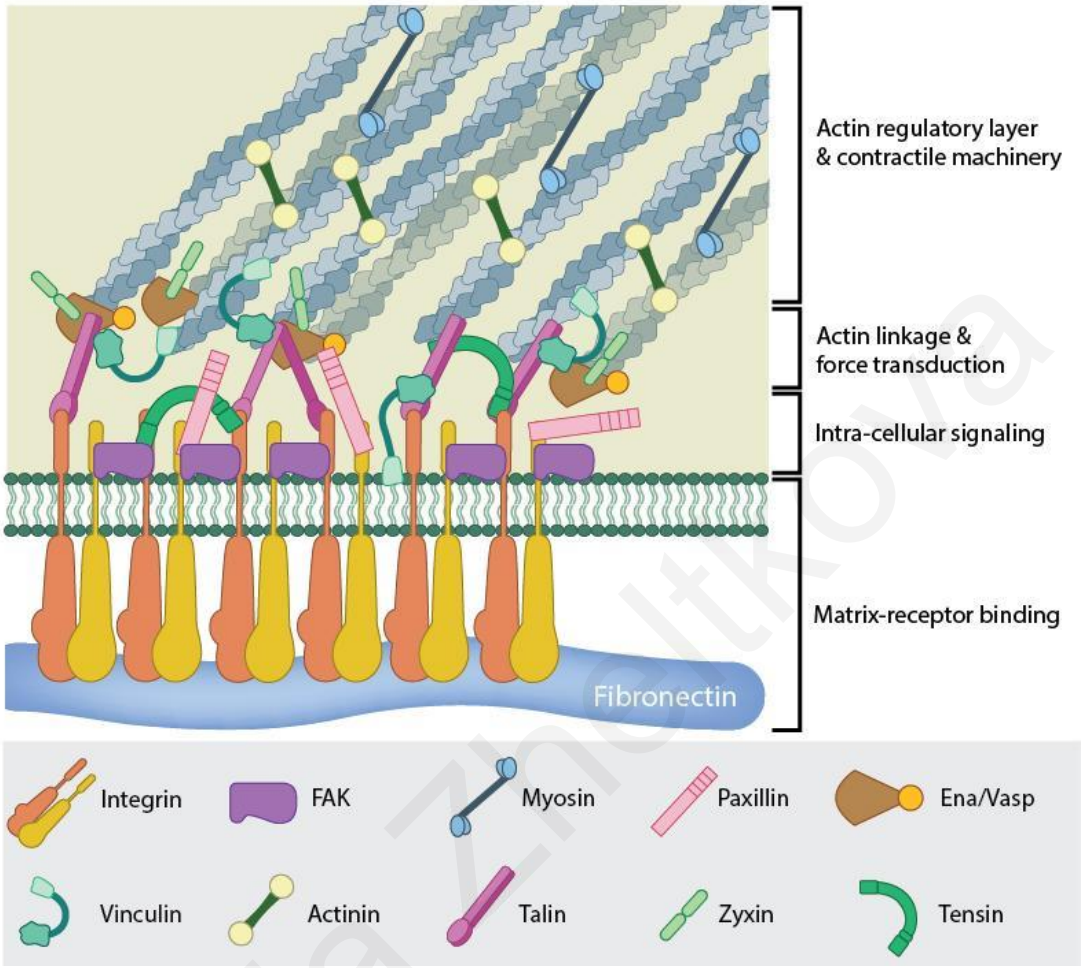

Figure 3: Focal Adhesion Complex. Focal Adhesions are multi-protein structures. Upon integrin activation, focal adhesion formation occurs, followed by the recruitment of numerous proteins to these sites, such as Vinculin, paxillin, and FAK (Adapted from: What are mature focal adhesions composed of? | MBInfo (mechanobio.info) [Accessed on 20/05/2022]).

3. Integrins

Integrins are a large family of transmembrane heterodimeric glycoprotein receptors, that mediate cell adhesion to the extracellular matrix and transmit bidirectional signals across the plasma membrane (Hynes, 2002). Upon integrin activation and clustering at the cell surface, the focal adhesion complex is formed, recruiting several proteins at these sites, and linking integrins with the actin cytoskeleton (Geiger et al, 2001). Thus, intracellularly integrins are linked with the actin cytoskeleton, while extracellularly they are coupled with extracellular proteins, including fibronectin and collagen (Su et al., 2016). In addition to cell adhesion, integrins are involved in tissue patterning and integrity, cell fate determination, immune response, cancer progression, and metastasis, as well as lead to pathologies such as thrombosis (Hynes, 2002; Bokel and Brown, 2002; Mahabeleshwar et al., 2007).

As mentioned above, integrins are heterodimers, consisting of noncovalently linked α and β subunits. Both subunits are tightly bound to each other via the interactions of the α-propeller and the β-I-like domain in the extracellular region of the receptor. So far, eighteen α and eight β subunits are identified, forming twenty-four different combinations of integrin heterodimers (Hynes, 2002). The major β subunit is integrin β1 since it can form heterodimers with almost all α subunits, is expressed in all cell types and tissues and lack of β1 leads to embryonic lethality in mice (Petit and Thiery, 2000; Hynes, 2002). Each heterodimer contains three domains, a large N-terminal extracellular head domain (80-150kDa), capable to bind extracellular matrix components, a single-span transmembrane domain (TMD), which promotes the stabilization of the dimer, and a small C-terminal cytoplasmic tail domain (10-40 amino acids long), which mediates the interaction with several proteins, leading to the connection of the receptor with the actin cytoskeleton (Hynes, 2002). The cytoplasmic tail of integrins contains two conserved motifs, the membrane-proximal NPx(Y/F) and the membrane-distal Nxx(Y/F). They are both phosphotyrosine-binding domain (PTB) sequences that can be recognized by several proteins, including Talin and Kindlin (Calderwood et al., 2003). The presence or the absence of the ligand-binding α-I domain, located in the top part of the extracellular head domain of the α subunit, appears to be the most significant structural difference between integrins. Specifically, nine heterodimers are with the α-I domain and fifteen are without, with the only functional difference being the mode of ligand binding. Integrins with the α-I domain can bind ligands via this domain,

while other integrins bind ligands in binding pockets formed by both α and β subunits (Bachmann et al., 2019).

Importantly, integrins can be classified based on structural features, their specificity for ligand binding, and their tissue and cellular expression (**Figure 4**). For instance, two β1 integrins (α5, α8) can recognize ligands containing an RGD tripeptide active site, like α5β1 that interacts with Fibronectin (Hynes, 2002). Additionally, several proteins of the immunoglobulin family can interact with integrins, such as VCAM-1, through their acidic motif, known as LDV (Rothlein et al., 1986). Moreover, four α subunits with the α-I domain (α1, α2, α10, α11) comprise a distinct laminin/collagen-binding subfamily. The expression of integrins in white blood cells is restricted to only β2 and β7 (Hynes, 2002). Furthermore, a different type of extracellular divalent cation can influence the affinity and specificity of ligand binding, since divalent-cation-binding domains are present in the extracellular part of α and β subunits (Ca^{2+} or Mg^{2+}) (Alberts et al., 2002).

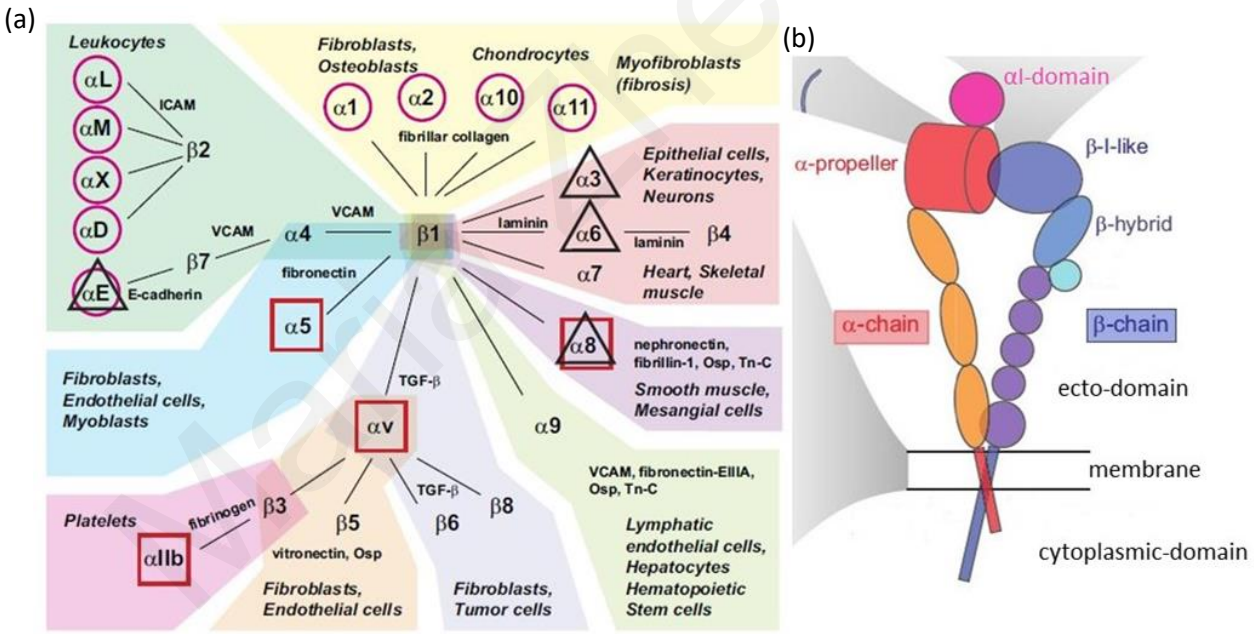

Figure 4: Classification and structure of integrins.

(a) Twenty-four different heterodimers are formed from the combination of α and β integrin subunits. They can be classified based on structural features, their specificity for ligand binding, and their tissue and cellular expression.

(b) Structural features of integrin heterodimer. Integrins consist of two subunits, α, and β, which are linked non-covalently. They are composed of three domains, a large extracellular domain, a single transmembrane domain, and a small cytoplasmic domain.
Courtesy of: Bachmann et al., 2019

Integrin activation promotes both receptor clustering at the cell membrane, which increases the avidity of molecular interactions, and changes in the ligand-binding affinity via the conformational changes of integrins. There are three distinct states of integrin conformation in response to activation: inactive state, intermediate state, and active state (**Figure 5**). When in the inactive state, integrins are bent with the head domain facing towards the legs generating a V-like structure, with the transmembrane domains being closely associated. In this state the affinity for ligand binding is low (Xiong et al., 2001). In the intermediate state, integrin legs are separated and extended, although the headpiece is closed, thus the affinity for ligands is intermediate. The active conformation, with high ligand-binding affinity, is obtained by separating and extending the legs, as well as opening the head domain of the receptors, which can be accomplished either by an inside-out (interaction between cytoplasmic tail and intracellular proteins) or outside-in (interaction between ligands and head domain) triggered mechanism (Takagi et al., 2002).
During inside-out signaling, intracellular proteins interact with cytoplasmic integrin tails, promoting the extension of the extracellular domains and stabilizing the intermediate state of the receptors. The conformational switch, from inactive to the intermediate state, results in the exposure of the ligand-binding site of the extracellular head domain and enhances the affinity for ligand-binding (Luo et al., 2007) (**Figure 5**). As mentioned above, Talin and Kindlin can interact with the cytoplasmic integrin tails and are known for promoting the inside-out activation of integrins. Specifically, it has been suggested that Talin can interact with the β cytoplasmic domain promoting the separation of the α and β subunit tails, while Kindlin contributes to integrin clustering (Ye et al., 2013).
Outside-in signaling occurs when the extracellular head domain of the receptor interacts with a ligand. This interaction leads to the conformational switch required for integrin activation. Subsequently, numerous proteins can bind the cytoplasmic integrin tails, forming the focal adhesion complex and connecting the receptor to the actin cytoskeleton (Hynes, 2002) (**Figure 5**).

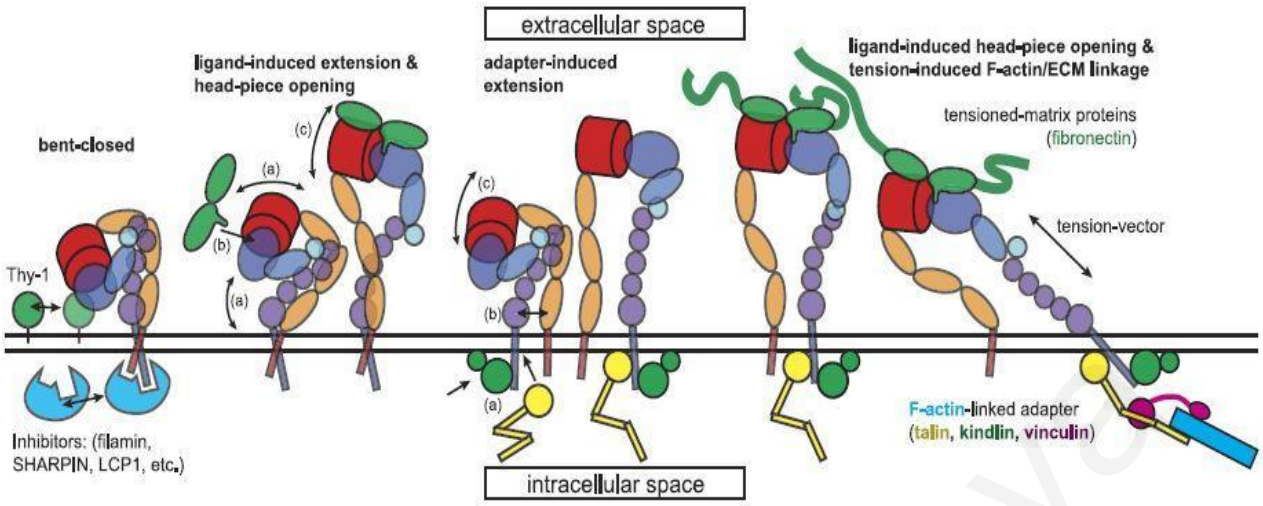

Figure 5: Integrin activation process. When integrins are not interacting with ligands, they adopt the closed bent conformation with low affinity for ligands. Outside-in signaling by ligand binding, or inside-out activation via interaction with intracellular proteins, promotes a conformational switch resulting in the intermediate state of integrin activation with intermediate affinity for ligands. After the connection of integrins with the actin cytoskeleton, the headpiece reaches the open conformation promoting the receptors to become fully activated, with a high affinity for ligand-binding.

Courtesy of: Bachmann et al., 2019

4. Focal adhesion and adherens junction crosstalk

As mentioned above, the coordinated regulation of cadherin and integrin functions is crucial for many physiological and pathological processes, such as tissue differentiation and renewal, wound healing, inflammatory response, and metastasis (Chen et al., 2012; Mui et al., 2016). Numerous studies suggested that a mechanically driven crosstalk between cadherins and integrins is involved in their spatial distribution, turnover, and dynamics, as well as in the regulation of intracellular force generation and the actin cytoskeleton. However, the exact molecular mechanisms underlying this regulated interplay between the two receptor classes remain unknown.

Several lines of evidence support the regulation of focal adhesion dynamics by adherens junction proteins, specifically showing that upon mechanical manipulation of VE-Cadherin, cell stiffening and F-actin increase promoting the activation of the PI3K kinase and integrins (Barry et al., 2015). In addition, when shear stress is applied to endothelial cells, the activation of PI3K kinase is promoted by PECAM1, VE-Cadherin, and VEGFR, leading eventually to the activation of integrins that can regulate the alignment of cells in response to the shear stress (Tzima et al., 2005). Furthermore, work by Bowler et al., showed that Cadherin-11 (CDH11) is involved in the regulation of focal adhesions and secretion of inflammatory cytokines to control valvular interstitial cell contractility (Bowler et al., 2018). Unpublished data from our lab showed that cadherin-based adhesions can stimulate and spatially guide ligand-independent activation of integrin receptors at the vicinity of AJs (Hadjisavva et al., Cell Reports- under revision).

The crosstalk between the two major adhesion systems appears to be bidirectional since integrins and focal adhesion proteins can also influence both positively and negatively AJ dynamics. For example, it has been shown that integrin β1 is essential for the localization of VE-Cadherin and p120 catenin at the AJs of endothelial cells, and therefore for junctional integrity (Yamamoto et al., 2015). Work from Howden et al., showed that α2β1 integrins can spatially restrict the activity of Cdc42 in keratinocytes to stabilize AJs (Howden et al., 2021). On the other hand, loss of α3β1 integrin promotes the disruption of cell-cell junctions in zebrafish and mouse kidney cells (Wang et al., 1999; Postel et al., 2013). Several studies showed that many focal adhesion resident proteins are recruited at AJs and play a critical role in their junction integrity. One of those is Src, a proto-oncogene tyrosine kinase (Roskoski et al., 2015). Specifically, inhibition of Src in tumor cells can promote E-cadherin-based cell-cell junction formation and restore the epithelial phenotype (Nam et al., 2002). Moreover, the recruitment of an E3 ubiquitin ligase, known as Hakai, is promoted through the phosphorylation of E-Cadherin by Src which leads to E-Cadherin degradation (Fujita et al., 2002). Along the same line, Piedra et al., showed that Src can phosphorylate β-catenin at Y654 residue resulting in disruption of the catenin-cadherin complex, thus promoting junctional instability (Piedra et al., 2003).

Several other focal adhesion proteins involved in this crosstalk are described below in more detail.

4.1 Focal Adhesion Kinase (FAK)

FAK is a 125 kD focal adhesion protein, widely expressed and conserved among tissues and different species (Parsons, 2010). It is classified as a cytoplasmic non-receptor tyrosine kinase, which is implicated in numerous fundamental cellular processes, including cell adhesion, proliferation, migration, and gene expression (Mitra et al., 2005; Goni et al., 2014; Tiede et al., 2018).

FAK is comprised of three main domains, that are linked via three proline-rich regions (PRR1-3): a FAT domain at the C-terminus, a FERM domain at the N-terminus, and a central kinase domain between the FERM and FAT domains. The focal adhesion targeting (FAT) domain interacts with Paxillin for promoting FAK at FAs, while the FERM domain provides docking sites for multiple proteins (Hildebrand et al., 1993).

Upon FAK recruitment at FAs through integrin activation or growth factor receptor activation, it becomes autophosphorylated at Y397, which is then recognized by the tyrosine kinase Src via its SH2 domain (Parsons, 2003). Assembly of the FAK-Src complex promotes the phosphorylation of FAK on two additional tyrosine sites, Y576 and Y577, resulting in the maximal FAK activation and phosphorylation of downstream protein targets, such as paxillin and p130Cas (Schaller et al., 1999; Hanks et al., 2003). Additional sites of FAK, including Tyr861 and Tyr925, get phosphorylated by Src, providing docking sites for Grb2 (Growth factor receptor-bound protein 2) and recruiting dynamin which will contribute to focal adhesion disassembly (Deramaudt et al., 2011).

Even though FAK is a well-characterized resident of focal adhesions, involved in their dynamics and functions, it also plays a central role in adherens junction integrity. Interestingly, several studies support both positive and negative regulation of AJs by FAK. For instance, in endothelial cells, FAK interacts with VE-Cadherin and enhances the phosphorylation of β-catenin at Y142. This phosphorylation decreases the affinity for cadherins, resulting in the disruption of the catenin-cadherin complex and thus in junctional instability and increased permeability of the endothelium (Chen et al., 2012). In addition, work from Wang et al., showed that VE- and N-Cadherin mediated intercellular contacts can be reduced by FAK, upon FA formation (Wang et al., 2006). On the contrary, FAK inhibition in tumor cells promoted the inhibition of cell-cell junctions by increasing RhoA activity, implying a positive role of FAK in AJ formation (Playford et al., 2008).

Additionally, increased expression of cadherins was observed upon FAK activation in fibroblasts (Mui et al., 2015). Along the same line, it was proposed that the strengthening of the epithelial barrier via the recruitment of E-cadherin to the cell periphery happens due to the activation of FAK (Quadri and Bhattacharya, 2007).

4.2 Paxillin

Paxillin is a 68kD multi-domain protein, a member of the FA complex. It is classified as an adaptor or scaffold protein since it interacts with several other proteins via its multiple docking sites (Schaller, 2001).

Paxillin contains several different motifs, including the five leucine- and aspartate-rich LD motifs, the four LIM domains, and the SH3- and SH2- binding sites, which promote the interactions with numerous binding partners (Turner et al., 1990). The LD motifs, within the N-terminus, are responsible for the interactions with several proteins as a response to cell signaling, while the LIM domains at the C-terminus, mediate the targeting of paxillin to FAs. Moreover, paxillin contains numerous tyrosine and serine/threonine phosphorylation sites (Brown and Turner, 2004). Importantly, phosphorylation of Y31 and Y118 by the FAK/Src complex is involved in cell migration and adhesion (Petit et al., 2000).

Paxillin is implicated in cell spreading and motility by coordinating the Rho GTPase family (Brown and Turner, 2004), as well as in cell migration through its involvement in growth factor and integrin signaling pathways (Brown and Turner, 2004). Furthermore, paxillin was found to be involved in embryonic development, since paxillin knockout mice showed embryonic lethality at day E9.5 (Hagel et al., 2002).

Importantly, Paxillin can also be found at AJs, where it can promote the formation of N-Cadherin-based adherens junctions, together with FAK, via the downregulation of Rac (Yano et al., 2004). Additionally, it is suggested that E-Cadherin-dependent junction integrity and contractility can be regulated by Paxillin through the control of RhoA and Rac1 activities (Gupta et al., 2021).

4.3 Vinculin

Vinculin is a 117 kD structural protein, a member of the focal adhesion complex (Geiger et al., 2001). It contains a large globular head domain and a tail region, linked via a short proline-rich sequence (Ziegler, 2006). When Vinculin is unbound, the interaction between the head and the tail domains promotes an auto-inhibited conformation, where the docking sites for Talin and actin are masked (Johnson and Craig, 1994; Johnson and Craig, 1995). Upon recruitment at FAs, Vinculin adopts the open conformation state, where the head domain interacts with the rod domains of Talin, and the tail is bound to actin bundles (Johnson and Craig, 1994; Johnson and Craig, 1995). It has been suggested that the interaction of Vinculin with Talin and actin is crucial for the maximal activation of Vinculin, as well as the phosphorylation of Y100, Y822, and Y1065 residues (Zamir and Geiger, 2001; Zhang et al, 2012). When activated, Vinculin can interact with numerous proteins, including paxillin and a-actinin, among others (Turner et al., 1990; Carisey et al., 2013). Vinculin is implicated in the transmission of extracellular and intracellular mechanical cues, which are required for the assembly, disassembly, and reorganization of FAs, as well as the assembly and remodeling of the actin cytoskeleton. Furthermore, Vinculin has a crucial role in cell migration, since Vinculin knockout cells showed altered migratory properties, cell spreading, and wound repair (Xu et al., 1998; Moese et al., 2007).

Although Vinculin is a member of the focal adhesion complex, it can be recruited to adherens junctions (AJs). The recruitment of Vinculin, as well as its role there, is less well understood. Several studies suggested that a multistep process involving α-catenin and β-catenin is responsible for the recruitment (Xu et al., 1998), while others proposed that external tension or tyrosine phosphorylation is crucial for Vinculin localization at AJs (Leckband et al., 2011). Specifically, activation of the Abelson tyrosine kinase (Ab1), in response to force on E-Cadherin and not integrins, leads to the phosphorylation of Y822. A mutant version of vinculin, Y822F, cannot bind β-catenin and is unable to localize at AJs (DeMali et al., 2014). Once localized at AJs, it has been suggested that Vinculin plays an essential role in cell-cell adhesion, through the stabilization of adhesion receptors. Specific depletion of Vinculin from AJs leads to the loss of E-Cadherin from the cell surface and a decrease in cell-cell adhesions (DeMali et al., 2017). Moreover, it has been shown that Vinculin can promote indirect binding of cadherins with the actin cytoskeleton, by interacting with α-catenin and exposing a cryptic site with a high affinity for F-actin (Yonemura et al., 2010). In addition, Vinculin has a crucial role in the force transmission to the actin

cytoskeleton by E-Cadherin, since cells lacking Vinculin or expressing the Y822F mutant, lose their mechanosensing capability (le Duc et al., 2010; DeMali et al., 2014).

4.4 Talin

Talin is a 270 kDa mechanosensitive protein that localizes at FAs. It contains multiple binding sites for other proteins, thus classified as an adaptor protein. Talin appears to be the main cytoplasmic protein mediating integrin adhesion to the extracellular matrix and linking integrins directly to the actin cytoskeleton. Additionally, Talin is involved in the regulation of integrin-adhesion strength, sensing matrix rigidity, and the regulation of T cell proliferation and survival (Chang et al., 2017; Klapholz and Brown., 2017).

Several studies showed that two conformational states of Talin exist, the inactive and the active. When inactive, an auto-inhibitory interaction between the N-terminal FERM domain and the C-terminal rod domain of Talin occurs, which can be disrupted by the PI(4,5)P2, an activator of Talin, thus promoting the active state of Talin (Moser et al., 2009). Once activated, the C-terminal rod domain interacts with actin filaments, exposing cryptic sites crucial for interaction with other proteins, including Vinculin, while the N-terminal FERM domain binds to the cytoplasmic tails of integrins. The interaction between Talin and Vinculin results in the conformational change of Vinculin, which enhances the recruitment of Vinculin at FAs (Izard et al., 2004). Moreover, Talin can promote the inside-out activation of integrins, where it converts integrins into a conformation with a high affinity for their ligands (Legate et al., 2011).

Not much information is available about the implication of Talin in AJ formation and function. However, it was shown that an argynilated proteolytic product of the C-terminal domain of Talin is localized at AJs, and the stabilization of VE-Cadherin at endothelial junctions is promoted through the Talin-dependent activation of endothelial cell β1 integrin (Zhang et al., 2012; Pulous et al., 2019).

5. Extracellular matrix (ECM)

As previously noted, integrin-mediated adhesions provide bidirectional links between the extracellular matrix and the actin cytoskeleton. Cell interactions with the extracellular matrix (ECM) affect numerous fundamental cellular processes, given that ECM appears to be a highly dynamic and multifunctional three-dimensional structure. ECM can be found within all tissues and organs, and it consists mainly of water, microfibrillar proteins, polysaccharides, and noncollagenous glycoproteins. However, a unique composition of ECM is present in each tissue, generated during tissue development via a reciprocal interplay between numerous cellular components, including epithelial and endothelial elements, and the cellular microenvironment (Frantz et al., 2010). Besides providing a substrate for cell anchorage and tissue scaffolding, ECM is essential for tissue morphogenesis, differentiation, and homeostasis, through the initiation of numerous biochemical and biomechanical cues. Additionally, ECM plays a critical role in cell migration during embryonic development and wound healing. Importantly, ECM can interact with several growth factors and cell-surface receptors, resulting in signal transduction and regulation of gene transcription to control cell growth, proliferation, survival, and death (Rozario and DeSimone, 2009). The fundamental and crucial role of ECM is highlighted by the wide range of syndromes, occurring from numerous genetic abnormalities in ECM components (Jarvelainen et al., 2009). For example, monogenic disorders of the connective tissue, such as osteogenesis imperfecta and Marfan's syndrome, manifest changes in the ECM (Glorieux, 2008), while an abnormal build-up of ECM components results in chronic kidney diseases, like glomerulosclerosis and tubulointerstitial fibrosis (Liu, 2006).

5.1 Fibronectin (FN)

Fibronectin (FN) is a core component of the ECM, which has a crucial role in numerous cellular processes, via the direct interaction with the integrin receptors. Fibronectin has been implicated in cell adhesion, survival, and differentiation, as well as in cell migration and wound healing. Mice lacking FN display embryonic lethality with defects in the mesoderm, neural tube, and cardiovascular network highlighting the crucial role of FN in embryogenesis (George et al., 1993). Moreover, several studies showed that FN can regulate vascular development and angiogenesis

(Hynes and Yamada 1982; George et al., 1993), while decreased FN expression was shown to be related to morphological changes observed in tumor cells (Hynes, 1990).

FN is secreted by a variety of different cell types as a disulfide-bonded dimer composed of subunits with a range in size from 230kDa to 270 kDa. Variation in the subunit size results from alternative splicing (Hynes 1990). FN is encoded by a single gene, whose transcript is alternatively spliced at three sites to generate multiple isoforms, as well as the two major forms of FN, plasma, and cellular FN. Plasma FN is abundant in blood and secreted by hepatocytes, while cellular FN can be incorporated into the fibrillar matrix and is secreted mainly by fibroblasts (Hynes, 1990). Each FN monomer consists of three types of repeating modules, known as type I, II, and III (Hynes 1990; Pankov and Yamada, 2002) (**Figure 6**). Specifically, there are 12 type I repeats, 2 type II repeats, and 17 type III repeats. However, the three positions of alternative splicing mentioned above are within the type III repeats, therefore 15 type III repeats are constitutively included in each monomer and 2 repeats (EIIIA, EIIIB) are included or omitted via the alternative splicing (Schwarzbauer et al., 1987; Hynes, 1990). The third region (V region) of alternative splicing can be included, partially included, or excluded from each monomer (Schwarzbauer and DeSimone, 2011). Type I and II repeats contain a pair of intrachain disulfide bonds to stabilize the folded structure (Pickford et al., 1997), while type III repeats have a 7-stranded β-barrel structure lacking the disulfide bonds, thus can undergo several conformational changes (Main et al. 1992). Interestingly, these repeats comprise a diverse set of binding domains on each FN monomer, mediating the simultaneous interactions between FN molecules and cell surface receptors, other ECM components (collagen), numerous extracellular enzymes, as well as with other FN molecules for FN dimer and fibrillar matrix assembly (Pankov and Yamada 2002; Singh et al. 2010) (**Figure 6**). For instance, at the carboxyl terminus is a pair of cysteines that form the disulfide-bonded FN dimer (Hynes 1990), while a major FN binding site lies within the N-terminal 1-5 type I repeats, required for fibrillar assembly (Sottile et al. 1991). In addition, sequences required for integrin binding, known as RGD and synergy sites, are in 9-10 type III repeats and the binding site for α4β1 integrin can be found in the V region of the FN molecule (Wayner et al., 1989).

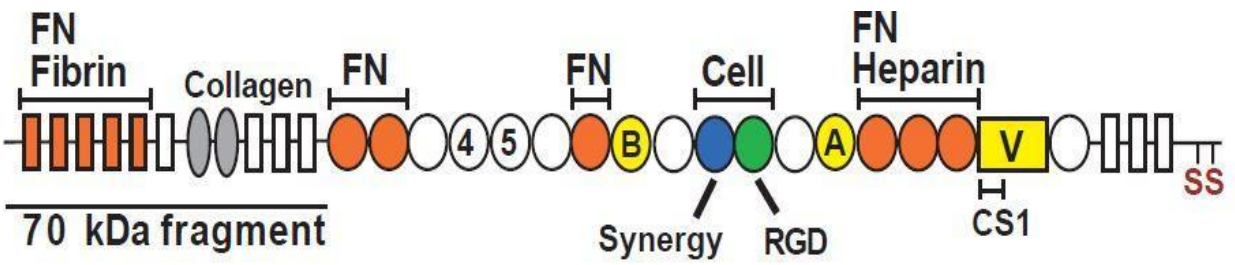

Figure 6: Fibronectin domain structure. FN is composed of type I (rectangles), type II (ovals), and type III (circles) modules. The three alternatively spliced repeats, EIIIA, EIIIB, and V region are indicated with yellow, while FN-binding sites and the assembly domain are indicated with orange. At the C-terminus, the SS indicates the cysteines required to form a dimer. Several binding domains, including the collagen-binding domain and fibrin, can be seen in the above scheme.

Courtesy of: Wierzbicka-Patynowski and Schwarzbauer, 2003

5.2 Fibrillogenesis

5.2.1 Cultured mammalian cells model

As previously described, FN is secreted as a soluble dimer molecule, which is then converted into insoluble, interlinked fibers via a multistep cell-dependent process, called Fibrillogenesis (McDonald et al. 1987). Mounting evidence supports that soluble FN must be activated first to assemble into fibrils given that even at extremely high concentrations of FN in solution it can't undergo fibril assembly due to its compact conformation as a dimer (Erickson and Carrell, 1983; Johnson et al., 1999; Schwarzbauer and Sechler, 1999; Sechler et al., 2001). Activation of FN is induced by the interactions with cell surface receptors, specifically with the α5β1 integrin. Inside-out signaling through cytoplasmic signals mentioned previously, promotes the conformational change required for switching integrin affinity for FN molecules from a low to a high state (Hynes, 2002; Takagi et al., 2002). Therefore, fibrillar assembly is initiated by the interaction of integrin receptors with FN molecules through the binding of the Arg-Gly-Asp (RGD) and the synergy sequences located in the 9 type III and 10 type III repeats, respectively, or the CS1 segment of the

alternative spliced V region (IIICS) (Argraves et al., 1987; Hynes, 1982; Hynes, 1990) (**Figure 7**). This specific interaction promotes the clustering of integrins, which are bound to FN dimers resulting in a high local concentration of FN at the cell surface required for FN-FN non-covalent interactions. The major FN binding domain lies within the N-terminal type I repeats, while a covalent interaction of FN subunits via a pair of disulfide bonds in the C-terminal is shown to be crucial for FN assembly as well (Sottile et al., 1991). It has been suggested that interaction with integrin receptors can induce conformational changes of FN, promoting the exposure of several FN-binding sites, some of which are hidden in the compact conformation of FN dimers. Subsequent events, in which cell contractility and tension play an essential role in promoting further the exposure of self-association sites lead to the switch of FN conformation from compact to extended required for fibrillogenesis (Zhong et al., 1998; Sechler et al., 2001; Schwarzbauer and DeSimone, 2011). In particular, integrins link FN molecules to the actin cytoskeleton, which can generate tension at the contact sites between the receptors and FN, while Rho GTPase activity provides further the contractility required for the FN assembly (Zhong et al 1998). Interestingly, cytoplasmic domains of integrins can stimulate intracellular signaling crucial for the initiation of matrix assembly, through several focal adhesion proteins such as FAK and Talin (Ilic et al. 2004; Green et al. 2009) (**Figure 7**). Finally, these events lead to the self-association of numerous FN dimers to form multimers and short fibrils with solubility in DOC detergent, which subsequently with continued deposition of FN molecules will irreversibly convert to DOC-insoluble fibrillar matrix characterized by rigidity and stability (McKeown-Longo and Mosher 1985). Therefore, the assembly of a functional fibrillar matrix requires the coordination between several extracellular events and intracellular pathways as well as tension and contractility.

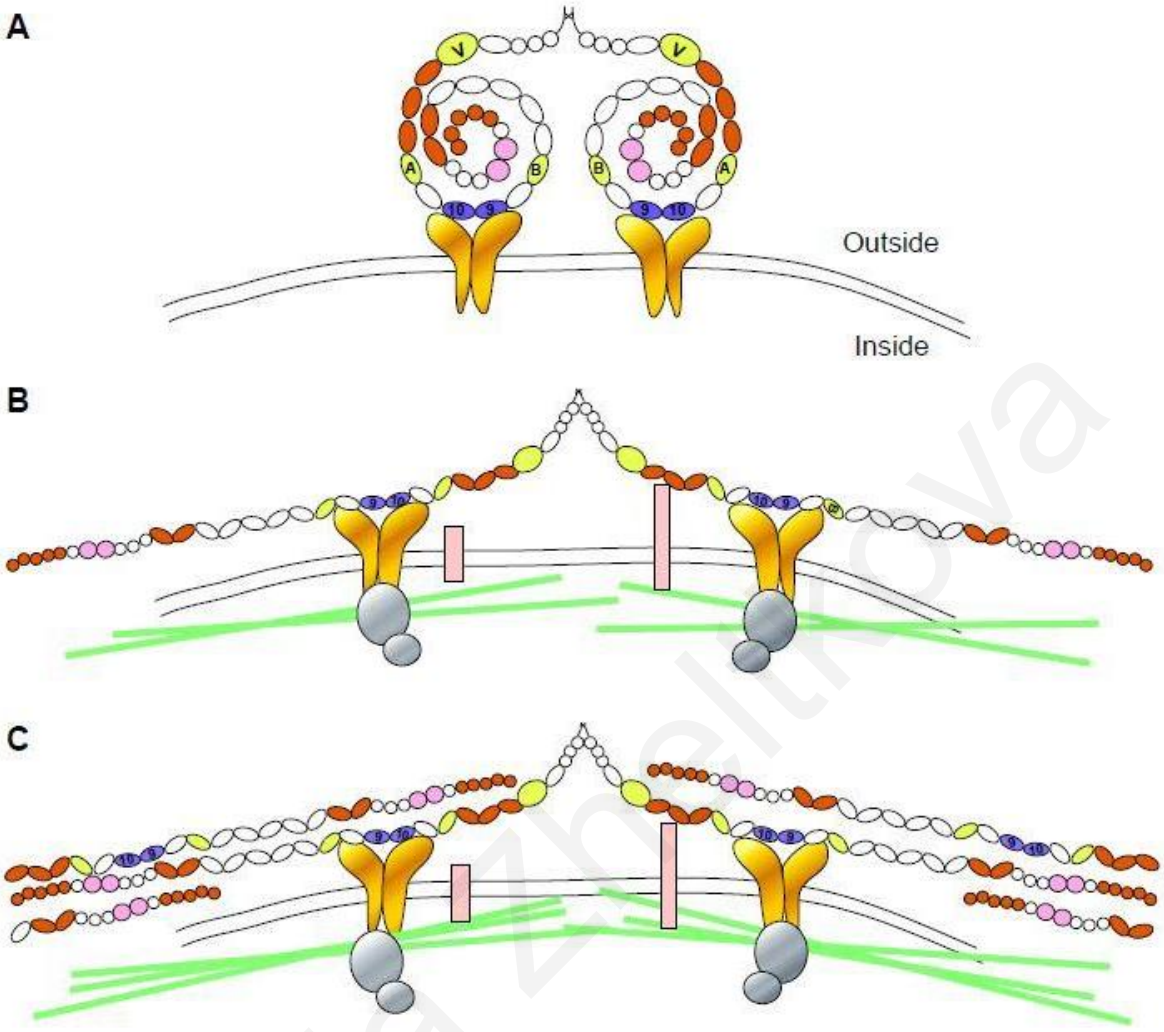

Figure 7: Major steps in fibrillar assembly. (A) Compact FN dimer binds to α5β1 integrin (gold structure). (B) Intracellular proteins (gray structures) are recruited to the cytoplasmic tail of integrins, linking them to the actin cytoskeleton (green lines). Induced cytoskeletal reorganization leads to increased cell contractility, which promotes the conformational change of FN dimer required for the exposure of the cryptic FN binding sites in the extended molecule. (C) Fibrillar matrix formation via multiple FN-FN interactions.

Courtesy of: Mao and Schwarzbauer, 2005

5.2.2 ECM assembly and remodeling in the Developing Embryo

Numerous studies on both avian and amphibian embryos showed that FN is expressed early in embryogenesis, however, the fibrillar assembly occurs before gastrulation (Lee et al. 1984; Boucaut et al., 1985). A pericellular nonfibrillar FN network can be detected initially only on the free surfaces of the blastocoel roof (BCR) in amphibians, which is opposed to the blastocoel cavity (Lee et al. 1984). Over time, this FN network develops into an elaborate fibrillar matrix crossing cell boundaries. Interestingly, at the early stages of embryogenesis, all cells express the main integrin receptor for FN, α5β1-integrin, and soluble FN can be detected in the blastocoel fluid showing that the presence of both the receptors and FN is insufficient to allow the fibrillar assembly in the embryo, therefore suggesting that it can be regulated both temporally and spatially to promote normal morphogenesis (Lee et al., 1984). Notably, it has been shown that free surface and lateral adhesive cell contacts are necessary for fibrillar assembly initiation as well (Winklbauer, 1998).

Mounting evidence shows the crucial role of FN expression and assembly in embryonic development, specifically as a migratory substrate, since mice lacking the FN gene are embryonic lethal, displaying defects in the mesoderm, neural tube, and cardiovascular development (George et al. 1993). Morpholino knockdowns of FN in zebrafish are also defined by faulty somite boundary formation and mesoderm migration (Ju¨lich et al. 2005). Moreover, FN assembly was shown to be involved in the convergent extension movements in *Xenopus* and zebrafish (Marsden and DeSimone 2001; Davidson et al. 2006).

Although the regulation of FN assembly is well characterized based on studies in cultured mammalian cells (Singh et al. 2010), where tension generated through integrin receptors is required (Pankov et al. 2000), the mechanisms of fibrillar assembly on the free surfaces of multi-layered tissues *in vivo* are still not well understood. Emerging evidence proposed that tissue tension regulated by adherens junctions between blastomeres plays an essential role in the fibrillar assembly (Dzamba et al. 2009). Specifically, it was observed that cells of the blastocoel roof change shape from round to polygonal during the initiation of FN assembly, indicating increased cell-cell adhesion and tension. Interestingly, by overexpressing cadherins in blastocoel-roof cells at earlier stages, the same changes in shape and early initiation of FN assembly were observed, while inhibition of cadherins blocked the assembly of fibrils. The same results have been seen by applying experimentally mechanical deformations that lead to increased or decreased tension in

the blastocoel roof. After investigating how these regional changes in cell adhesion can regulate FN assembly, work from Dzamba et al., proposed a model where cadherin-dependent changes via the noncanonical Wnt/PCP signaling pathway, lead to the reorganization of the cortical actin cytoskeleton and myosin phosphorylation through the activation of the small GTPase Rac and Pak. This contractile event is required for the integrin-FN translocation from cell-cell contact sites across the free surfaces of adjacent cells, generating additionally high mechanical tension (**Figure 8**). Therefore, this enhanced cell-cell junction formation is analogous to the role of focal adhesions *in vitro,* described previously, to generate the tension required for exposing the cryptic binding sites within the FN molecule for self-interaction and eventually fibrillar formation (Dzamba et al., 2009).

Other mechanisms have also been suggested to regulate the fibrillar assembly in embryonic development. For instance, FAK and Ena/VASP are implicated in fibrillar formation at the intersomitic boundaries of *Xenopus* embryos, while during gastrulation syndecan-1 and -2 play an essential role as well (Kramer and Yost 2002; Kragtorp and Miller 2006). Moreover, in the somite borders of zebrafish, FN matrix assembly is influenced by the Eph/Ephrin signaling pathway (Julich et al., 2009).

The integrin-cadherin crosstalk described in the previous section has a role in developmental processes, including the fibrillar assembly. In mammalian cells reduction in N-Cadherin adhesion was observed when fibrillogenesis was initiated. Similarly, during the development of zebrafish, the expression of N-Cadherin promotes the stabilization of the integrin inactive state at the lateral junctions between cells to restrict fibrillar assembly in areas lacking cell-cell adhesion (Julich et al., 2015). Contrary, as mentioned above, in *Xenopus* embryos fibrillar formation, which is an integrin-dependent process, is initiated by the increased cell-cell adhesion and AJ generated tension (Dzamba et al., 2009). Furthermore, data from our lab showed that adherens junction formation can spatially guide ligand-independent integrin activation and thus influence ECM topology (Hadjisavva et al., Cell Reports-under revision).

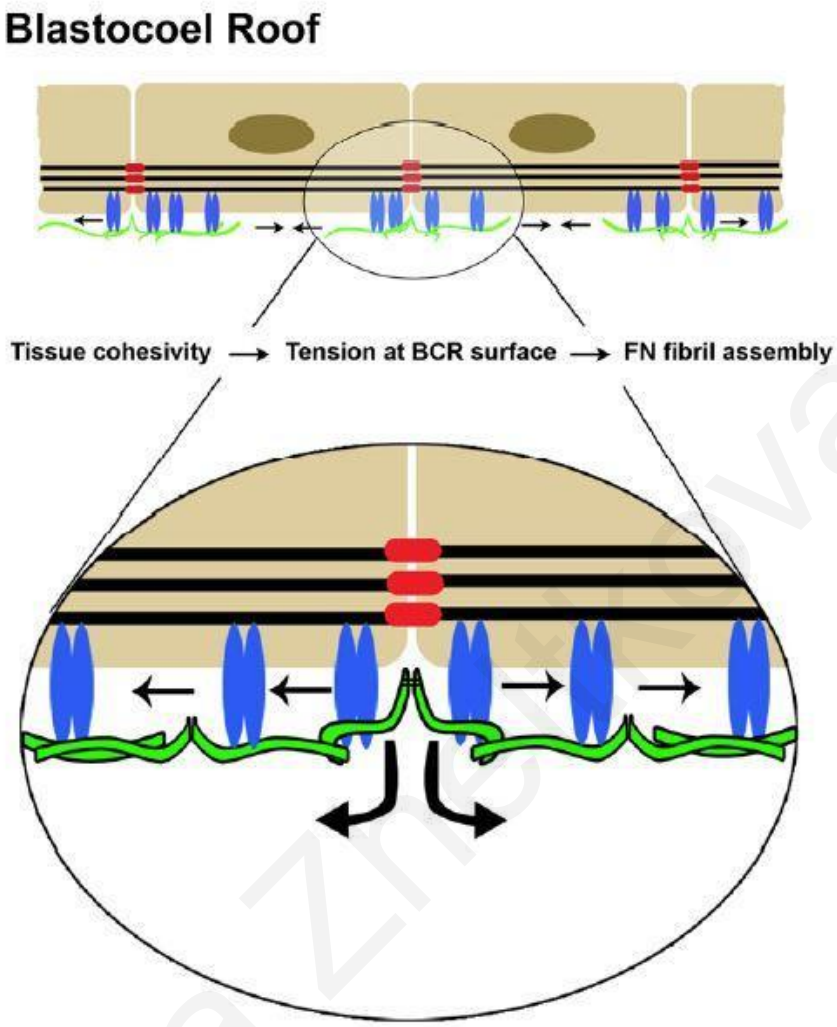

Figure 8: Model of fibrillar assembly in *Xenopus.* Local tension generated by an increased cell-cell junction (red structure) formation linked to the actin cytoskeleton (black lines), is transmitted to α5β1 integrin receptors bound to FN dimers, resulting in the conformational change of FN and exposure of cryptic FN binding sites. As integrin/FN complexes move from cell-cell contact sites across the free surfaces of adjacent cells, fibrillar assembly is promoted.

Courtesy of: Dzamba et al., 2009

MATERIALS AND METHODS

Cells, Cell Culture, and Transfection

HeLa (CCL2, American Type Culture Collection, ATCC) and HEK293 (CRL-1573, ATCC) cell lines, as well as NIH3T3 (CRL-1658, ATCC), Talin KO HeLa Kyoto and YPet-Talin reconstituted HeLa Kyoto cell lines, were cultured at 37°C with 5% CO2 in Dulbecco's modified Eagle's Medium (PAN-Biotech$_{TM}$) supplemented with 10% Fetal Bovine Serum (Biosera) and 1X Antibiotic/Antimycotic solution (Biosera). Transient transfections in HeLa, NIH3T3, and HEK cells were performed with Lipofectamine 2000 (11668019, Invitrogen) according to the manufacturer's protocol. For the experiments in which cells were seeded either on conA, on N-Cadherin Fc substrates, or for live imaging, cells were detached with cold EDTA solution (10mM EDTA, 2% BSA in 1XPBS), followed by one wash with 1XPBS and diluted in serum-free DMEM medium (Dulbecco's modified Eagle's Medium without Calcium Chloride, 21068-028, gibco) before seeding.

Silanization of coverslips

Glass coverslips were initially sonicated for 15 minutes, washed in distilled water, and incubated in isopropanol, before being air-dried at 65°C. Coverslips were then exposed to plasma treatment for 5 minutes. Subsequently, coverslips were incubated in concentrated silane (3-Aminopropyl) triethoxy-silane (Alfa Aesar) for 15 minutes and then washed 5-10 times with isopropanol. Then coverslips were baked at 100°C for 30 minutes. Coverslips were either used immediately or stored in a sealed container for use for up to one week.

Substrate coatings

Silenized coverslips were coated with bovine plasma Fibronectin (33010018, Thermo Fisher Scientific) at a concentration of 10 μg/ml in 1XPBS for 60 minutes at 37°C, followed by two washes with 1XPBS before seeding of cells. For Concanavalin A (C5275, Sigma-Aldrich) coated coverslips, silenized coverslips were incubated with concanavalin A at a concentration of 250μg/ml in 1XPBS for 30 minutes at 37°C. Excess liquid was aspirated, and coverslips were allowed to air-dry at 37°C, before seeding cells. For N-Cadherin substrate generation, coverslips were initially incubated with Goat Anti-Human IgG (10 μg/ml, SSA015 Sino Biological) for 1 hour at 37°C. Afterward, coverslips were coated with N-Cadherin Fc (Recombinant CDH2/Fc, Sino Biological) at a concentration of 10 μg/ml for 1 hour at 37°C, followed by two 1XPBS washes.

Drug treatments

Regarding the ROCK inhibitor (Rho-kinase inhibitor, Y-27632) and RO-3306 inhibitor (CDK1/cyclin B1, CDK1/cyclin A inhibitor) experiments, cells were either cultured for 12 hours in the presence of inhibitors (25μM and 50μM) separately or allowed to first form doublets and then treated for 15 minutes with the inhibitors (50μM) before fixation.

Fibrinogen and mem stain incubation

Regarding the Fibrinogen-Alexa Fluor 674 (5mg/ml, Invitrogen 11584816) cells were cultured for 12 hours in the presence of Fibrinogen before fixation. Regarding the Deep Red Plasma membrane stain (5mg/ml, Invitrogen C10046) experiments, cells were incubated in media supplemented with the mem stain for 10 minutes at 37°C. After two washes with PBS cells were ready to use for live imaging.

Generation of agarose gels for doublet formation

1% agarose gels were generated and placed for equilibration in DMEM for 60min at RT, before the addition of suspended cells. Cells were detached with cold EDTA solution (10mM EDTA, 2% BSA in 1XPBS), followed by one wash with 1xPBS, resuspended in serum free DMEM medium, added on top of gels, and allowed to form doublets for 30 minutes before fixation.

Generation of polyacrylamide gels

Glass coverslips were initially sonicated for 15 min. After several washes with distilled water, the coverslips were incubated in isopropanol, before being air-dried at 65°C. Next, they were incubated in Rain-X (Water Repellent, 500 ul each) for 2 min at room temperature, followed by several washes with distilled water. For the generation of the polyacrylamide gels, based on the required stiffness, several mixtures were used, as described in the table below (**Table 1**). Afterward, 20μl of each mixture was added to each Rain-X-coated coverslip and finally a silanized (vapor-APTES, 2x2 min) coverslip was placed on top of each gel. For the gels to set, they were left for 60 min at room temperature, and afterward, they were incubated in distilled water for 45min. The coverslips were separated, and the polyacrylamide gels remained on the top of the silanized coverslips, which were used for the following steps. Subsequently, the coverslips were incubated in a Sulfo Sanpah mixture (A35395, Thermo Scientific, 20 μl per coverslip) under a UV lamp (UVP BLACK-RAY B-100AP LAMP, 365 nm) for 5 min. After several washes with 1xPBS, they were coated with Vitronectin (10 μg/ml) in 1XPBS overnight at 4°C. The next day, coverslips were washed several times with 1XPBS and placed for equilibration in DMEM and 1% Antibiotics for 60min at 37°C, before seeding cells. For live-imaging DMEM was replaced by FN-YPet serum free media for live imaging on a Zeiss LSM 910 airyscan laser confocal microscope.

	40% Acrylamide stock	2% Bis-acrylamide stock	H20	Antibiotic	10% APS	Temed
30 kPa	100 ul	25 ul	364.5 ul	5 ul	5 ul	0.5 ul
66 kPa	100 ul	62.5 ul	313 ul	5 ul	5 ul	0.5 ul

Table 1. Gel recipes in ul for a total of 500 ul mix.

Soluble FN YPET generation

Transfection of HEK293 cells with the pHLSec2-FN-YPet (#65421, Addgene) construct was performed with Lipofectamine 2000 (11668019, Invitrogen) according to the manufacturer's protocol. Upon removal of the transfection reagent, cells were cultured in serum-free DMEM for 2 days, followed by the collection of the medium. For the removal of leftover detached or dead cells, the medium was centrifuged for 5 min X 2000rpm. For live imaging, the FN YPet containing medium was diluted.

Immunostaining on cells

HeLa cells as well as NIH3T3, Talin KO HeLa Kyoto, and YPet-Talin reconstituted HeLa Kyoto cell lines were washed three times with 1XPBS and fixed for 12 minutes in 4% paraformaldehyde (PFA) solution in 1XPBS. PFA fixation was followed by incubation in a 50 mM glycine solution (pH=7.8) in 1X PBS for 10 minutes. Next, permeabilization of cells was done using 0,1% Triton-X solution in 1X PBS for 10 minutes. After several washes with 1XPBS, cells were blocked using 10% donkey serum in 1X PBS for 30 minutes. Following that, cells were incubated with primary antibodies diluted in 10% donkey serum solution in 1X PBS for 1 hour at room temperature or overnight at 4°C. The primary antibodies used were: β-catenin rabbit (Sino, 11279R021) 1:1000, N-Cadherin mouse (Thermo, MA1-159) 1:300, N-Cadherin rabbit (Sino, 11039-R014) 1:500, N-Cadherin rabbit (Sino, 11039-R020) 1:500, N-Cadherin rat (Hybridoma, MNCD2) 1:50, 9EG7 rat

(BD Biosciences, 553715) 1:800, Mab13 rat (Millipore, MaBT821) 1:500, 12G10 mouse (Santa Cruz, sc-59827) 1:500, Phalloidin Alexa 633 (Invitrogen, A22284) 1:400, HUTS mouse (BD Biosciences, 556048) 1:500, Human FN mouse (Hybridoma, HFN 7.1) 1:500, Fibronectin Fragment 2 rabbit (Sino Biological, 10314-RP03) 1:500, Paxillin mouse (BD transductions, 610051) 1:600, Vinculin mouse (Santa Cruz, sc-73614) 1:400, FAK mouse (ProteinTech, 66258-I-1g), pY20 (tube Eppendorf, co210) 1:500, pFAK rat (RD Biosciences, MAB4528) 1:500, pPaxillin Tyr31 rabbit (Santa Cruz, sc-14035) 1:600. The primary antibodies were washed 3x5minutes in 1XPBS before the addition of secondary antibodies (in block solution) for 1 hour at room temperature. The following secondary antibodies were used: 488 Donkey anti-Rat (Invitrogen, 1:500), 568 Donkey anti-Mouse (Invitrogen, 1:250), 568 Donkey anti-Rabbit (Invitrogen, 1:500), 647 Donkey anti-Rabbit (Invitrogen, 1:300), Alexa 647 Donkey anti-Rat (Jackson Immunoresearch, 1:100), Cy3 Donkey anti-Rat (Jackson Immunoresearch, 1:500), 488 Donkey anti-Rabbit (Invitrogen, 1:500), 488 Donkey anti-Mouse (Invitrogen, 1:500). The secondary antibodies were washed three times in 1XPBS. For mounting, ProLong anti-fade mounting agent (Invitrogen, P36961) was used on a microscope slide and the glass coverslip was placed inverted on top of it.

Plasmids and DNA constructs

Most of the plasmids used in this thesis for molecular cloning purposes or protein expression in cells were already available in the lab [pHLSec2-FN-YPet (#65421, Addgene), Pcs2+ N-Cadherin GFP ΔCP (provided by Dr. Carl Philipp Heisenberg), mCherry-Beta-Catenin-20, mCherry N-Cadherin (provided by Dr. Roberto Mayor), mCherry Talin-18 (#55137, Addgene), pCS2++ mKate FAK, mScarlet Paxillin (#112956, Addgene), pActinin-miRFP670nano (#127432, Addgene), pmiRFP680-tubulin (#136575, Addgene), pCS2+ N Cadherin Scarlet WT, GFP-Talin (mTalin1) (#80027, Addgene), pCDNA3.1 catenin conformational FRET sensor (#71709, Addgene), mRuby-Vinculin-23, pCS2+ N-Cadherin GFP).

The pmiRFP680 Fibronectin was constructed using standard molecular biology techniques.

Generation of the miRFP680 Fibronectin was performed in one step using pmiRFP680-tubulin as a template and the following primers:

F: aaaACCGGTatggcggaaggctccgtcg

R: aaaGAATTCTAActcttccatcacgccgatct

The PCR product was inserted in frame in the pHLSec2-FN-YPet plasmid, using AgeI and EcoRI restriction sites. The YPet gene sequence, which was situated between the AgeI and EcoRI restriction sites of the pHLSec2-FN-YPet plasmid, was removed during the digestion.

Cell lysis

Cells were rinsed with 1XPBS and lysed in lysis buffer (130mM NaCl, 20mM HEPES pH 7,2, 3mM EDTA, 0,3% Triton X-100, 10% Glycerol, supplemented with protease and phosphatase inhibitors) on ice, followed by cell scraping, collection in 1,5 ml Eppendorf tube, sonication (Hielscher Ultrasound Technology), centrifugation (10000 rpm X 12 minutes) and incubation at 95°C for 2 minutes, after the addition of 5X Laemmli Buffer (10% SDS, 50% Glycerol, 0.02% bromphenol blue, 0.3125M Tris HCl, pH 6.8) supplemented with 25% β-mercaptoethanol. Lysates were used for western blot analysis.

Western Blot Analysis

Lysates were loaded into 6% or 10% SDS-polyacrylamide gels with BlueStar Prestained Protein Marker (NIPPON genetics) and blotted onto nitrocellulose membranes (Porablot NCP-MACHERY-NAGEL). Afterward, blots were blocked in 5% milk (Fluka® analytical) in PBS-Tween 20 (1XTBS and 0.1% Tween 20) or 5% BSA (A9647, Sigma-Aldrich) in PBS-Tween 20 (1XTBS and 0.1% Tween 20) for 30 minutes and then incubated with the primary antibodies in 5% milk or 5% BSA, respectively, overnight at 4°C. The primary antibodies used were:

Fibronectin Fragment 2 rabbit (Sino Biological, 10314-RP03), Paxillin mouse (BD transductions, 610051), pPaxillin Tyr31 rabbit (Santa Cruz, sc-14035). Blots were washed in PBS-Tween 20 for 3X10 minutes and then incubated with a Goat anti-Rabbit IgG-HRP (1:5000, SantaCruz Biotechnology) secondary and a Donkey anti-Mouse IgG (H+L) Alexa Fluor™ Plus 800 (A32789, Invitrogen) secondary in 5% milk or 5% BSA, respectively, for 1 hour at room temperature. After three 10-minute washes in PBS-Tween 20, visualization of fluorescent secondary antibody was performed immediately, while for the HRP-conjugated secondary the signal detection was performed with the use of the Immobilon Forte Western HRP Substrate (WBLUF0500, Millipore). Images were acquired with the use of the ChemiDocTM MP – Imaging System (BIO-RAD).

Imaging

After immunofluorescence staining, cells were imaged either with a Zeiss Axio Imager Z1 microscope equipped with a Zeiss Axiocam MR3 and the AxioVision software 4.8 or with a Zeiss LSM 710 scanning laser confocal microscope, with the Zen 2010 software, or with a Zeiss LSM 910 airyscan laser confocal microscope with the Zen 2010 software.

Quantification and Statistical analysis

All quantifications were performed with the AxioVision LE software, ImageJ, and Zen (Blue + Black edition) software. Intensities were measured using ImageJ. Profiles were generated using the Zen (Blue edition) software. Statistical analysis was performed with the GraphPad Prism software (Version 7.01).

RESULTS

6.1 Establishing a protocol to monitor FN localization and fibrillar assembly during live imaging and in fixed samples

The aim of this study was to examine the possible impact of AJs both on ligand binding on the cell surface and on fibrillar assembly. Previous work revealed that ECM deposition is regulated indirectly by tissue tension and cadherin-based interactions; however, the exact mechanism through which AJs could influence ECM assembly and deposition was unclear (Dzamba et al.,2009). Nevertheless, unpublished data from our group revealed that AJs can stimulate and spatially guide ligand-independent integrin activation creating spatially restricted pools of high ligand affinity receptors at cell-cell contact sites (Hadjisavva et al., Cell Reports-under revision). Thus, we wanted to examine if those AJ-driven pools of integrins can a) spatially influence ligand binding on the cell surface and b) impact ECM deposition and remodeling. Since the ECM is a three-dimensional network consisting of several extracellular molecules, we decided to select and examine Fibronectin, a core component of the ECM, the importance of which is demonstrated by the embryonic lethal phenotype of knockout mice (George et al., 1993). In an effort to address the above questions, we had to initially develop a protocol that would allow monitoring fibronectin assembly both during live imaging as well as in fixed samples.

6.1.1 Use of Fibrinogen to monitor fibrillar assembly

In order to fluorescently label fibronectin we initially examined the possibility to use Fibrinogen covalently labeled with Alexa 647. Fibrinogen is a glycoprotein shown to interact with fibronectin via the cryptic high-affinity FN-binding site in the alphaC domain, accessible only when fibrinogen converts into fibrin (Makogonenko et al., 2002). Fibrinogen is much more stable than fibronectin and is readily available prelabeled from various vendors while fibronectin is very sensitive and very few options of pre labeled fibronectin exist in the market. To test the Alexa Fluor conjugated Fibrinogen , we incubated HeLa and fibroblasts with different

concentrations of Fibrinogen (250ng/µl, 150ng/µl, 100ng/µl) for 24 hours and then fixed them and stained against Fibronectin. As shown in **Figure 9**, only a few fibrils were labeled by Fibrinogen; however, in order to get a better picture of the percentage of fibrils incorporating Fibrinogen vs. the fibrils stained with the FN antibody, intensity profiles were generated in parallel with the fibrils, with the FN antibody represented by the green line and Fibrinogen with the red line. We observed that a high percentage of fibrils were completely devoid of Fibrinogen and the labelling was uneven since some of the fibrils were fully labelled, others displayed discontinuous staining, and others were completely incapable of incorporating Fibrinogen, compared to the FN antibody that stained completely and continuously all the fibrils. By increasing the concentration of Fibrinogen, more fibrils positive for Fibrinogen were observed, however, nonspecific labelling was increasing as well, creating nonspecific, large aggregates of Fibrinogen resulting in background, both in HeLa and fibroblasts (**Figure 9**).

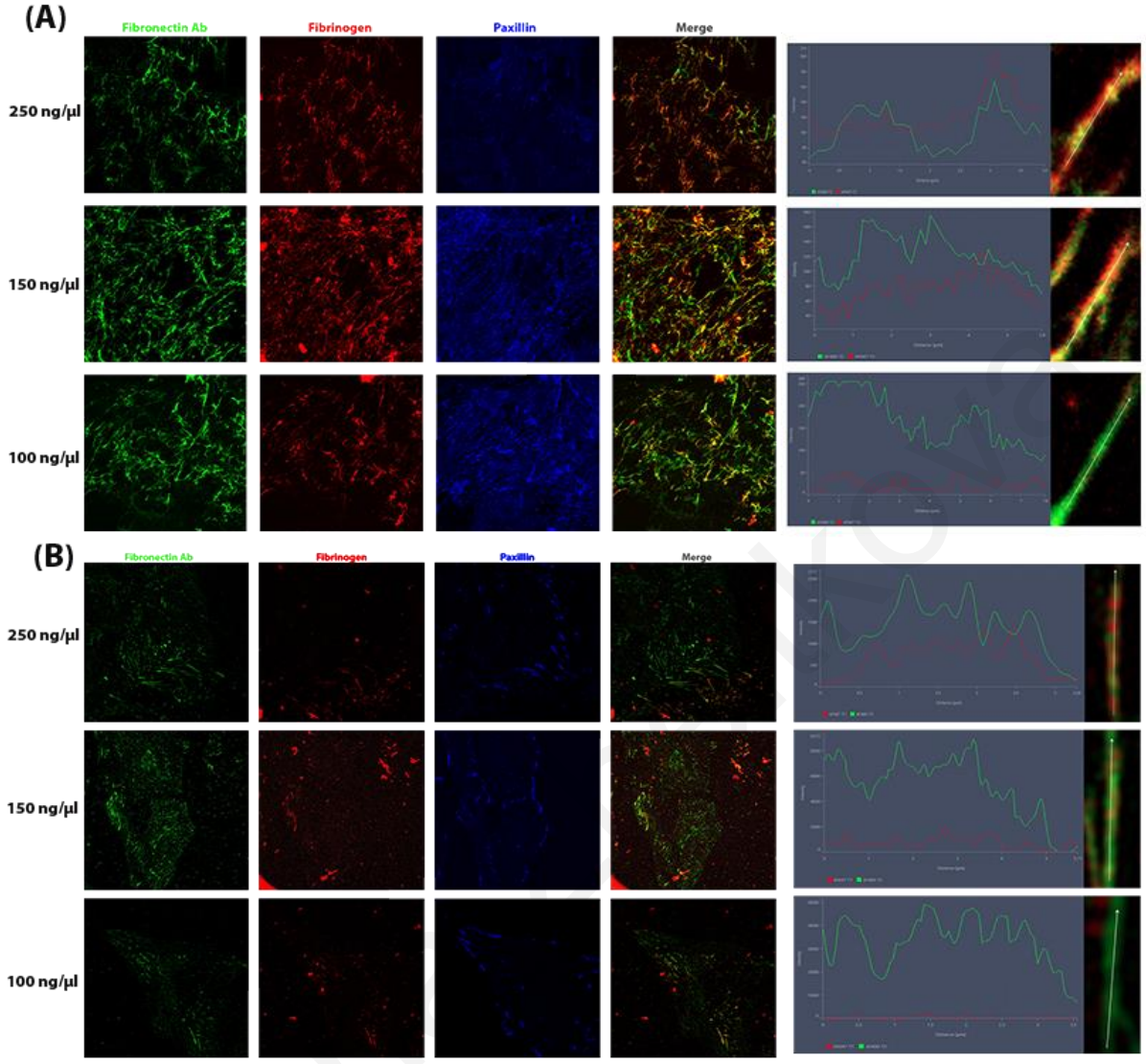

Figure 9. Use of fibrinogen leads to discontinuous labeling of fibronectin fibrils

(A) Confocal images of NIH3T3 cells cultured for 24 hours in the presence of several concentrations of Fibrinogen (250ng/µl, 150ng/µl, 100ng/µl), were fixed and stained for FN and Paxillin. Profiles generated parallel to each fibril revealed that Fibrinogen display discontinuous fibrillar staining or even fails to stain fibrils at all.

(B) Confocal images of HeLa cells cultured for 24 hours in the presence of several concentrations of Fibrinogen (250ng/µl, 150ng/µl, 100ng/µl), were fixed and stained for FN and Paxillin. Profiles generated parallel to each fibril revealed that Fibrinogen display discontinuous fibrillar staining or even fails to stain fibrils at all.

6.1.2 Use of fluorescent protein Fibronectin fusion (FN-YPet) to monitor fibrillogenesis

Given the poor results obtained using fluorescently labeled fibrinogen we turned to a fluorescent protein fusion of fibronectin (Ohashi et al., 2002). We initially attempted direct transfection of the target cells however this was problematic. Given the fact that our experiments required high sensitivity detection of FN binding of the cell surface, direct transfection of target cells led to high levels of FN-YPet accumulating in the ER and Golgi as well as in exocytic vesicles. This masked lower intensity signal from secreted FN binding on the cell surface. To bypass this issue we generated a fluorescently labeled fibronectin using HEK293 cells and the FN-YPet construct. We postulated that expression in the highly amenable to transfection HEK293 cells would lead to sufficient FN accumulation in the media to allow their conditioning and subsequent use on the target cells. A schematic representation of the protocol for the generation of the fluorescently labeled FN conditioned media established in our lab is presented in **Figure 10**, as well as the schematic representation of the full-length FN and FN-YPet construct. We decided to use HEK293 cell line for the generation of the FN-YPet conditioned media, since HEK293 cells display high transfection rates that result in efficient protein secretion in the media. Specifically, HEK293 cells were transfected with FN-YPet construct and cultured for two days in serum-free media. Serum contains various ECM ligands including fibronectin. This would compete with our fluorescently labeled FN for binding to cells and thus would reduce the fluorescent signal in our experiments. This conditioned media was collected, cells and cell debris were removed by centrifugation and added to fibroblasts for 24 hours before fixation, in order to examine if this media would lead to fluorescent labeling of FN fibrils. Hence, immunofluorescence (IF) experiment and intensity profiles were carried out using an antibody against Fibronectin. As shown in **Figure 11**, most of the fibrils were fully labeled with the FN-YPet in a continuous manner, as a clear correlation between the signal intensity variation of FN antibody and the signal from FN-YPet can be observed in the intensity profiles made parallel to the fibrils.

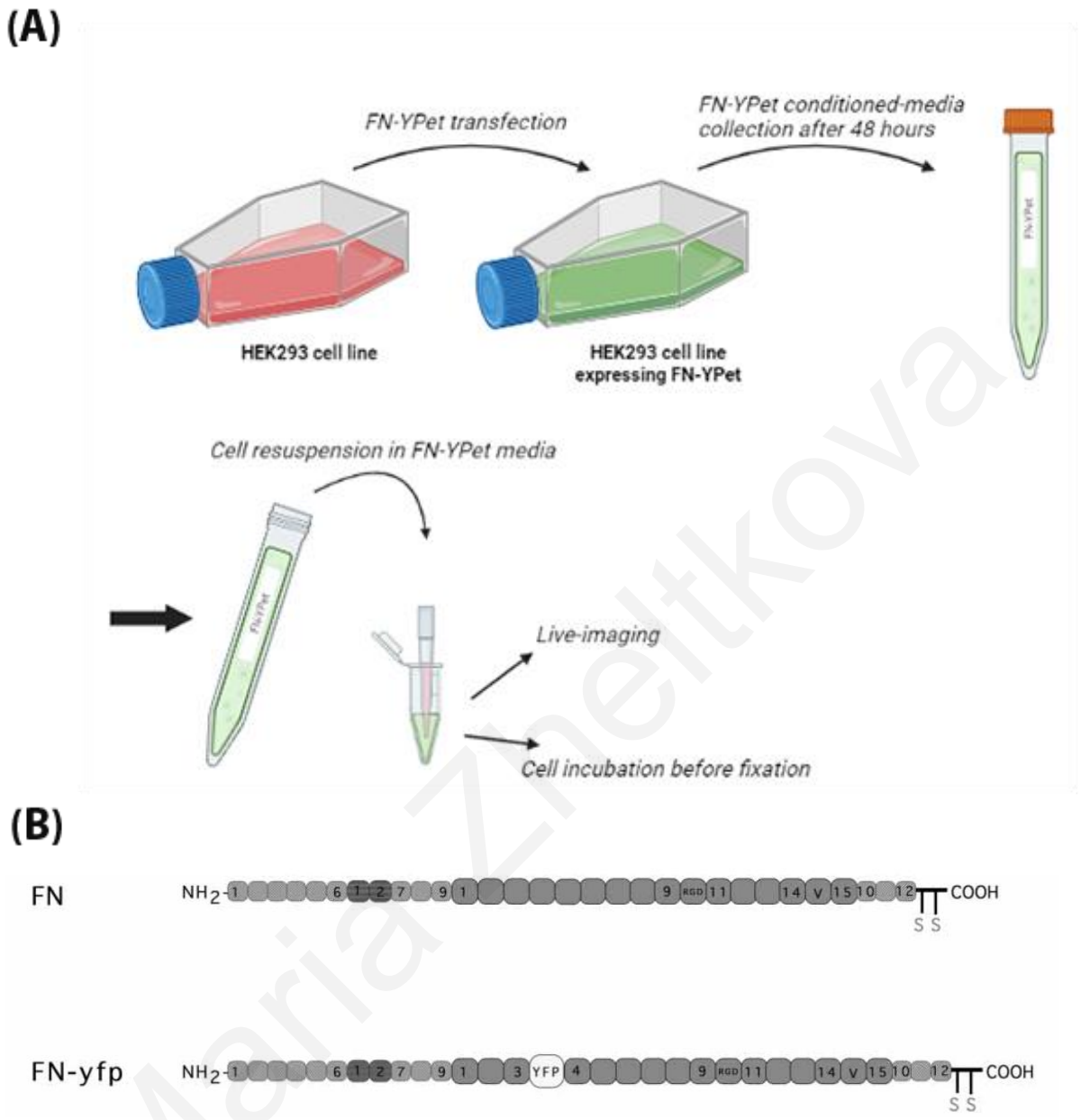

Figure 10. Schematic representation of the protocol used for FN-YPet conditioned media production.

(A) Schematic representation of the protocol followed for the production of FN-YPet containing media. This scheme was made by using BioRender.com.

(B) Schematic representation of the structure of the full-length FN and the FN-YPet, in which YFP was fused between 3 and 4 domains. Adapted from Ohashi et al., 2001

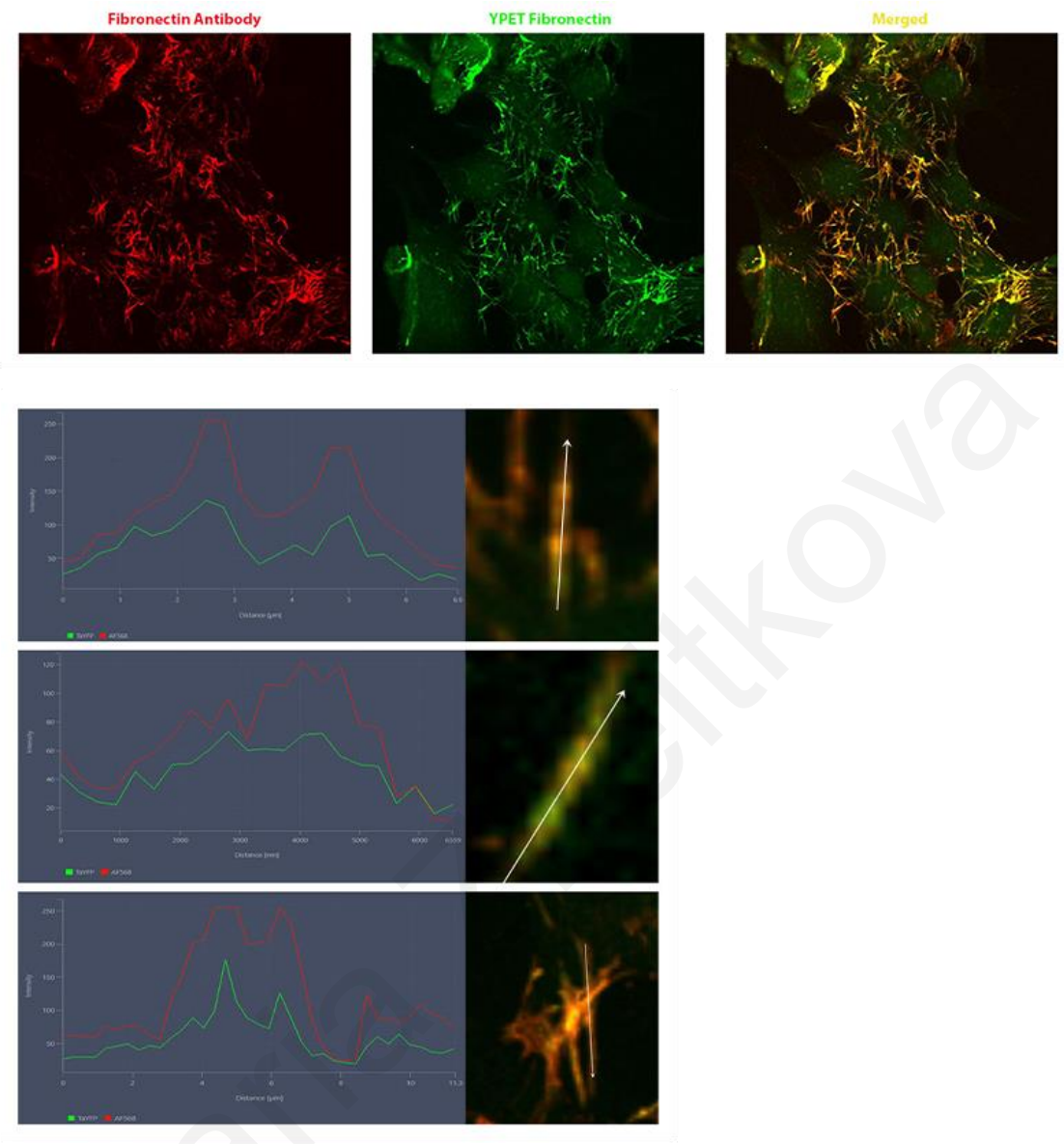

Figure 11. FN-YPet can efficiently label fibronectin fibrils formed by the cells

Confocal images of NIH3T3 cells cultured for 24 hours in the FN-YPet conditioned media were fixed and stained for FN. Profiles generated parallel to each fibril reveal that FN-YPet is capable of labeling the fibrils in a continuous manner.

Since we had tested both options, Fibrinogen and FN-YPet, on fixed samples, we proceeded to examine them during live imaging. Similar results were obtained with FN-YPet labeling the majority of fibrils, compared to the Fibrinogen, which incorporated discontinuously in a very small number of fibrils and created a strong background with non-specific aggregates (**Figure 12A**). Interestingly, Fibrinogen labeling not only displayed discontinuity, but it also showed a delayed appearance within the fibrils, compared to the FN-YPet labeling, as shown in **Figure 12B** suggesting that its incorporation into FN fibrils does not take place at the earliest stages of fibrillogenesis. Overall, we concluded that the fluorescently labeled FN was the most suitable option for monitoring both ligand binding on the cell-surface as well as fibronectin fibrillogenesis during live imaging and in fixed samples and thus we proceeded to use it for our experiments.

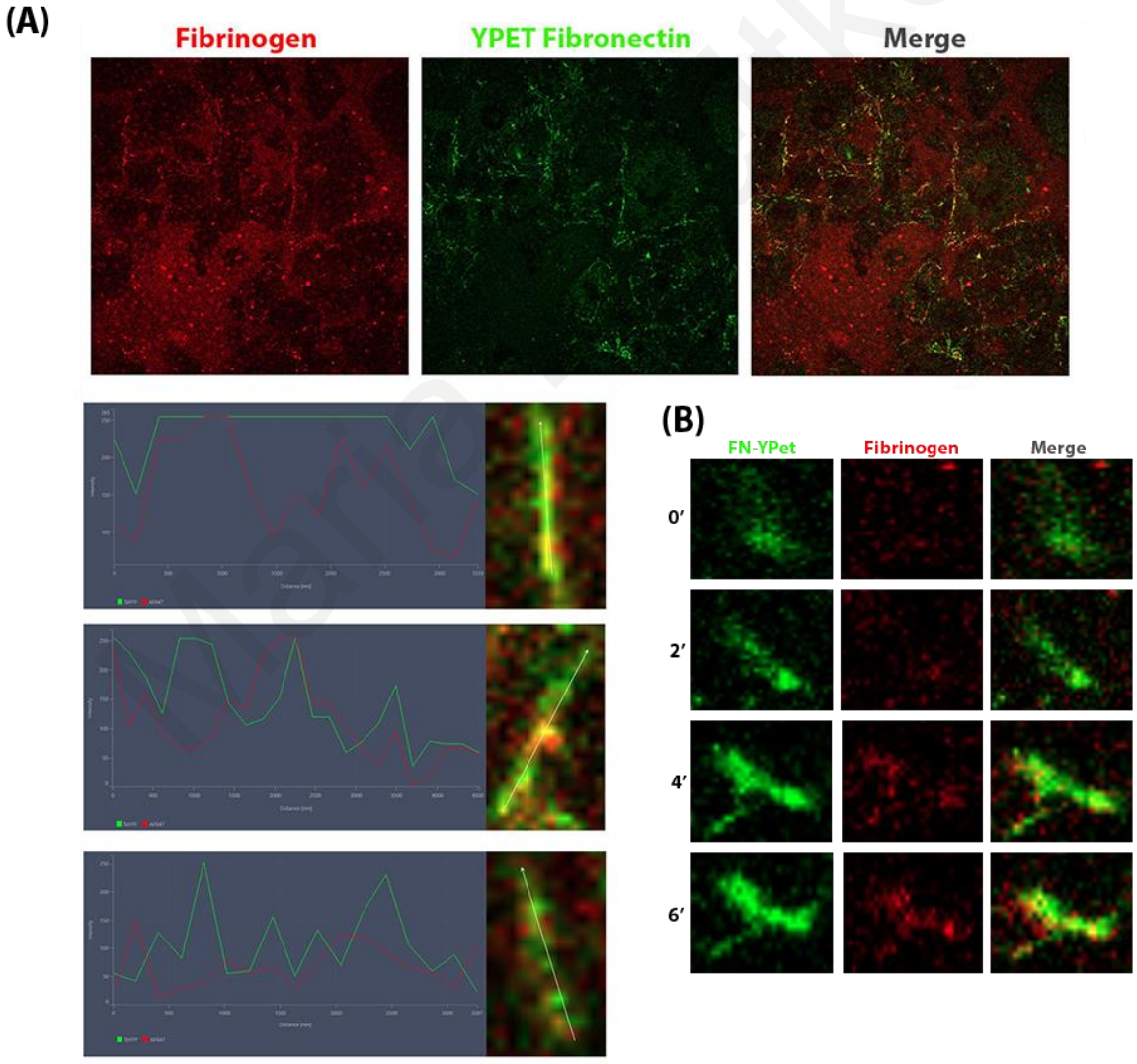

Figure 12. Live imaging of Fibrinogen and FN-YPet confirmed the discontinuous fibrillar staining of Fibrinogen compared to the FN-YPet and revealed that the fibrillar labeling via Fibrinogen is delayed

(A) Still images from a live movie of NIH3T3 cells in the presence of both Fibrinogen and FN-YPet. Profiles generated parallel to each fibril confirmed the continuous fibrillar staining from FN-YPet, in comparison with the discontinuous fibrillar staining from Fibrinogen.

(B) Close-up of a single fibril over time revealed the delayed appearance of Fibrinogen compared to the FN-YPet.

6.1.3 Cloning of the miRFP680 Fibronectin construct and verification of its stability and size

Before moving forward, given the need to combine FN with other labelled proteins simultaneously, we attempted to switch the fluorescent molecule of the FN-YPet construct from YPet to a near-infrared emitting protein (NIR). As shown in **Figure 13A**, both the excitation and emission spectra of the YPet molecule overlap with the spectra of the Green Fluorescent Protein (GFP) and the Red Fluorescent Protein (RFP), and this leads to an imaging issue, known as bleed-through. During imaging of more than one fluorophore, bleed-through can occur, where a signal from one fluorophore leaks to the channel of another and is detected there, resulting in false results. Since we wanted to examine the impact of AJs on FN deposition during live imaging as well, we needed to have more than one fluorophore available for multi-imaging. Specifically, the idea was to simultaneously image FN, an AJ component (N-cadherin or β-catenin), and Talin, which acts as a surrogate for integrin activation, given that it is directly interacting with active integrin tails. However, most of the constructs available in the lab, including N-cadherin, β-catenin, and Talin, were either GFP or RFP. Given that, using them together with the FN-YPet was not an option. Notably, when media containing FN-YPet was added to cells transfected with N-Cadherin GFP during live imaging, those two fluorophores could not be spectrally resolved adequately even when using a spectral confocal system. Thus, we went on to take advantage of the fluorophores emitting near-infrared (NIR), such as the miRFP680 and the miRFP670nano. Their spectra do not overlap with the GFP or RFP spectra, hence bleed-through could be avoided (**Figure 13B**). Importantly

the NIR region of the spectrum is ideal for live imaging since there is very little autofluorescence in this region and low energy photons are less toxic to the cell. For this reason, we thought to remove the YPet molecule from the FN-YPet construct and switch it with the one from the miRFPs that were available in the lab via standard molecular cloning techniques.

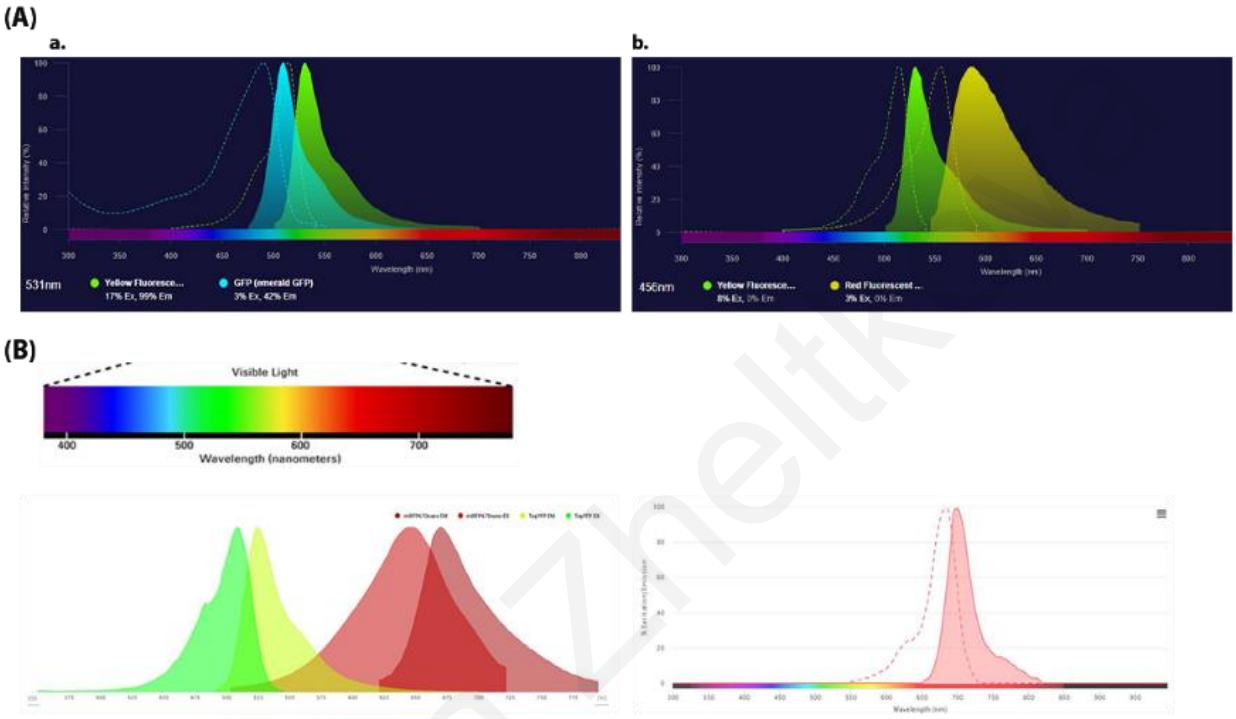

Figure 13. Emission and excitation spectra of several fluorescent proteins

(A) Emission and excitation spectra overlap between (a) YFP and GFP and (b) YFP and RFP. Adapted from thermoficher.com/spectraviewer.

(B) Emission and excitation spectra of YFP, miRFP670 nano, and miRFP680. Adapted from fp.base.org.

Before moving on with the cloning, we first had to decide which miRFP construct was the most suitable in our case. We had two available options in our lab, a miRFP680 fused with tubulin, and a miRFP670nano fused with Lifeact. This was especially critical given that NIR protein fluorophores typically exhibit very low quantum yields and as a result are quite dim. At the same time both photomultipliers and CCD sensors display reduced sensitivity at the NIR region of the spectrum making the detection of these fluorophores challenging. In order to determine which fluorophore was the brightest and most photostable, we transfected cells with either the miRFP680 Tubulin or the miRFP670nano Lifeact construct and live imaged them for 70 minutes keeping the same laser power and exposure times between them (**Figure 14**). In agreement with the FPbase database, our results showed that miRFP680 was brighter and more photostable compared to the miRFP670 nano (**Figure 14C**). Since NIR emitting fluorophores are characterized by dim light emission and high stability, we ended up selecting the miRFP680 instead of the miRFP670 nano, due to its better characteristics.

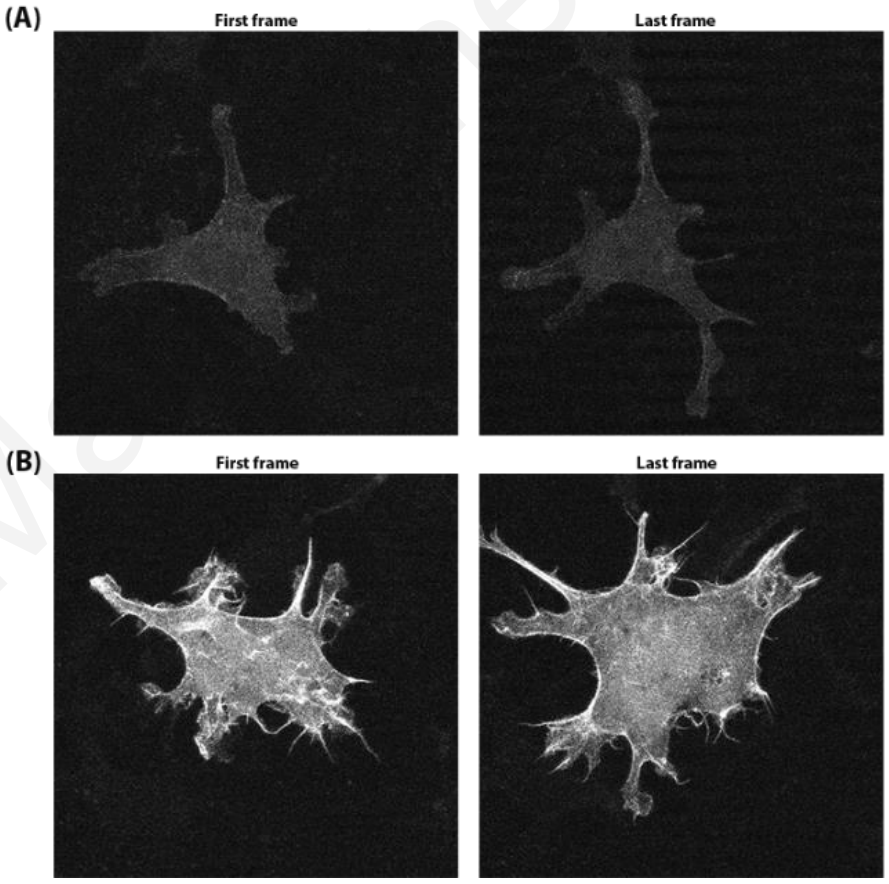

(C)

	miRFP 680	*miRFP 670nano*
Brightness	13.63	10.26
Photostability	980 t1/2 (s)	490 t1/2 (s)

Figure 14. Live imaging of miRFP680 tubulin and miRFP670nano lifeact revealed that miRFP680 is a more suitable option due to its increased brightness and photostability compared to the miRFP670nano

(A) First and last still images from a live movie of a cell transfected with miRFP670nano Lifeact.

(B) First and last still images from a live movie of a cell transfected with miRFP680 tubulin.

(C) Table referring to the characteristics of both miRFP670nano and miRFP680 protein (Adapted from Fpbase.org).

Following standard molecular cloning techniques, we generated a new construct by replacing the YPet domain of FN-YPet with miRFP680. The cloning of this construct is thoroughly described in the Material and Methods section. The molecular weight and stability of the FN-miRFP680 were verified by Western Blot. Lysates from FN-miRFP680 transfected HEK293 cells, FN-YPet transfected HEK293 cells, and control untransfected HEK293 cells were used for this experiment. Using an antibody against FN, a single band was detected at the expected molecular weight of around 300 kDa (**Figure 15**).

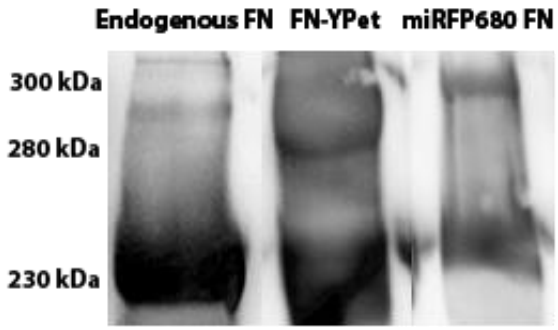

Figure 15. Confirmation of size and stable expression of miRFP680 FN in HEK293 cells

Western Blot analysis of lysates from miRFP680 FN and FN-YPet transfected HEK293 cells, and untransfected HEK293 cells (control). The miRFP680 FN construct in transfected cells is detected at 300 kDa, while FN-YPet is detected at 290 kDa and endogenous FN is detected at 230 kDa in HEK293 cells.

We went on to examine whether FN-miRFP680 can label fibrils as efficiently as the original FN-YPet construct could. HEK293 cells were transfected with FN-miRFP680 and cultured for two days in serum-free media, before the collection of the conditioned media. Subsequently, NIH3T3 cells were cultured in that media for 24 hours and then fixed and stained against Fibronectin. Despite being functional, we observed that FN-miRFP680 didn't colocalize perfectly with the FN antibody staining on fibrils and exhibited discontinuity along fibrils (**Figure 16**). Additional analysis of these data with the generation of profiles parallel with the fibrils confirmed that there was a mismatch between FN-miRFP680 and FN antibody labeling, as well as the discontinuous fibrillar labeling from FN-miRFP680.

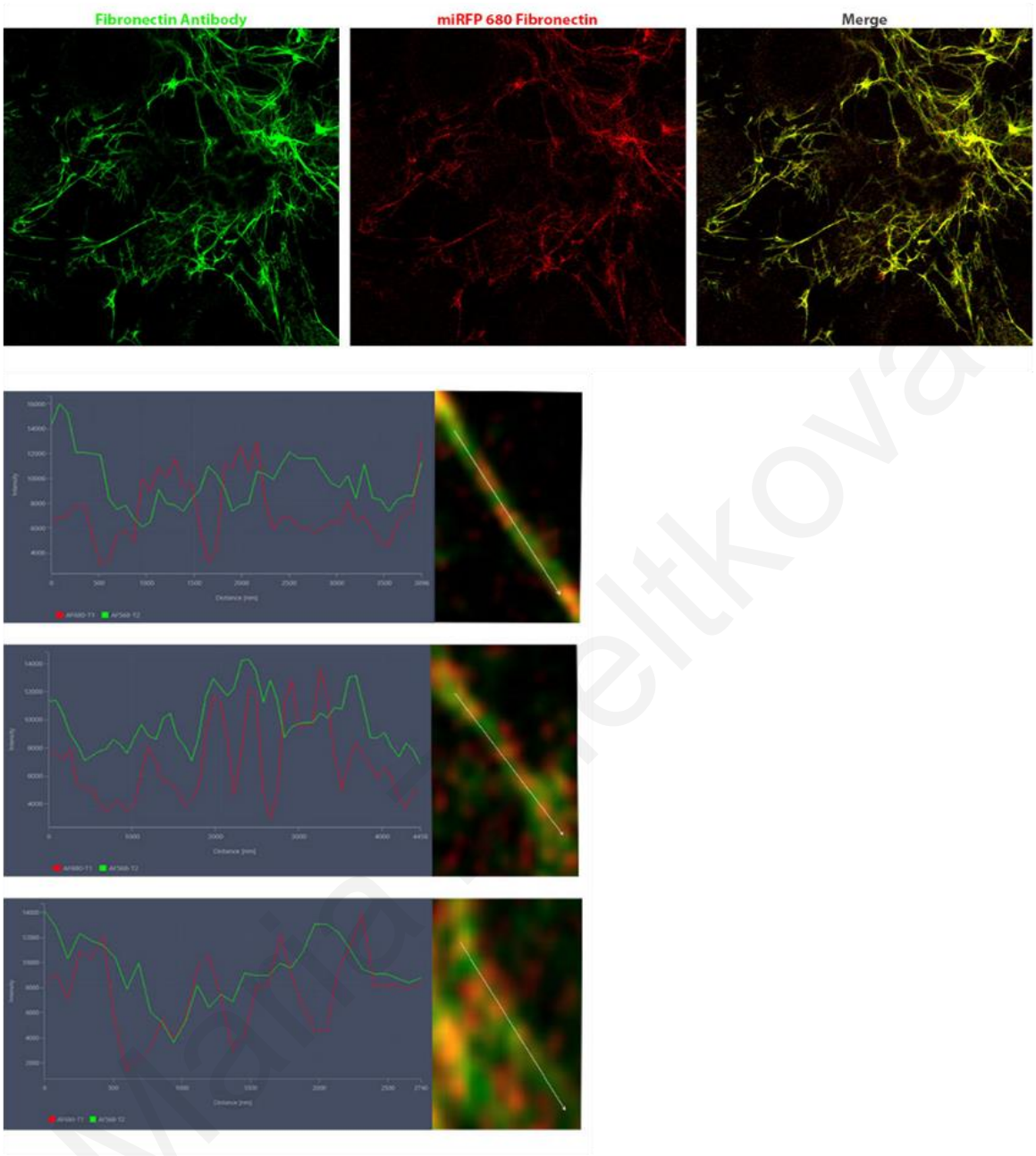

Figure 16. miRFP680 FN displays discontinuous fibrillar staining

Confocal images of NIH3T3 cells cultured for 24 hours in miRFP680 FN conditioned media were fixed, and stained against FN. Profiles generated parallel to each fibril revealed the discontinuity of staining along fibrils by miRFP680 FN.

Nonetheless, we proceeded to examine the new construct during live imaging and compare it with the original FN-YPet. Therefore, we imaged cells live, to which we externally introduced media from HEK293 cells containing both FN-miRFP680 and FN-YPet. As shown in **Figure 17**, the FN-miRFP680 signal was not detectable at all even after 30 minutes, compared to the FN-YPet signal. Further analysis confirmed that the FN-miRFP680 signal cannot be detected, probably due to the fact that the fluorophore is very dim and not detectable at such low levels within short time periods (**Figure 17B**). Although our construct is useful for long term experiments since it does become incorporated into fibrils when cells were cultured for 24 hours (**Figure 16**), in the short term, during live imaging it was undetectable, and since it did not fulfil the requirements for these experiments, we went on to use the original FN-YPet construct only.

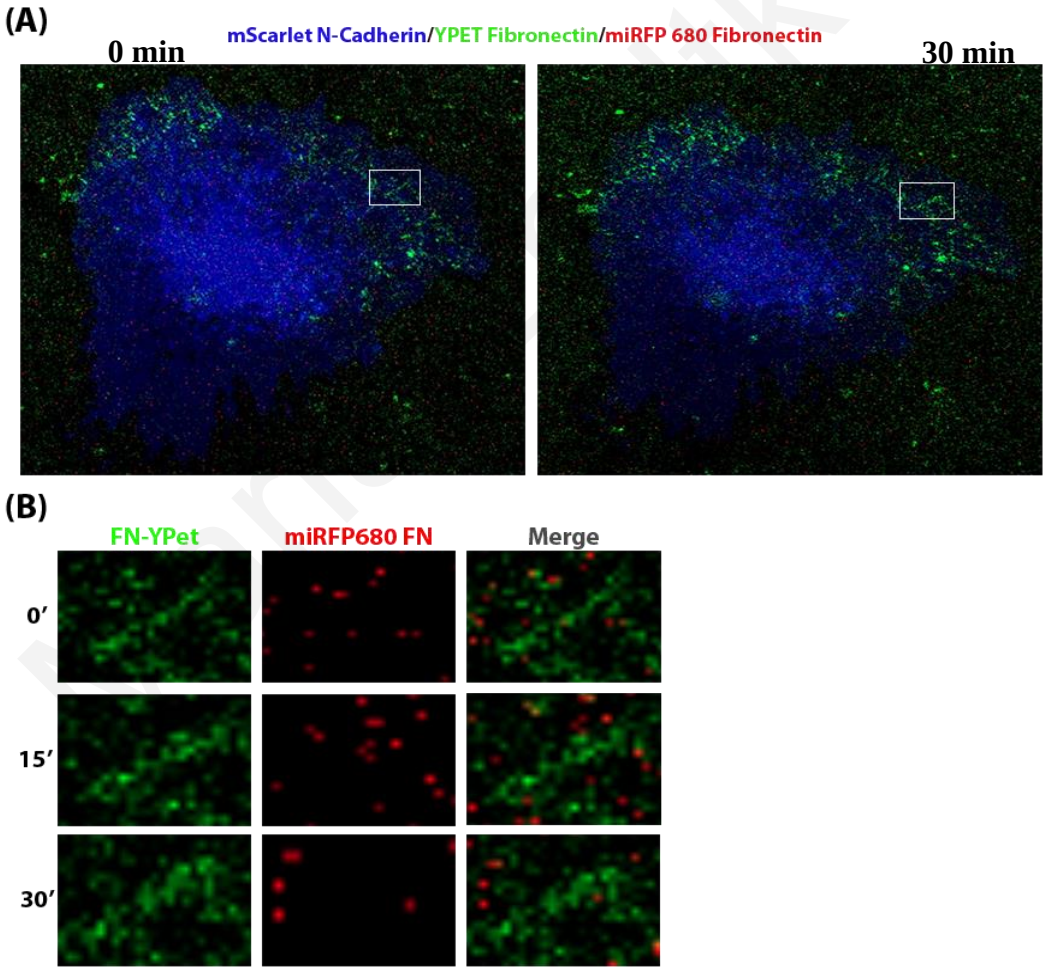

Figure 17. Live imaging of miRFP680 FN revealed that unlike FN-YPet it cannot be detected during the early stages of fibril formation

(A) Still images (0 min and 30 min time points) from a movie of HeLa cell in media containing both miRFP680 FN and FN-YPet, showing the incorporation of FN-YPet into newly formed fibrils in comparison with the undetectable signal from miRFP680 FN.

(B) Close-up of a single fibril over time revealed that miRFP680 FN is not detectable at such low levels and within short time periods.

6.1.4 Selection of appropriate cellular model with the use of FN-YPet

6.1.4.1 Selection based on the capacity for FN fibril formation

We then moved on to select the appropriate cell lines for our experiments that would allow the monitoring fibrillar assembly with the use of FN-YPet and the study of the impact of AJs on both the cell-surface ligand binding and fibrillogenesis. Specifically, we examined various cell lines available in our lab, including NIH3T3 and Paxillin null cells, which are both mouse embryonic fibroblasts, as well as the human cervical carcinoma cell line HeLa and the human embryonic epithelial kidney cells HEK293. Of all the cell lines tested the most appropriate to show in this study were those four that covered all the possible outcomes concerning FN deposition (**Figure 18**). In order to find the most suitable cellular model, we initially cultured all the different cell lines for 12 hours in media containing FN-YPet before fixation. Remarkably, both fibroblast cell lines created an impressive dense meshwork of fibrils, in comparison to HeLa cells that showed a small number of individual fibrils and HEK293 cells that were almost completely unable to deposit fibrils (**Figure 18**). These results were in agreement with previous studies, that showed that fibroblasts are to a large extent responsible for the synthesis and deposition of fibrillar ECM components of the stroma (Hynes, 1990; Strutz and Zeisberg, 2006; Qureshi et al., 2017), however, epithelial cells were shown to respond to fibrotic stimuli and produce components of the ECM as well (Humphreys et al.,2010). At this point, we decided to move on with the NIH 3T3 cells instead

of using Paxillin null cells, since this cell line lacks the protein Paxillin, and therefore could impact several cellular properties, such as cell spreading (Hagel et al., 2002) and complicate data interpretation. Additionally, HeLa cells were chosen over HEK293 cells since HEK293 were not able to deposit FN fibrils. Collectively, we decided to proceed with NIH3T3 and HeLa cells.

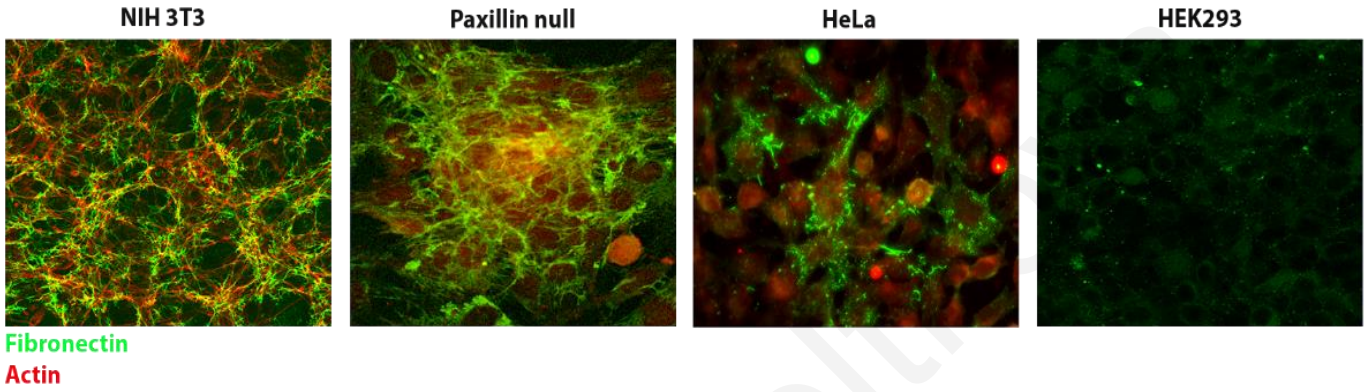

Figure 18. Fibroblasts generate a dense fibrillar network, compared to HeLa and HEK293 which show a limited and no fibril formation, respectively

Images of various cell lines cultured for 12 hours in the presence of FN-YPet, fixed, and stained for FN. Both fibroblasts formed an extremely dense fibrillar meshwork in comparison with HeLa and HEK293.

6.1.4.2 Cellular model selection based on AJ formation

Considering that we wanted to address the role of AJs on fibronectin assembly, we had to find a cell line that not only produces fibrils, but it also expresses adherens junction components at sufficient levels to form adherens junctions, since different cell lines express different cadherin types and at different levels, leading to differences in the ability to form AJs or the appearance of the AJs. Numerous studies showed that both NIH3T3 and HeLa cells express N-cadherin and β-catenin via WB analysis, with fibroblasts displaying more scattered phenotype with punctuated AJs, while HeLa cells showed more strong and large AJs along the cell-cell contacts (Islam et al., 1996). In agreement with these studies, we performed immunofluorescence experiments, using

antibodies that recognize β-catenin and N-Cadherin both in NIH3T3 and HeLa cells and showed that HeLa displayed very strong and robust enrichment of those components at AJs, compared to NIH3T3 fibroblasts (**Figure 19A**). Quantification of the intensity levels of N-cadherin and β-catenin respectively, localized at the AJs of HeLa and NIH3T3 cells confirms the above observation (**Figure 19B**). Collectively, our results showed that we came up with two different contexts, HeLa cells with a limited fibrillogenesis but with strong enrichment levels of AJ components at those sites, and fibroblasts that display very fast and dense fibrillar matrix assembly but moderate AJ formation. Taking this into account, we thought to take advantage of both contexts in our future experiments.

Conclusively, we have established a protocol to monitor ligand binding on the cell surface and fibronectin matrix assembly, both during live imaging as well as in fixed samples, in an effort to address the impact of cell-cell junctions in these processes.

(A)

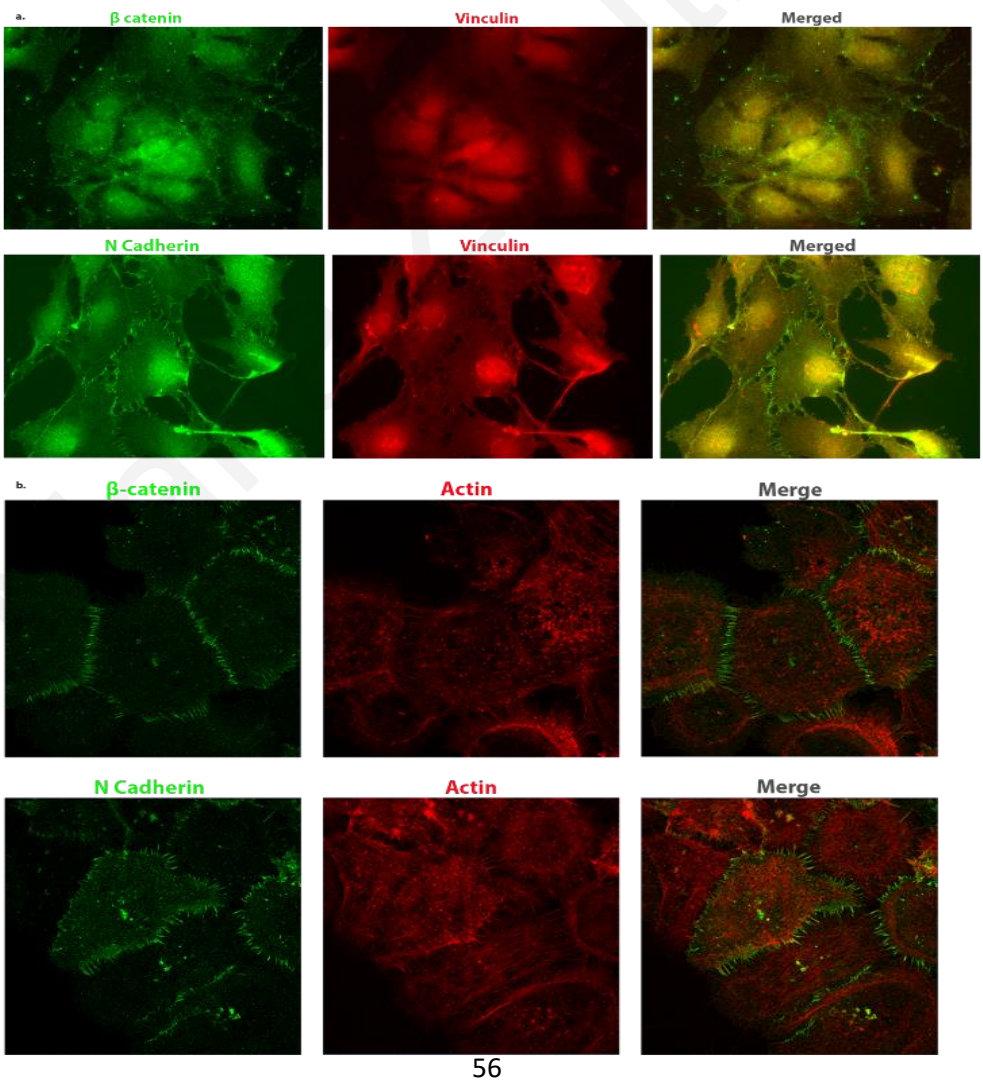

(B)

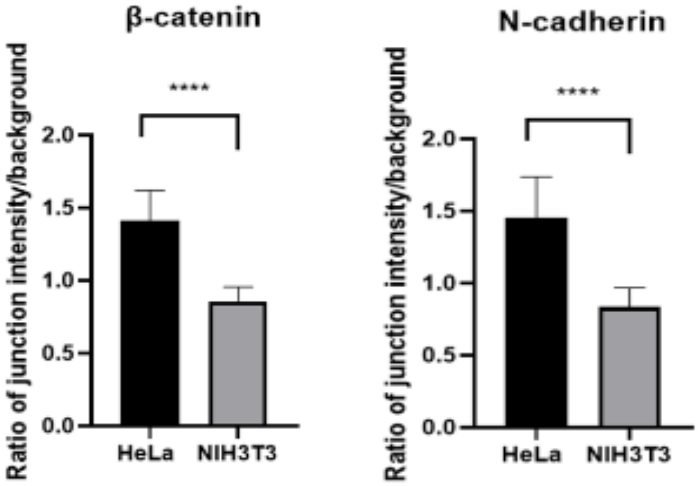

Figure 19. HeLa cells form stronger and larger AJs compared to NIH3T3 cells

(A) (a) Images of NIH3T3 cells stained against β-catenin and N-cadherin, respectively, showed minimal enrichment of both components at the AJs

(b) Images of HeLa cells stained against β-catenin and N-cadherin, respectively, showed strong enrichment of both components at the AJs

(B) Quantification of junction/background mean intensity ratio from β-catenin positive AJs and N-cadherin positive AJs of NIH3T3 and HeLa cells, from a two-tailed unpaired t-test. Error bars represent S.E.M. The mean intensity of β-catenin in HeLa cells is 1,411±0,07233, n=15 and in NIH3T3 cells is 0,8589±0,07233, n=15. The mean intensity of N-cadherin in HeLa cells is 1,455±0,08957, n=18 and in NIH3T3 cells is 0,8364±0,08957, n=18. n, number of AJs measured from three independent experiments.

6.2 Preferential accumulation of high ligand affinity receptors on AJs guides the selective binding of FN-YPet on cell-cell contacts

As mentioned in the introduction, unpublished work from our lab has revealed that AJs can regulate the spatial distribution and activation of integrins in the absence of ECM ligands (Hadjisavva et al., Cell Reports-under revision). Therefore, increased tension at the cell-cell junction sites results in the creation of high ligand affinity extended integrin pools and given the fact that the formation of fibrils relies on increased tension and the presence of AJs, we hypothesized that AJ-driven activation and distribution of integrins could spatially influence ligand binding on the cell surface. We thus wanted to examine if integrin activation driven by AJ-generated tension can spatially guide ECM ligand binding. For this purpose, we initially used N-cadherin Fc substrates, on which cells spread through the formation of linear AJs in contact with the glass, formed through the interaction of the cell's cadherins with the cadherins grafted onto the glass surface, as shown in **Figure 20A**. Specifically, we seeded HeLa cells on N-cadherin Fc substrate until integrin activation was detected at AJs and introduced externally FN-YPet to cells. Immunofluorescence experiment was carried out using antibodies against β-catenin and active integrin β1, followed by imaging of the AJs using super-resolution microscopy. As shown in **Figure 20B**, FN preferentially accumulated at the β1-integrin positive linear AJs. Additional analysis of these data with the generation of intensity profiles perpendicular to the adhesions revealed that there was enrichment of FN, β-catenin, and active integrin β1 on each linear AJ. This experiment clearly showed that, AJs can spatially guide integrin activation, which have high affinity for ligands and can promote the enrichment of soluble ligands at the AJs. These results show that AJs can influence ligand binding on the cell surface via the creation of localized high ligand affinity pools of integrins.

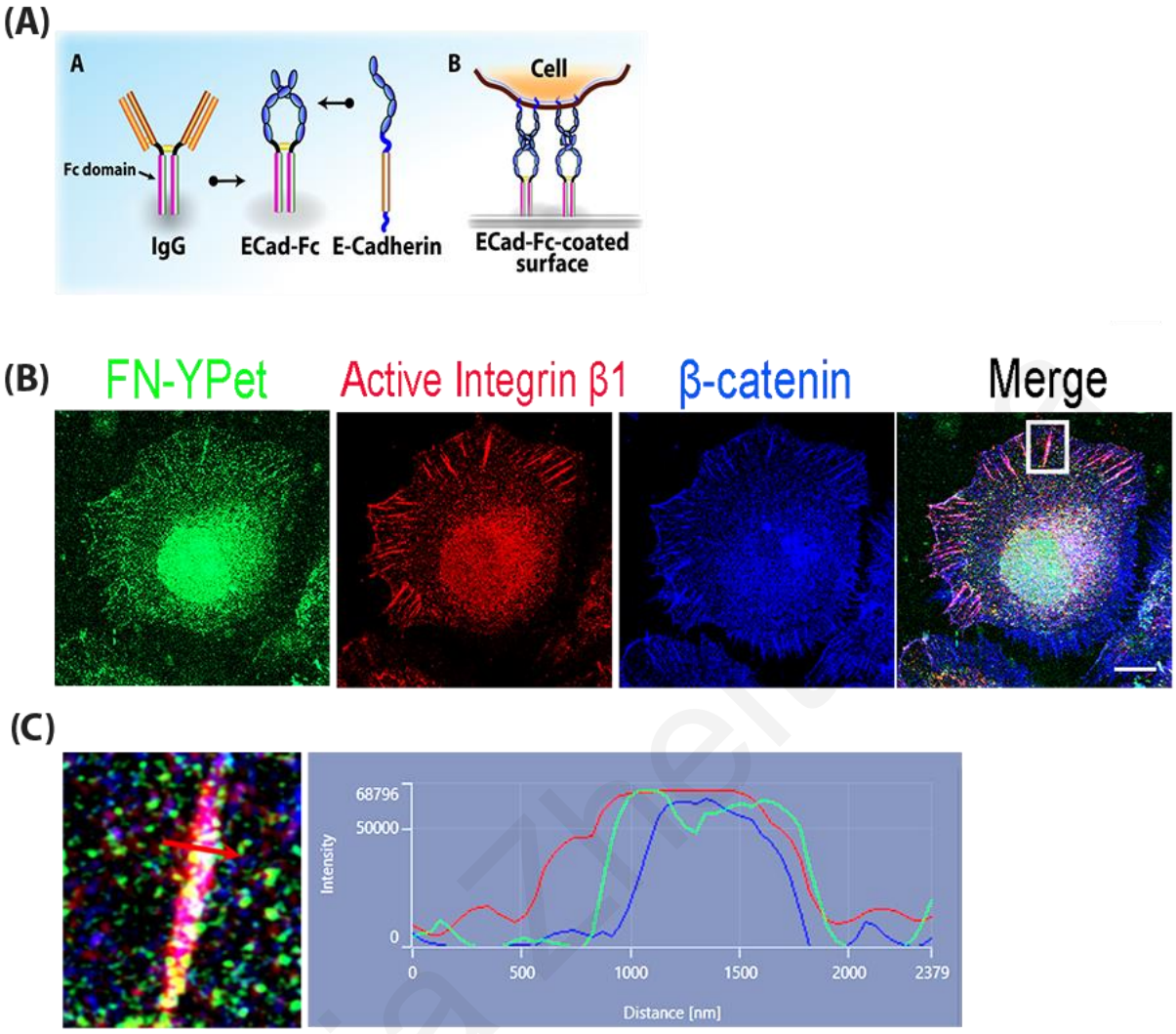

Figure 20. Preferential accumulation of FN at β1 positive linear AJs

(A) Schematic representation of N-cadherin Fc substrate (Adapted from Nag et al., 2014).

(B) Confocal images of HeLa cell spread on N-cadherin Fc were fixed at 60 minutes upon the introduction of soluble FN-YPet in the medium and stained for β-catenin and active integrin β1.

(C) Intensity profile generated perpendicular to the FN-YPet positive AJ, revealed that FN is sharing the same area within the adhesion as β-catenin and active integrin β1.

However, given the artificial nature of the AJs generated by cells attached on Fc coated glass coverslips, we went on to examine whether preferential ligand accumulation would take place in a more physiologically relevant condition. Cells in suspension can form cell doublets which can form ring like AJs between their contact area. AJs between cell doublets were previously shown to be positive for both cadherin and active integrin β1, clustered at the rim of the contact area of two cells (Hadjisavva et al., Cell Reports-under revision). In order to address this, cells incubated with soluble FN-YPet were allowed to form doublets for 20 minutes, fixed, and stained for antibody against N-cadherin. As shown, we observed a clear FN accumulation at the AJ between the two cells, suggesting that cell-cell adhesion elicits integrin activation which then spatially guides FN binding, in agreement with what we observed on glass Cadherin substrates (**Figure 21A**). A 3D reconstruction of the doublet clearly showed the accumulation of FN along the circular AJ formed between the two cells (**Figure 21B**). Similarly, cells attached on charged glass substrate in the presence of FN-YPet, also display selective accumulation of FN at the N-cadherin positive cell-cell contact regions, further confirming that AJs spatially influence ligand-binding on the cell surface via controlling integrin distribution and activity (**Figure 21C**).

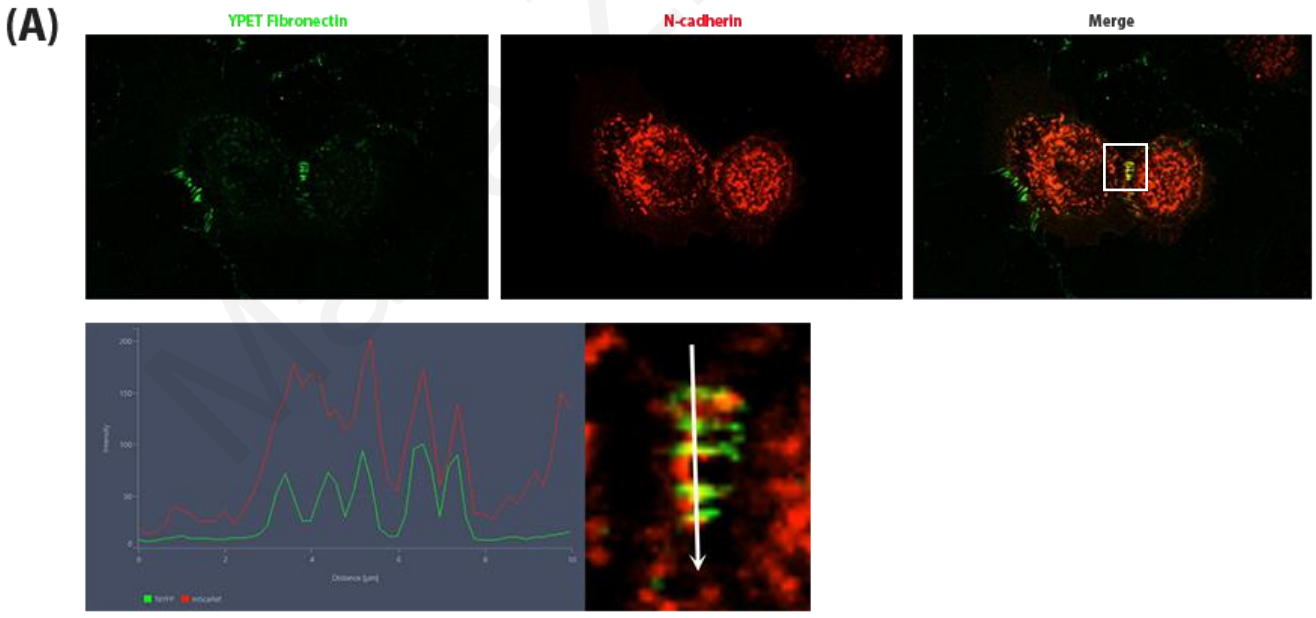

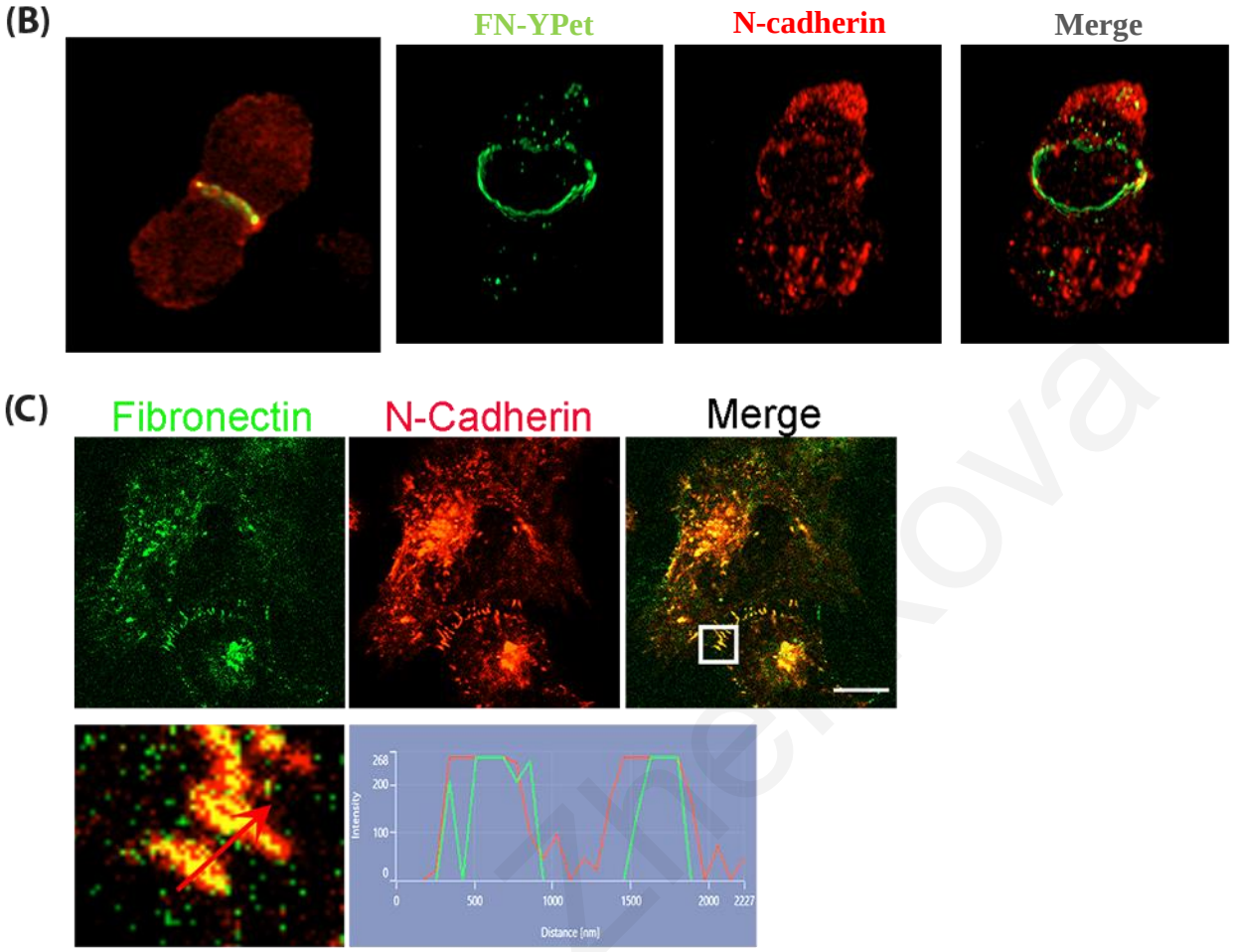

Figure 21. FN is selectively enriched at the cadherin positive cell-cell contact sites

(A) Confocal images of a cell doublet incubated with soluble FN-YPet, fixed and stained against N-cadherin showed the recruitment of FN at cell-cell junction sites.

(B) 3D rendering images of cell doublet showed clear FN accumulation at the cadherin positive ring formed between the two cells.

(C) Confocal images of cells seeded on charged glass substrate in the presence of soluble FN-YPet showed the preferential ligand accumulation at AJs. Profile was generated perpendicular to two AJs at cell-cell contact.

6.3 Use of conformational-specific integrin antibodies revealed the sequence of events taking place at the integrin positive cell-cell junctions

After showing the selective accumulation of FN at integrin positive cell-cell junctions, we went on to determine the sequence of events taking place at those sites. Specifically, we went on to examine whether activated integrins are localized at AJs prior to the sequestering of ligands at the junction, as we hypothesized. In order to achieve this, we took advantage of the well-characterized monoclonal antibodies against β1, specific for the extended, closed, and open headpiece conformational states. As mentioned in the introduction, integrins display at least three distinct conformational states correlated with the ligand affinity of the receptor. The bent-closed and extended-closed conformational states, which are ligand-free, and the extended-open conformation which is the ligand-bound conformational state. During integrin activation, the bend low-affinity state undergoes reversible conformational changes to increase ligand affinity, by completely extending the extracellular domains and separating the cytoplasmic domains resulting in an extended high-affinity receptor (Xiong et al., 2001; Takagi et al., 2002). Hence, in order to examine the exact conformation of the receptor during cell doublet formation, cell doublets were fixed at two distinct time points, at an early time point (30 minutes) without serum and at a late time point (1 hour) of which serum was supplemented after 30 minutes, and were stained for extended conformation-specific antibodies (9EG7 or HUTS21), closed-headpiece specific antibody (mAb13), open-headpiece specific antibody (12G10), AJ marker (N-cadherin or β-catenin) and FN. As shown in **Figure 22A**, at the early time point in serum-free conditions, the extended conformation-specific antibodies 9EG7 and HUTS21 were detected at the cell-cell contact areas together with the closed-headpiece specific antibody mAb13, while no FN or open-headpiece specific antibody staining were observed at that time point, suggesting that receptors with extended closed-head conformation are recruited first at the cell-cell junctions. Within 60 minutes after switching to serum-containing media, open-headpiece-specific antibody 12G10 and FN were observed at the cadherin positive cell-cell junction together with the extended conformation-specific antibody 9EG7 (**Figure 22B**). Collectively, these data revealed that integrin receptors with extended closed-headpiece conformation are recruited first at the cell-cell junctions and then preferentially guide ligand accumulation there, further supporting our initial hypothesis. Notably, the above results are in agreement with what has been shown recently by our group, when

they characterized the integrin conformational state at the linear AJs on Fc substrates (Hadjisavva et al., Cell Reports-under revision).

(A)

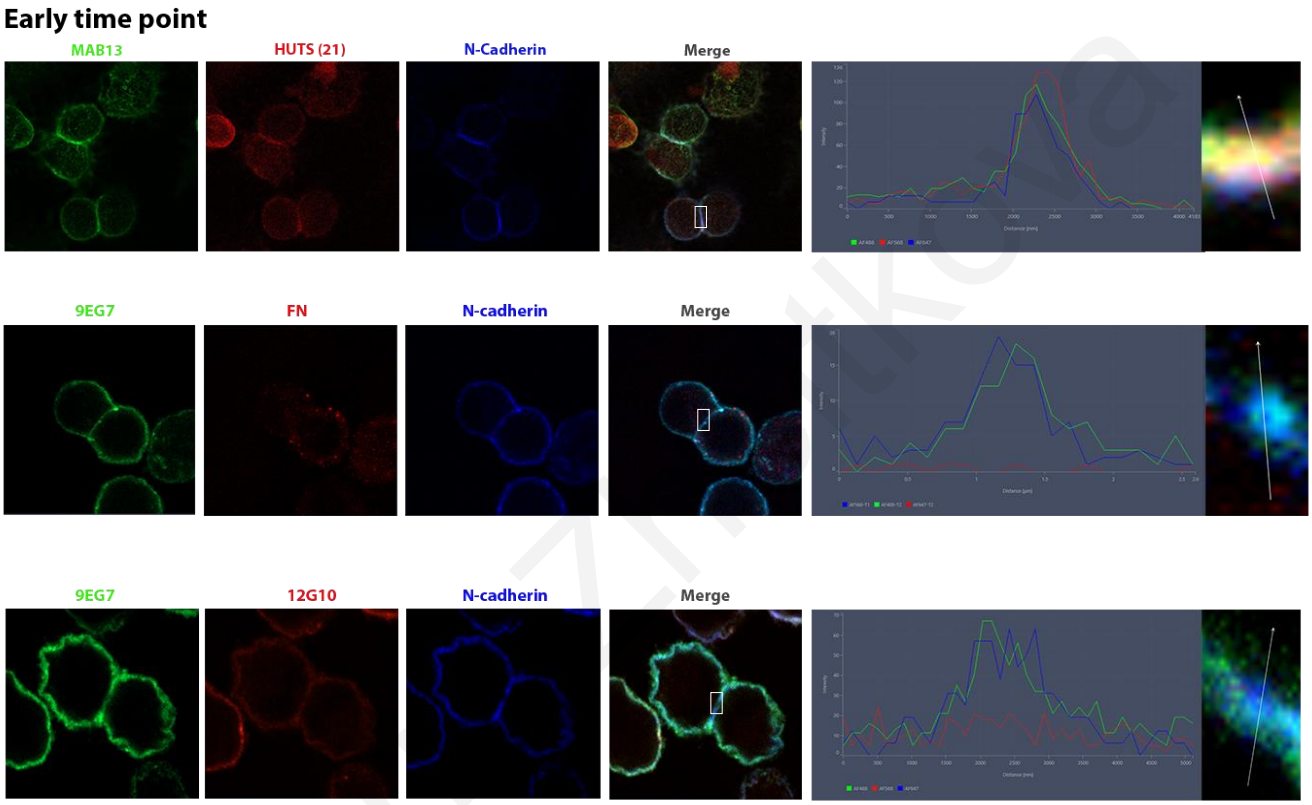

(B)

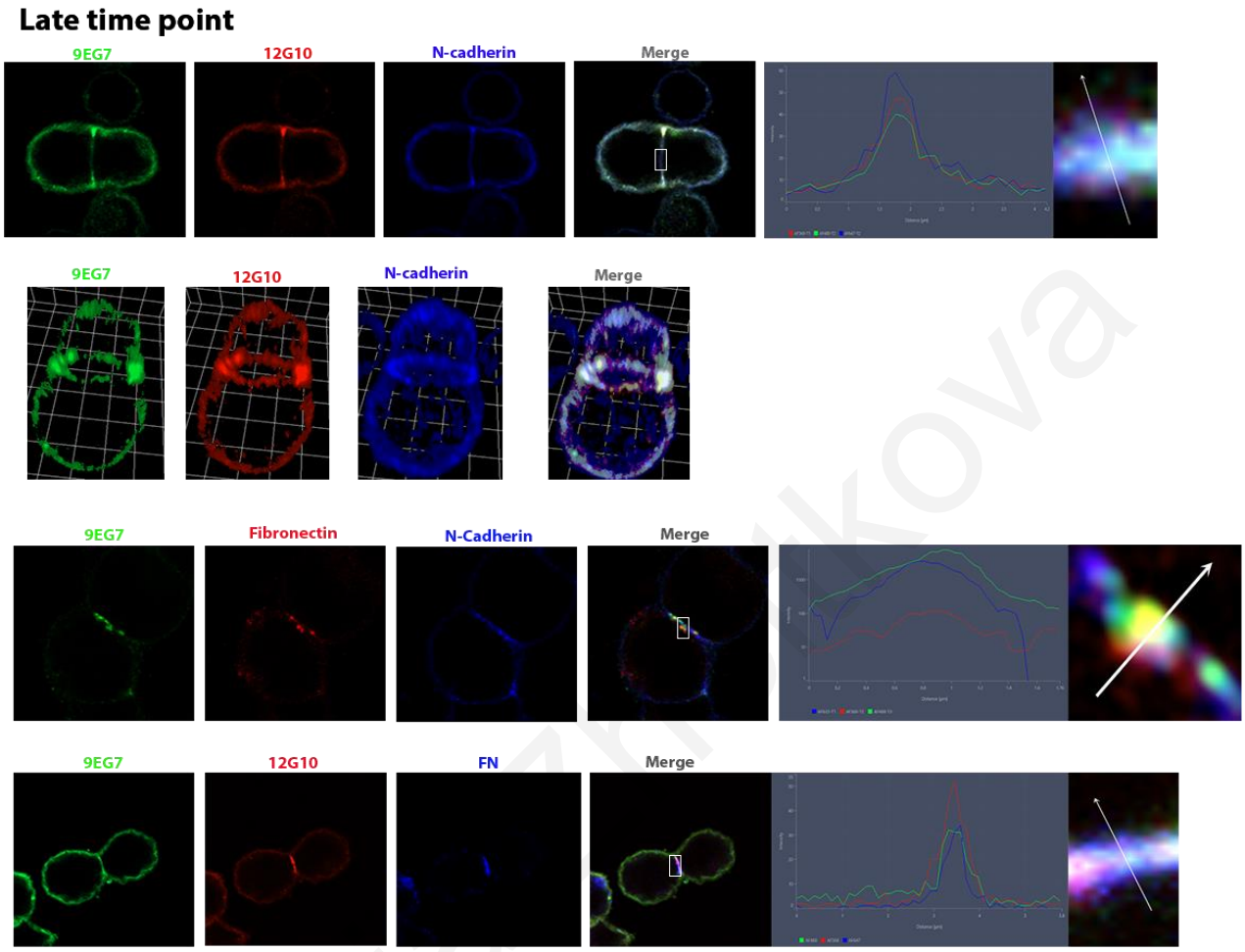

(C)

	Close headpiece mAb13	Open headpiece 12G10	Extended 9EG7, HUTS21
Early time point	+		+
Late time point		+	+

Figure 22. Selective FN accumulation is achieved via the AJ-driven activation and recruitment of closed-headpiece extended conformation integrins at the cell-cell junction sites

(A) Confocal images of cell doublets in serum-free conditions, fixed at 30 minutes and stained for FN, N-cadherin, and several conformational specific integrin antibodies. Intensity profiles were made perpendicular to the AJs. At an early time point, only closed-headpiece-specific and extended-specific antibodies were observed.

(B) Confocal images of cell doublets in media supplemented with serum, fixed at 60 minutes and stained for FN, N-cadherin, and several conformational specific integrin antibodies. Intensity profiles were made perpendicular to the AJs. At a late time point, open-headpiece-specific antibody, extended antibody, and FN were observed at the cell-cell contact sites. 3D rendering image of a cell-doublet clearly showed the co-localization of the extended-specific and open-headpiece-specific antibodies on the cadherin positive circular AJ.

(C) Table summarizing the appearance of the different conformation-specific integrin antibodies.

6.4 Talin and contractile force are involved in the ligand accumulation at cell-cell contacts

After the characterization of the sequence of events taking place at cell-cell junctions, concerning the order of appearance of the conformational states of integrins and ligand enrichment, our results so far supported that cadherin-based interactions influence integrin distribution and activation, creating pools of receptors with extended closed headpiece conformation, that guide selectively FN accumulation at those sites. Therefore, this brought up the question of how these high-ligand affinity integrins are stabilized in their extended conformation in those regions at early time points, in the absence of ligand presence. Several studies suggested that plasma membrane tension (PM) elicits integrin activation in the absence of ligands in a variety of contexts (Ferraris et al.,2014; Petridou and Skourides, 2016), with the more recent one showing that physical events deforming the cell membrane structure, including stretch, shear stress, or osmotic pressure, can induce integrin activation via disrupting the association of the integrin transmembrane domains (Kim et al.,2020). Interestingly, unpublished data from our lab revealed that integrin activation and

clustering at AJs are dependent on AJ-generated tension, since AJs are regions of high intrinsic tension when coupled to the actin contractile cytoskeleton (Hadjisavva etl., Cell Reports-under revision). It is well documented that Talin links integrins directly to the actin cytoskeleton, strengthening their activation and increasing their affinity for ligands via the transmission of actin-mediated forces (Klapholz and Brown, 2017). Therefore, it was proposed that AJ-generated tension leads to the accumulation of extended integrin receptors which can interact with Talin and thus with the actin cytoskeleton resulting in the stabilization of their extended state (Hadjisavva et al., Cell Reports-under revision). However, those experiments were performed using an artificial system, where cells were seeded on cadherin Fc coated substrates.

Thus, we went on to investigate if these pools of extended integrin receptors at the cell-cell contact area of doublets are dependent on Talin and subsequently on contractile force. In an effort to address this, we initially used both Talin KO and Talin-YPet reconstituted cell lines, which were allowed to generate doublets for 45 minutes in serum-free conditions, fixed, and stained for antibodies against N-cadherin and active integrin β1. As shown in **Figure 23A**, no active integrin β1 can be detected in association with N-cadherin at the cell-cell contact area of Talin KO cells, compared to the Talin-YPet reconstituted doublets, which showed a clear accumulation of active integrin at the Talin-positive cell-cell junction. To further confirm our hypothesis, we repeated the experiment in serum-containing media staining against N-cadherin and FN. As expected, we observed FN accumulation on the Talin positive cell-cell contacts of Talin reconstituted doublets, in comparison with Talin KO doublets that showed nonspecific recruitment of FN along the cell surface with no correlation between FN and N-cadherin (**Figure 23B**). These data conclusively showed that preferential accumulation of ligands at cell-cell junctions is due to the recruitment and stabilization of extended conformational state integrins at those sites by Talin.

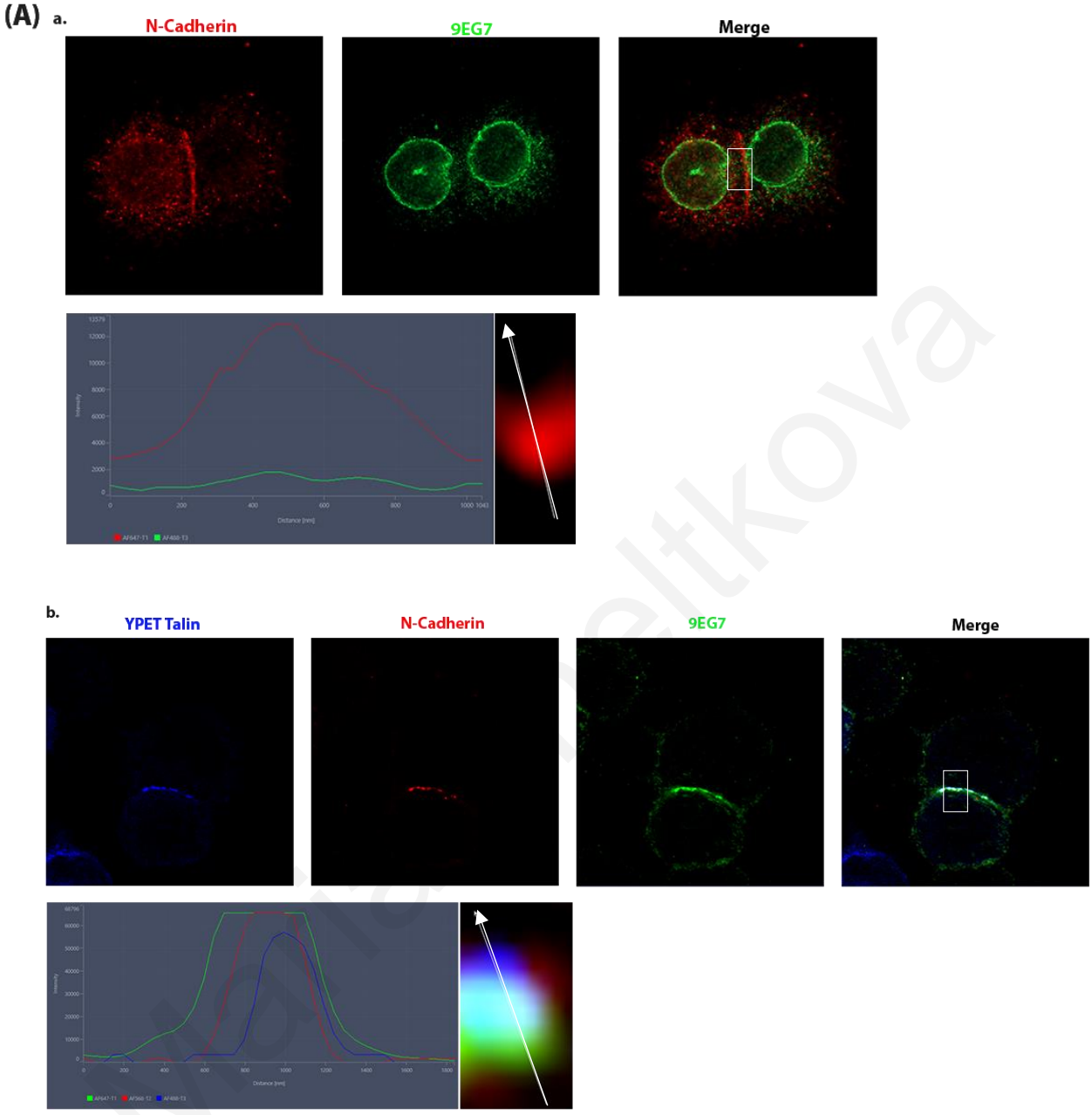

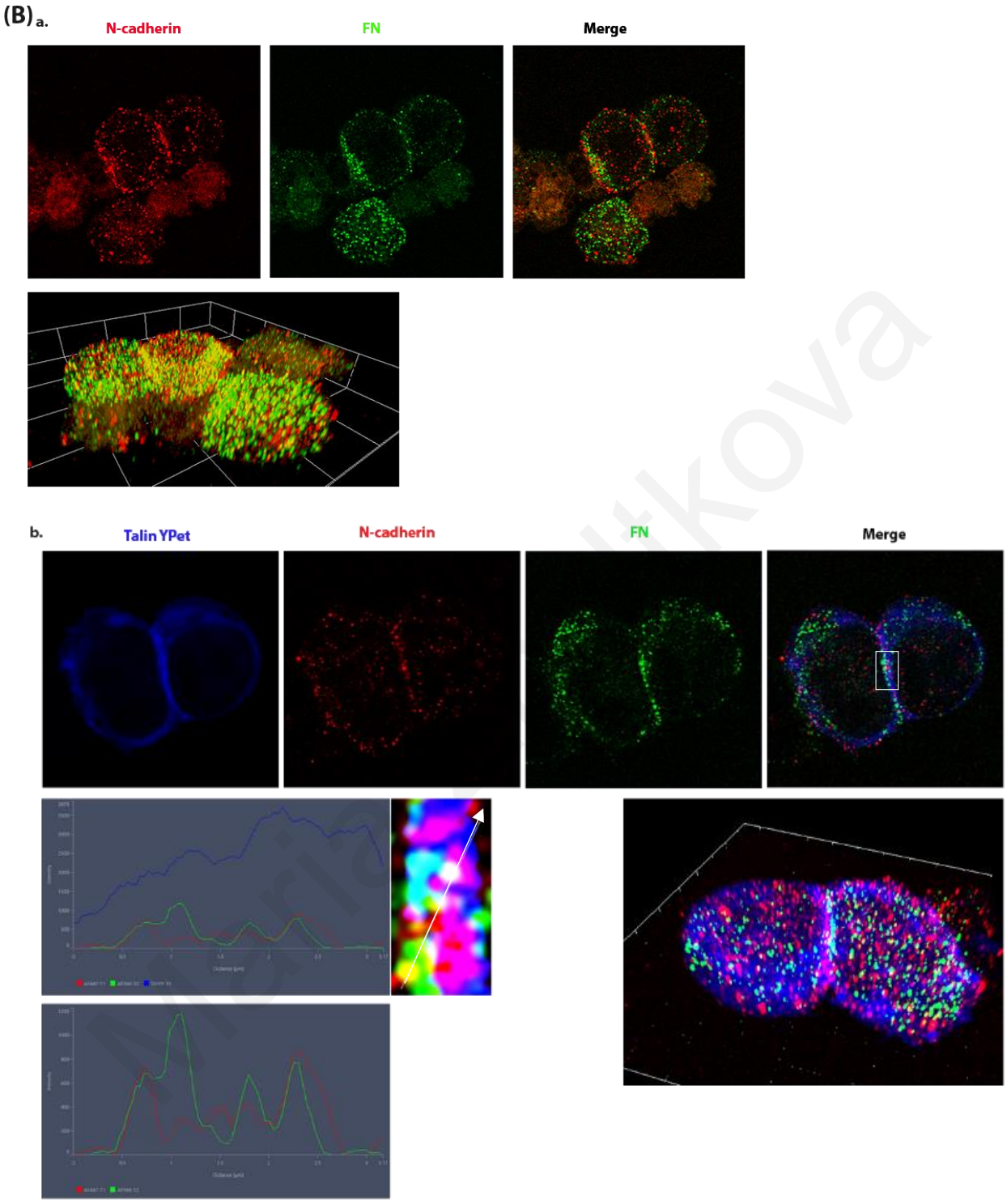
(B) a.
N-cadherin
FN
Merge
b.
Talin YPet
N-cadherin
FN
Merge

Figure 23. FN accumulation on cell-cell junction sites is strictly dependent on Talin

(A) (a) Confocal images of Talin KO cell doublet fixed and stained against N-cadherin and active integrin β1 showed a cell-cell contact site negative for active integrin β1 suggesting that Talin is essential for the stabilization of integrins at those sites. Intensity profile generated perpendicular to the AJ showed that no integrin activation is detected at those sites.

(b) Confocal images of Talin-YPet reconstituted cell doublet fixed and stained against N-cadherin and active integrin β1 showed clear recruitment of active integrin β1 at the Talin positive cell-cell contact. Profile generated perpendicular to the AJ revealed that active integrin β1 is co-localized at AJs enriched with N-cadherin and Talin.

(B) (a) Confocal images of Talin KO cell doublet fixed and stained against N-cadherin and FN showed no FN accumulation correlated with cell-cell junctions. 3D rendering image of the cell-doublet showed clearly the distribution of FN along the whole cell surface without any correlation with cell-cell contact sites.

(b) Confocal images of Talin-YPet reconstituted cell doublet fixed and stained against N-cadherin and FN showed the preferential accumulation of FN at the cell-cell junction sites positive for both N-cadherin and Talin, revealing the crucial role of Talin for FN accumulation at those sites. Intensity profile generated perpendicular to the AJ and a 3D rendering image of the cell-doublet showed that FN is recruited selectively at the cell-cell junction.

In an effort to directly address the role of contractile force on AJ-driven integrin activation and ligand accumulation we treated cells with a ROCK inhibitor (Rho-kinase inhibitor Y-27632) to reduce contractility. Cells were allowed to form doublets for 20 minutes in media containing FN-YPet and then treated with the ROCK inhibitor for 15 minutes before fixation. Immunofluorescence experiments were carried out using antibodies against N-cadherin and Vinculin. Vinculin staining was used as a reference for reduced contractility since it is known that Vinculin interacts with Talin stabilizing the Talin-F-actin interactions and it was expected to be reduced by the ROCK inhibitor (Humphries et al., 2007). As expected, upon treatment, Vinculin

is lost from the cell-cell junction compared to the untreated doublet, confirming reduced contractility (**Figure 24A**). As shown in **Figure 24B**, FN localization on cell-cell contact sites is lost, upon the addition of ROCK, confirming that AJ-generated tension plays an essential role in the stabilization of the extended state of integrins receptors and therefore accumulation and binding of FN.

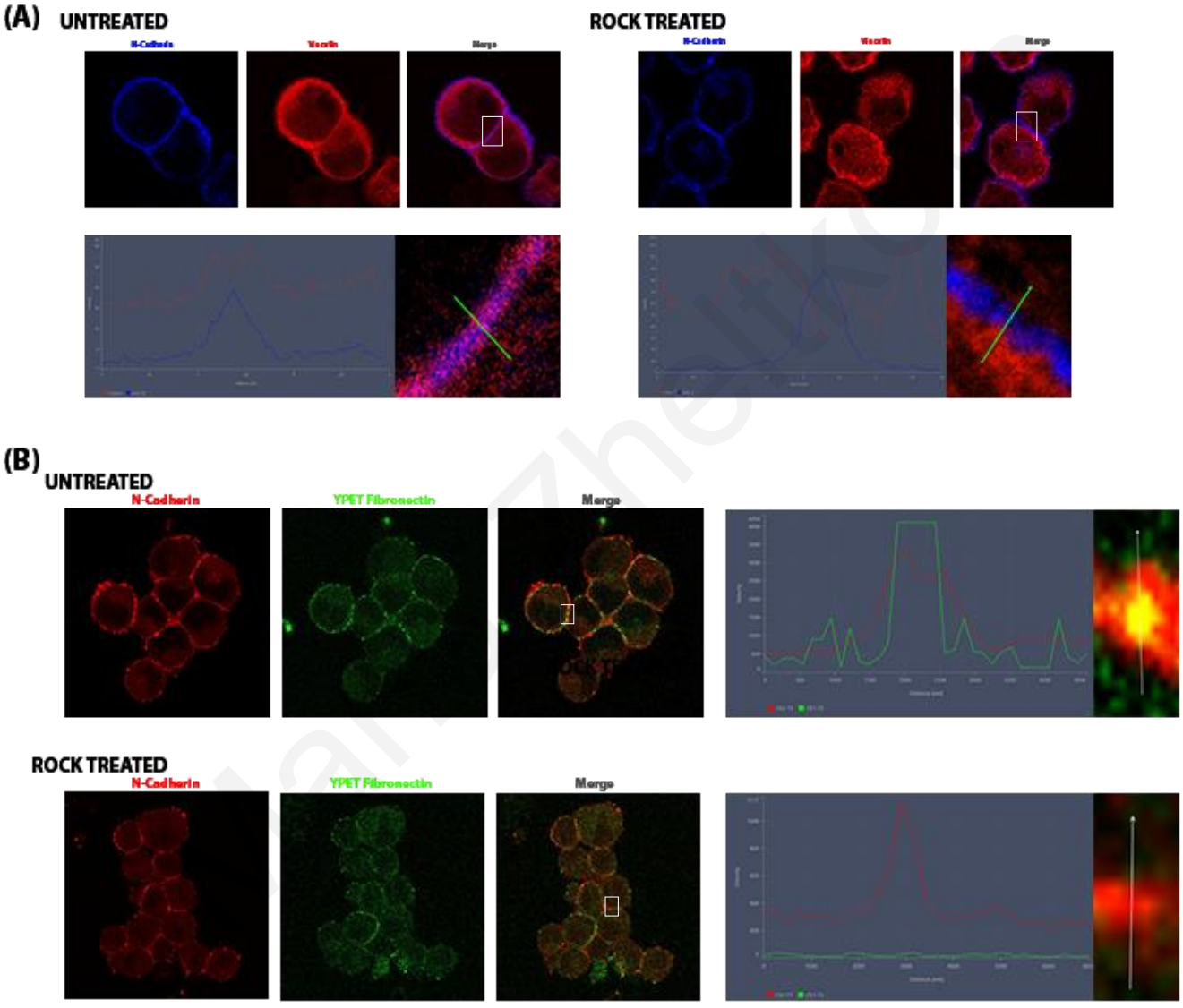

Figure 24. Selective recruitment of FN on cell-cell junctions is dependent on contractile force

(A) Confocal images of cell doublets fixed upon treatment with ROCK inhibitor for 15 minutes and stained for N-cadherin and Vinculin revealed that contractility is reduced at the AJs since Vinculin is lost. Profiles generated perpendicular to the AJ showed a clear loss of Vinculin from AJs, compared to the untreated cell doublet.

(B) Confocal images of multi doublet cells incubated with soluble FN-YPet and treated for 15 minutes with the ROCK inhibitor, were fixed and stained against N-cadherin. Upon contractility reduction, no FN accumulation is detected on cell-cell junctions suggesting that the contractile force is necessary for integrin stabilization at those sites. Profile generated perpendicular to the AJ revealed that upon contractility reduction the co-localization of FN at the AJ with N-cadherin is lost.

6.5 AJ modulation reveals the role of AJs in ECM formation and FN fibrillogenesis

6.5.1 Reduction of Calcium levels results in stronger and denser fibrillar formation

We have so far shown that the preferential recruitment of ligands at cell-cell junctions is due to the AJ-driven distribution and activation of extended conformation integrins at these sites, which are stabilized in that conformational state via Talin and actin contractility. We went on to directly explore the role of AJs in ECM formation and FN fibrillogenesis by modulating AJs using various approaches. As a first option, we sought to reduce calcium levels, given the fact that calcium is essential for AJ formation, and in the absence or even in low levels of calcium cadherins undergo conformational changes that lead to AJ disruption (Pokutta et al., 1994). For this purpose, we cultured both HeLa and NIH3T3 cells for 12 hours in Calcium free media, and as a control, cells that were cultured for 12 hours in media with Calcium Chloride were used. Should be noted that these are not calcium-free conditions since despite using calcium-free DMEM the media contained serum that does contain calcium. After fixation, we stained cells with antibodies against FN and actin. Same experiments were done in parallel using an antibody against N-Cadherin to ensure that calcium reduction resulted in weaker AJs since both Fibronectin and N-Cadherin primary

antibodies were the same species and couldn't be used simultaneously in one experiment (**Figure 25A**). Surprisingly, we observed increased fibrillogenesis with more dense fibrils generated by cells cultured without calcium (**Figure 25B**). Analysis of the outcomes by quantifying the average fibril intensity between cells cultured with and without calcium revealed that calcium reduction led to a 4.5-fold and 2.5-fold increase in fibril signal intensity in HeLa and NIH3T3 cells respectively, further confirming our observations (**Figure 25C**). A possible explanation for this would be that by reducing calcium levels we not only affect AJs, but we may promote integrin activation as well. As mentioned in the Introduction, integrins can interact with calcium through the divalent-cation-binding domains on their extracellular subunits (Alberts et al., 2002). Notably, several studies suggested that calcium can either suppress or enhance the binding ability of integrin receptors to regulate cell behavior (Santoro et al., 1986; Kirchhofer et al., 1991). However, removal of Ca2+ or addition of Mn2+ does increase ligand binding affinity and adhesiveness of almost all integrins (Zhang and Chen, 2012). Therefore, in this case, calcium may act as a negative regulator of integrin activity, and by reducing its levels we are promoting integrin activation. Conclusively, this approach generated data that are hard to interpret, since calcium is probably modulating the function of both AJs and integrin receptors. However, this needs to be further investigated and the effects of calcium on FN fibrillogenesis need to be examined since the effect of calcium levels of FN fibrillogenesis is dramatic and has not been previously reported.

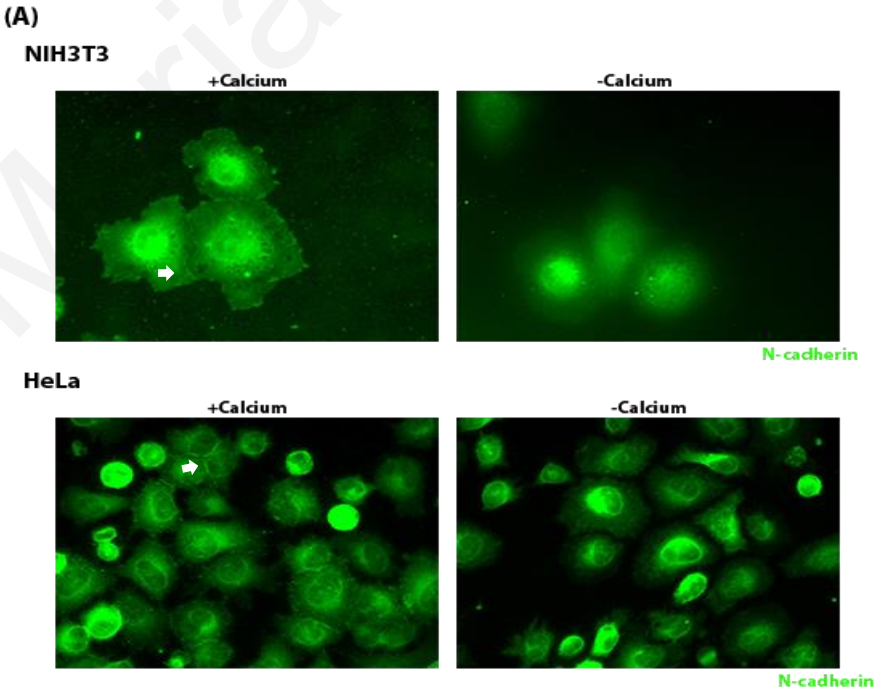

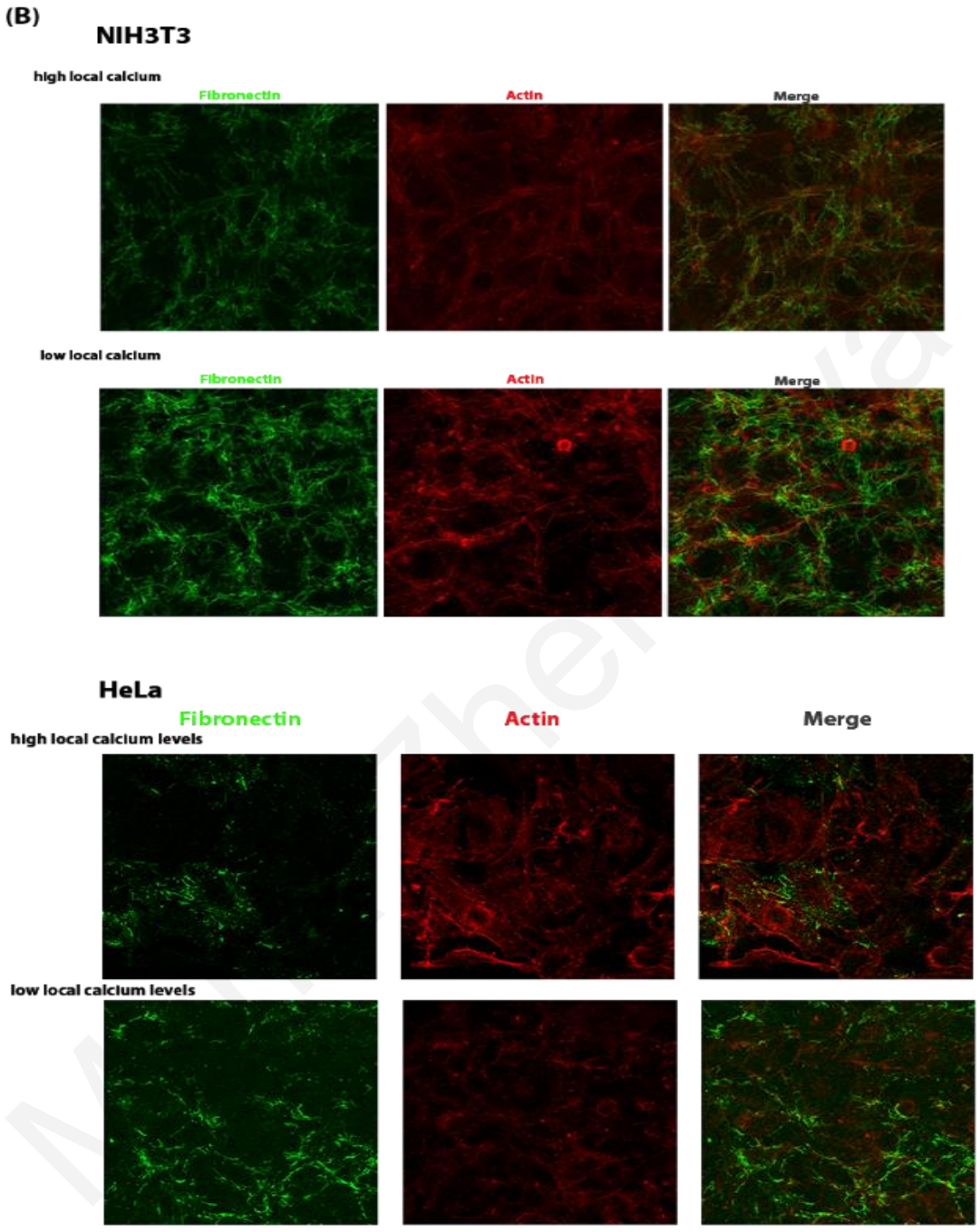
(B)
NIH3T3
high local calcium
Fibronectin
Actin
Merge
low local calcium
Fibronectin
Actin
Merge
HeLa
Fibronectin
Actin
Merge
high local calcium levels
low local calcium levels

(C)

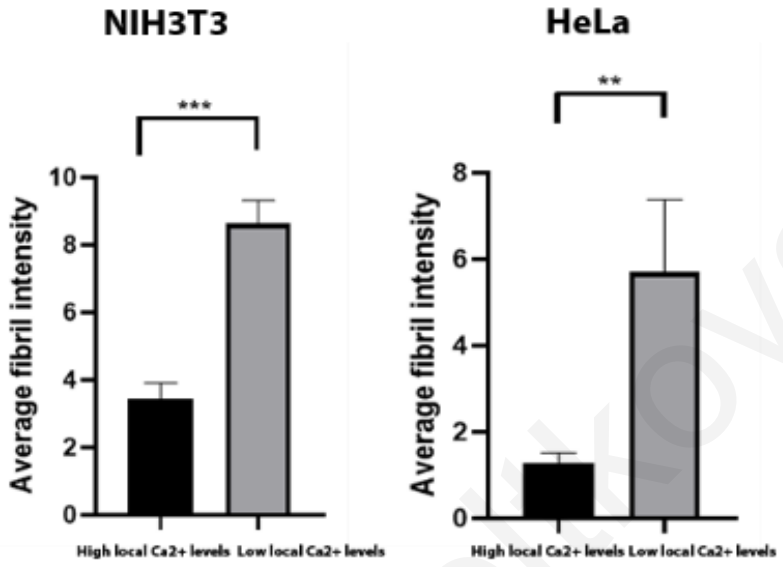

Figure 25. Reduction of calcium levels leads to the formation of more dense fibrils in both NIH3T3 and HeLa cells

(A) Images of NIH3T3 and HeLa cells cultured for 12 hours in calcium-free and calcium-plus conditions, fixed, and stained against N-cadherin, were used as a control to ensure that AJ formation would be reduced upon the reduction of calcium.

(B) Confocal images of NIH3T3 and HeLa cells respectively, cultured for 12 hours in calcium-free and calcium-plus conditions were fixed and stained against FN and actin. Both cell lines display stronger fibrillar assembly upon the reduction of calcium.

(C) Quantification of average fibril intensity from cells cultured in calcium-free and calcium-plus conditions, from a two-tailed unpaired t-test. Error bars represent S.E.M. The mean intensity of fibrils in NIH3T3 cells in calcium-plus conditions is 3,440±0,4733, n=6, and in calcium-free conditions is 8,636±0,4733, n=6. The mean intensity of fibrils in HeLa cells in calcium-plus conditions is 1,291±0,8378, n=9, and in calcium-free conditions is 5,716±0,8378, n=9. n, number of regions measured in two independent experiments.

6.5.2 Expression of a function-blocking cadherin mutant leads to the elimination of both ligand binding on the cell surface and FN fibril formation

Modulation of Calcium ion levels failed to provide a clear understanding on the role of AJs on FN fibril formation. For this reason, we went on to explore an alternative approach to modulate AJ function in a more specific manner. We decided to use a Cadherin mutant that lacks the cytoplasmic domain, known as N-cadherin ΔCP. This mutant can effectively interact with other cadherins via the extracellular domain; however, it cannot interact with the actin cytoskeleton and thus fails to cluster (**Figure 26A**). Work by Hadjisavva et al., has also shown that expression of this mutant suppresses AJ-driven integrin activation. Importantly, expression of this mutant does not eliminate cell-cell attachment and thus does not eliminate force application between cells (Hadjisavva et al., Cell Reports-under revision). Control cells and cells expressing N-cadherin ΔCP were allowed to form doublets for 20 minutes, fixed, and stained against active integrin β1 and FN. As shown in **Figure 26B**, both active integrin β1 and FN were not detected in expressor doublet cells, compared to the controls, where recruitment of active integrin and FN accumulation were observed in the cell-cell contact area. Intensity profiles made perpendicular to the AJ and quantification of FN intensity in control and expressor cells further confirmed that the expression of the N-cadherin ΔCP mutant suppresses integrin activation and thus eliminates ligand accumulation and fibril formation at the cell-cell junction (**Figure 26C**). These data suggested that FN accumulation at cell-cell contact sites is governed by the AJ-generated tension through the activation and clustering of integrin receptors at these sites.

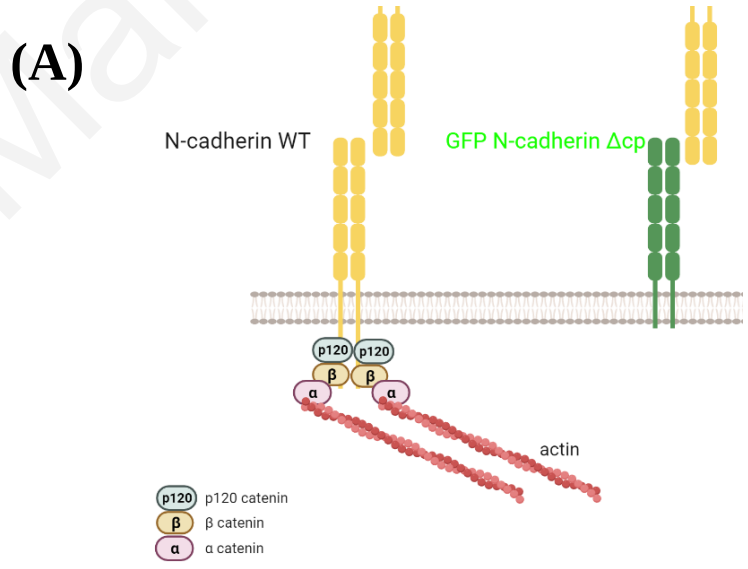

(B)

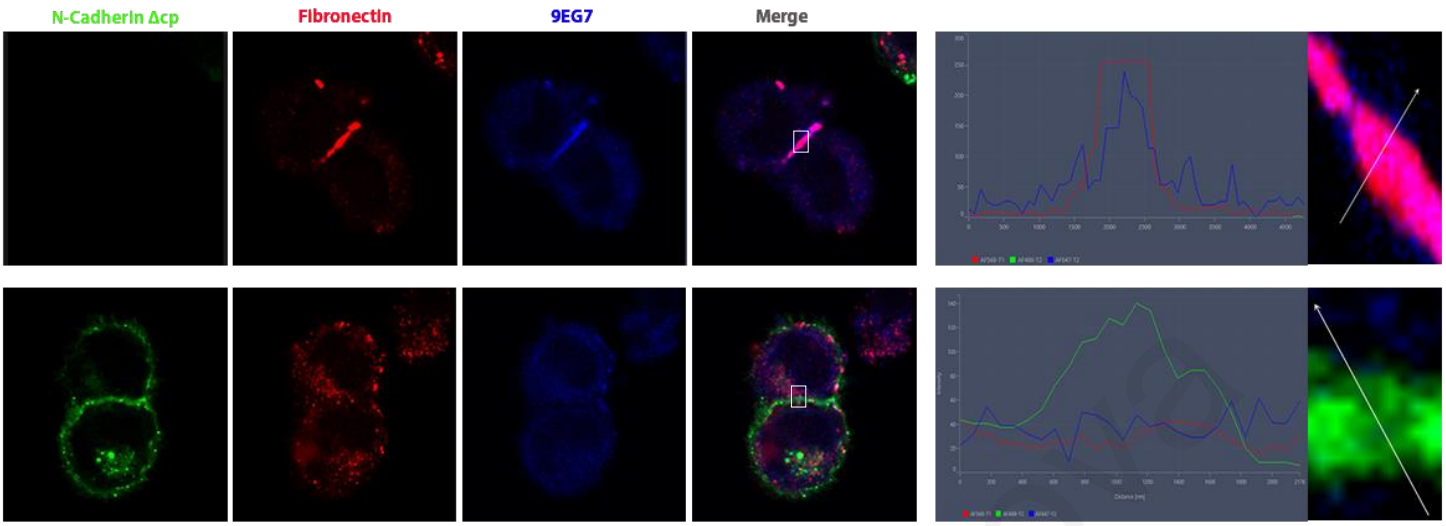

(C)

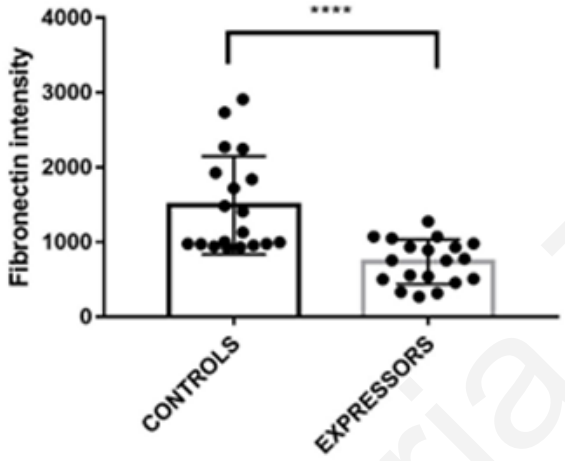

Figure 26. Expression of N-cadherin Δcp mutant results in suppression of integrin β1 recruitment at the cell-cell contact site and consequently of FN accumulation

(A) Schematic representation of N-cadherin WT and Δcp mutant structures. Scheme made by online program Biorender.org

(B) Confocal images of a control cell doublet and a doublet expressing N-cadherin Δcp revealed that FN accumulation is not detected at cell-cell junctions upon the expression of the mutant, suggesting that AJs are essential for the selective accumulation of FN via the recruitment of active

integrins at cell-cell contact sites. Profiles generated perpendicular to the AJs revealed that upon mutant expression FN is not detected at the AJ compared to the control doublet.

(A) Quantification of the distribution of FN intensity between control and N-cadherin Δcp expressing cells, from a two-tailed unpaired t-test. Error bars represent S.E.M. The mean intensity in control cells is 1449±150,4, n=19 and in expressors is 737,5± 69,09, n=19. n, number of doublets measured from three independent experiments.

The above results show that we have established a reliable approach to address the input of AJ-driven integrin activation and the resulting spatial guidance of ligand binding on the cell surface in a manner that does not impact focal adhesion-based fibrillogenesis. In an effort to address the impact of AJs in the fibrillar matrix assembly and remodeling, NIH3T3 cells were transfected with the N-cadherin ΔCP mutant and N-cadherin W.T. respectively, cultured for 12 hours, fixed, and stained against FN. Interestingly, cells expressing the mutant displayed a significantly reduced capacity to form fibrils, compared to cells expressing the WT protein (**Figure 27A**). Quantification of the average fibril intensity revealed that N-cadherin ΔCP expression led to a 1.5-fold reduction in the average fibril intensity in ΔCP expressors, confirming that N-cadherin ΔCP mutant suppresses fibril formation (**Figure 27B**). These data show that AJs have a major impact not only on determining the ligand binding on the cell surface but also in the generation and remodeling of the complex fibrillar network.

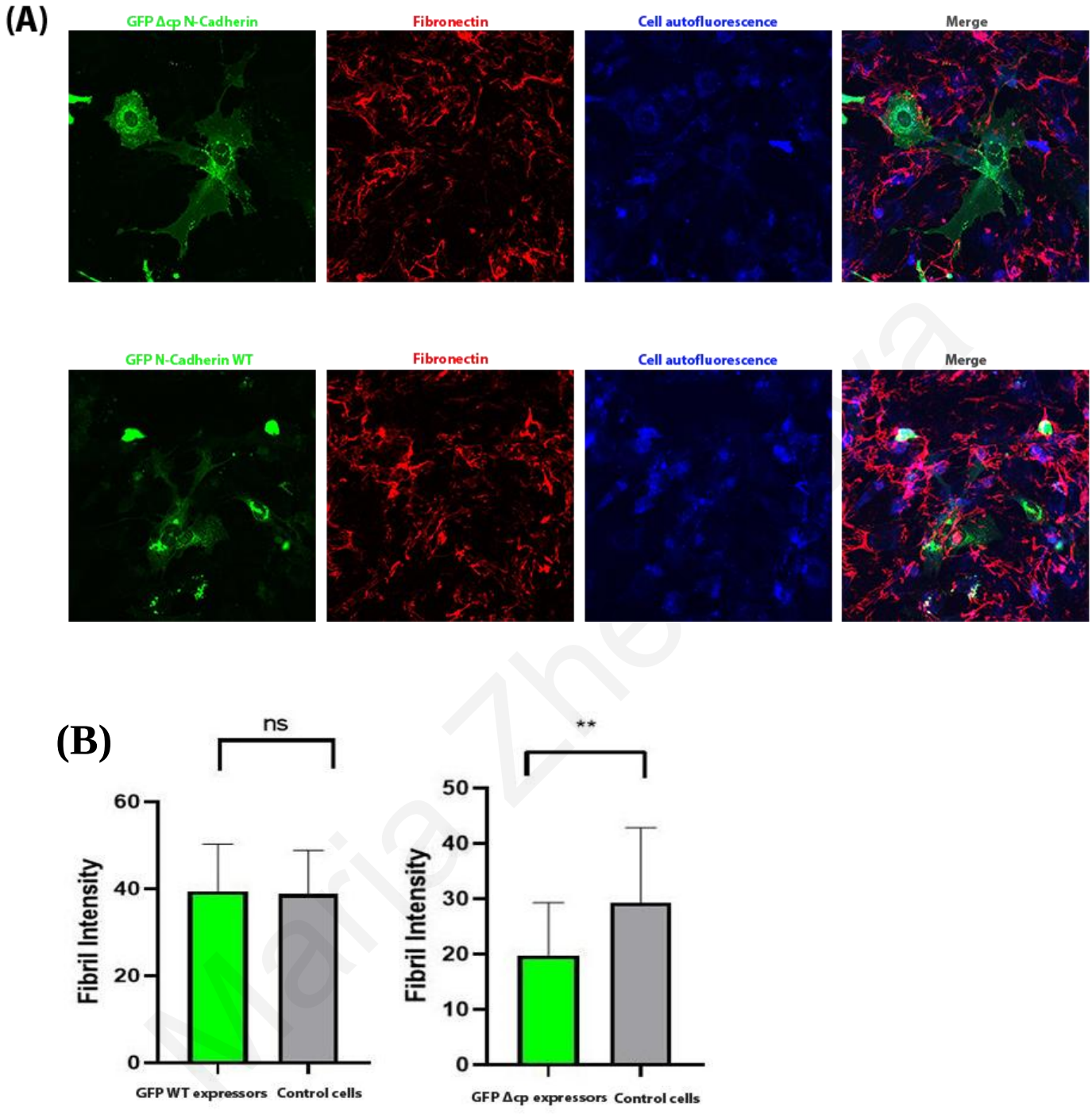
(A)
GFP Δcp N-Cadherin
Fibronectin
Cell autofluorescence
Merge
GFP N-Cadherin WT
Fibronectin
Cell autofluorescence
Merge
(B)
ns
Fibril Intensity
60
40
20
0
GFP WT expressors
Control cells
**
Fibril Intensity
50
40
30
20
10
0
GFP Δcp expressors
Control cells

Figure 27. Expression of N-cadherin Δcp mutant leads to suppression of FN fibril formation

(A) Confocal images of cells transfected with N-cadherin Δcp and N-cadherin WT, respectively, cultured for 12 hours, fixed, and stained against FN. Cells expressing the mutant fail to form fibrils compared to the control cells and cells expressing the WT protein.

(B) Quantification of the average fibril intensity from cells expressing N-cadherin Δcp and control cells, from a two-tailed unpaired t-test. Error bars represent S.E.M. The mean intensity in control cells is 29,30±3,781, n=15 and in expressors is 19,77±4,781, n=15. Quantification of the average fibril intensity from cells expressing N-cadherin WT and control cells, from a two-tailed unpaired t-test. Error bars represent S.E.M. The mean intensity in control cells is 38,90±4,234, n=15 and in expressors is 39,50±4,234, n=15. n, number of cells measured from three independent experiments.

6.6 Optimization of a protocol to generate a more physiologically relevant substrate to allow monitoring fibrillar assembly during live imaging

With the above experiments, we uncovered a profound influence of AJs not only on ligand binding on the cell surface via the recruitment of active integrins at cell-cell junctions but also on the 3D architecture of the ECM generated by cells in culture. However, all of our experiments so far were done statically, and in order to acquire more mechanistic insights we went on to examine this process with live imaging.

As shown previously, NIH3T3 cells can form a very dense meshwork of fibrils compared to HeLa cells within the same period of 12 hours (**Figure 18**), suggesting that fibroblasts can form fibrils faster. Given that, the use of HeLa cells would make the experiment more challenging, since it would take hours to see fibril formation live, while we aimed to keep the live imaging of cells short, we opted to use NIH3T3 for the live imaging experiments. We also needed a way to image cell protrusions and to identify cell-cell contact areas as they developed. We chose a plasma membrane stain (Deep Red Plasma membrane stain, 0.01ng/μl) as an indicator for AJs, as it was conjugated with a far-red emitted molecule (Deep Red), and thus it t could allow the simultaneous imaging of AJs, active integrin, and FN. This membrane staining stains the plasma membrane, and

when cells come in contact then the intensity increases as shown in **Figure 28A**, indicating where we would expect an AJ to form. Talin or FAK were used as an indicator for active integrin since Talin is the first one to bind integrin tails after activation and directly after FAK is the first one to be recruited. The use of an antibody recognizing active integrins during live imaging was not an option since it could potentially elicit integrin activation and or/prevent inactivation resulting in false results, since most of the conformational antibodies are functional and can alter the state of the integrin. By imaging FN, AJs, and integrins together we wanted to explore the sequence of events taking place at a newly formed AJ. Considering our results in fixed cells (**Figure 22**), we expected to observe AJ formation first, then recruitment of Talin or FAK, and finally the accumulation of FN at those sites. Therefore, cells stained with mem stain and transfected with Talin or FAK, respectively, were live imaged in media containing FN-YPet. Unfortunately, during live imaging, we came across several problems. First, although mem stain could potentially indicate where an AJ would form, it was not guaranteed that indeed an AJ was there, hence it was not clear whether the subsequent localization of Talin or FAK there was due to the formation of an AJ. Given that, in order to examine the sequence of events, we need to be able to observe the formation of AJs by transfecting cells with a fluorescently labeled cadherin or β-catenin. Another problem was that we didn't manage to have sufficient temporal resolution to distinguish the exact order the proteins were recruited at the junction (**Figure 28B)**, since the presence of a ligand in the media, in this case, FN-YPet, made the whole process to be almost instantaneous, something that will require extremely high frame acquisition rates in order to be imaged efficiently, which can lead to fluorophore photo-bleaching or photodamage. However, the most challenging problem that we came across was the basal deposition of FN by individual cells, an artifact of seeding cells on extremely stiff substrates, like glass. As mentioned in the Introduction, force is required to expose cryptic sites on FN molecules essential for fibril formation (Schwarzbauer and DeSimone, 2011). Notably, it was shown that lateral adhesive cell contacts are crucial for the initiation of fibrillar assembly since very small BCR explants from *Xenopus laevis* failed to generate fibrils (Winklbauer, 1998). Although single cells *in vivo* cannot form fibrils, cells seeded on stiff substrates form stress fibers, a contractile bundle of actin, anchored on FAs, resulting in sufficient force essential to expose cryptic sites on FN molecules and promote fibril formation upon contraction. As shown in **Figure 28C**, this basal deposition of FN on the glass substrate masks any initial accumulation of FN at cell-cell contact sites that we wanted to investigate. In an effort to

resolve this problem, we went on to optimize a substrate that will closely mimic the *in vivo* state, where single cells cannot deposit fibrils and thus will eliminate basal FN deposition in single cells.

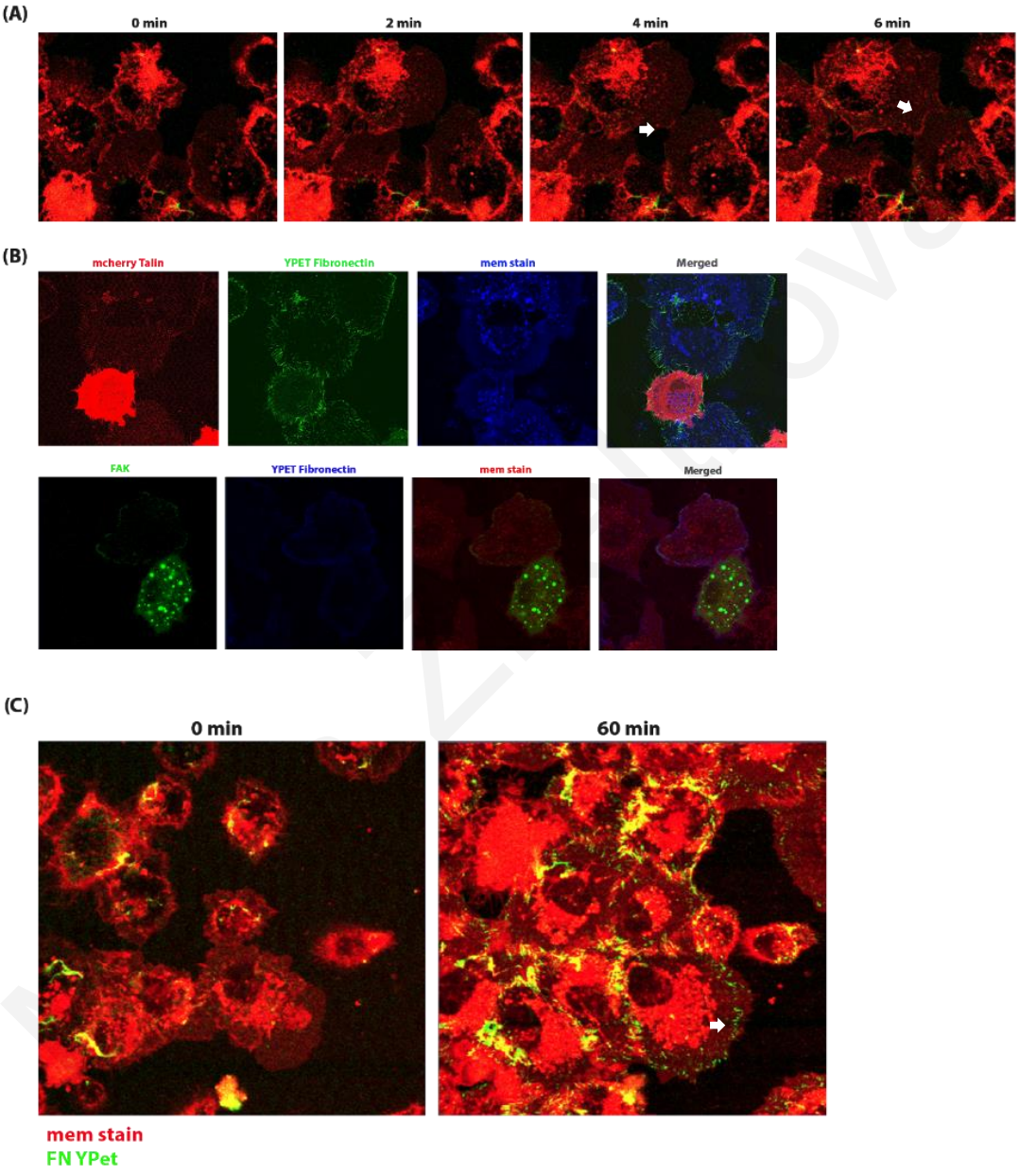

Figure 28. Basal deposition of FN, an artifact of stiff substrates, masks any initial accumulation of FN at cell-cell contact sites during live imaging

(A) Still images from a live movie of NIH3T3 cells stained with mem stain. White arrowheads indicate the cell-cell contact site where an AJ potentially would form.

(B) Still images from live movies of NIH3T3 cells expressing Talin or FAK, respectively, stained with mem stain and incubated with soluble FN-YPet. Basal deposition is observed in both movies.

(C) Still images (0 min and 60 min) from live movie of NIH3T3 cells stained with mem stain and incubated with soluble FN-YPet showing the basal deposition of FN that could potentially mask any accumulation of FN at the cell-cell junction sites.

6.6.1 Use of PLL for the promotion of non-specific attachment of cells on glass

To bypass FN basal deposition, we initially decided to use Poly-L-Lysine (PLL). PLL is a cationic polymer that can be strongly adsorbed to glass surfaces, leaving free cationic sites. Given the fact that the cell surface is negatively charged, PLL coating promotes cell adhesion through electrostatic interactions (Minigo et al., 2006) (**Figure 29A**). Therefore, cells would spread without forming FAs, and potentially single cells would not be capable of fibril formation. For that reason, we cultured cells expressing N-cadherin in media containing FN-YPet for 2 hours before fixation. As a control, we used cells cultured on a glass coverslip and a plasma-treated glass coverslip. The plasma treatment makes glass substrates more hydrophilic by adding polar oxygen-based functional groups and hence they allow integrin-based cell spreading. Additionally, Bovine Serum Albumin (BSA) coating was done after the PLL coating, since it is well known that BSA monolayer minimizes nonspecific binding of cells on the substrate (Ma et al., 2020). As shown in **Figure 29B**, although basal deposition was partially suppressed and stronger fibrils were observed between cells, cell spreading was drastically affected compared to cells on charged glass substrates. Within 30 minutes the spreading of cells on PLL was limited in comparison to cells on plasma glass, where cells were almost fully spread, suggesting that PLL coating delays cell spreading. The time limitation was an issue for us since we wanted to monitor ligand binding

during live imaging and thus, we wanted a substrate that could both eliminate basal deposition and promote fast cell spreading to allow monitoring of the process.

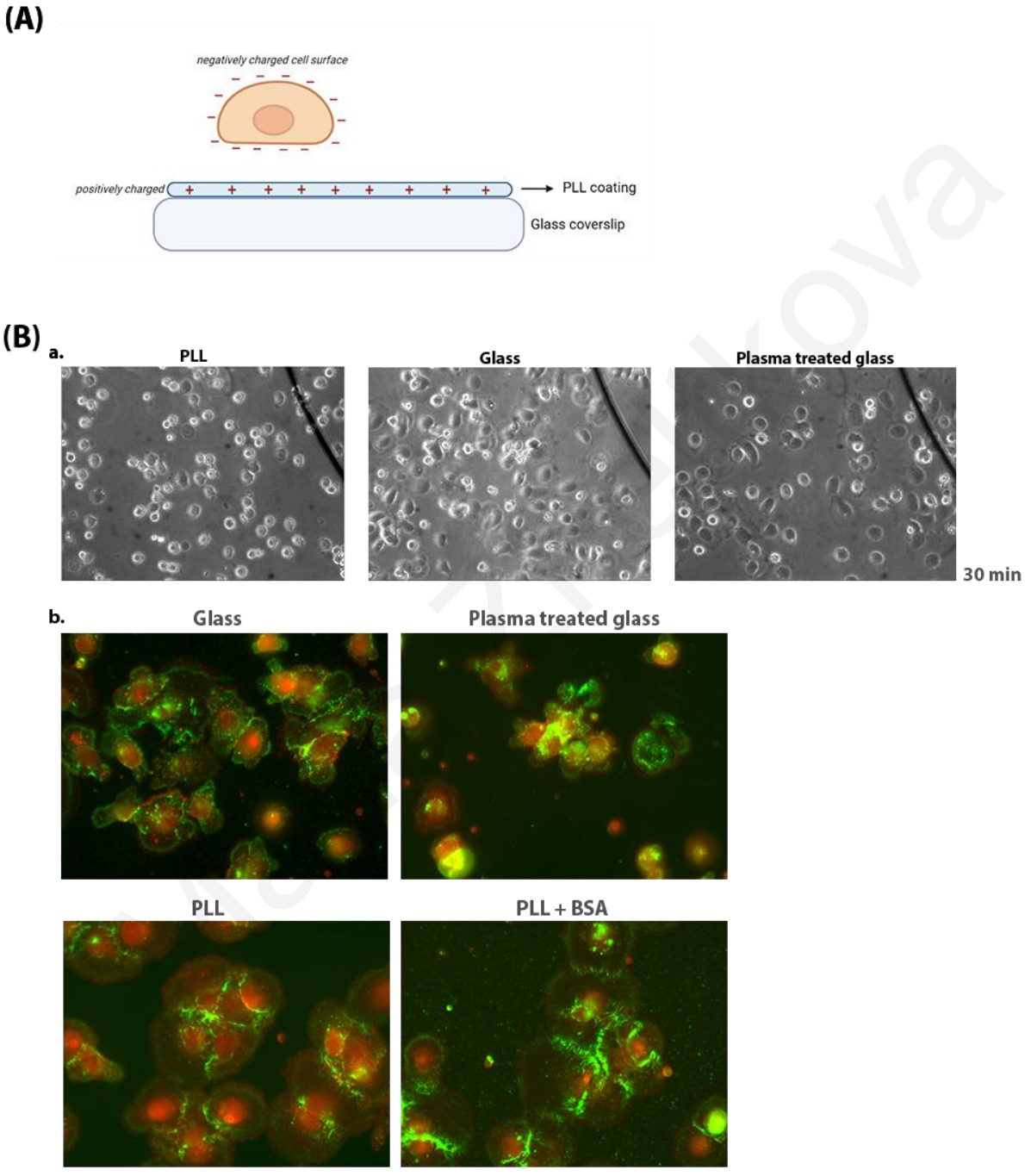

Figure 29. PLL coating coupled with BSA block delays cell spreading

(A) Schematic representation of the electrostatic interactions between the cell surface and PLL coated coverslip. This scheme was made by using BioRender.com.

(B) (a) Brightfield images of cells seeded on PLL coated coverslip, glass, and plasma-treated glass coverslips for 30 minutes showed a delayed cell spreading of cells seeded on PLL.

(b) Images of cells transfected with N-cadherin and incubated in soluble FN-YPet for 2 hour before fixation on differently conditioned coverslips. Partial elimination of FN basal deposition was observed.

6.6.2 Use of ECM proteins with main integrin receptor different than α5β1, as an option for substrate optimization

Since efficient spreading of cells was not achieved on PLL coated glass, we went on to follow a different approach. We hypothesized that, if we used a different ECM ligand instead of Fibronectin in order to coat the glass surface, we would promote efficient cell spreading while ensuring that the FN specific integrin receptor α5β1 will all be available to interact with the exogenous FN-YPet, and at the same time preventing the formation of fibrils at the basal surface. Specifically, we proceeded with the use of Gelatin and Vitronectin (VN).

6.6.2.1 Use of Gelatin as a substrate produces background generation via the interactions with the FN molecules

Gelatin is a natural biomaterial, obtained from partial hydrolysis of collagen, which is the most abundant ECM protein. The main gelatin-binding integrin receptor is αvβ3 (Davidenko et al., 2016). Cells transfected with N-cadherin were seeded on gelatin-coated coverslips for 2 hours before fixation. In addition to gelatin-coated only glass coverslips, silenization was done before the gelatin coating to increase the hydrophilicity of the glass and BSA coating was done after the gelatin coating to minimize non-specific binding (**Figure 30**). Silenization was performed with the use of silane, an inorganic compound that gets covalently conjugated on glass making it more hydrophilic by providing free positively charged amino groups for proteins to attach on. We

observed that FN basal deposition was almost fully eliminated in cells seeded on all the four gelatin-based coverslips compared to the cells seeded on the control substrates. However, unfortunately, despite the fact that gelatin eliminated the formation of fibrils basally, it promoted a strong diffuse background, shown in green, probably by interacting directly with the FN-YPet molecules via the gelatin-binding domain of FN. Notably, it has been shown that *in vitro* FN can bind gelatin with a higher affinity than native collagen (Speziale et al., 2008) (**Figure 30**). This strong background was supressed by BSA however even with BSA it still masked low level early-stage FN accumulation at AJs, thus this approach was not chosen for subsequent experiments.

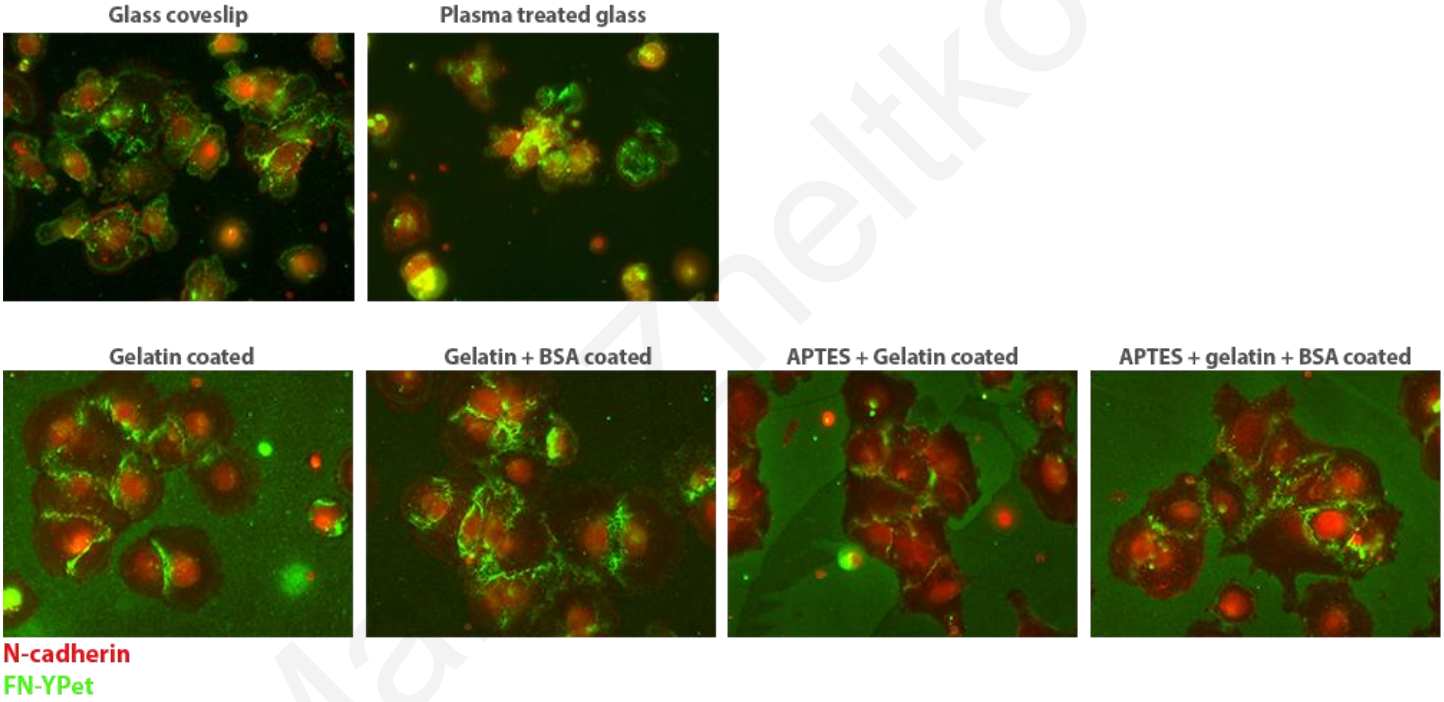

Figure 30. Gelatin coating leads to strong fluorescent background due to the adsorption of FN-YPet on gelatin.

Images of cells transfected with N-cadherin and incubated in soluble FN-YPet for 2 hour before fixation on differently conditioned coverslips. Although elimination of basal FN deposition was observed, a very robust background was formed rendering the gelatin coat unsuitable.

6.6.2.2 Use of Vitronectin as a substrate fails to eliminate basal deposition of FN

Another major ECM component is Vitronectin. Hence, we went on to test whether VN-coated coverslips would eliminate the basal deposition of FN fibrils. There are at least four known integrin receptors capable of binding vitronectin, including αvβ1, αvβ3, and αIIbβ3 (Felding-Habermann and Cheresh, 1993). For this purpose, cells expressing N-cadherin seeded on VN-coated coverslips were cultured in media containing FN-YPet for 2 hours before fixation. Unfortunately, as shown, VN-coated coverslips did not work in the way that we hoped since they failed to eliminate basal deposition of FN (**Figure 31**).

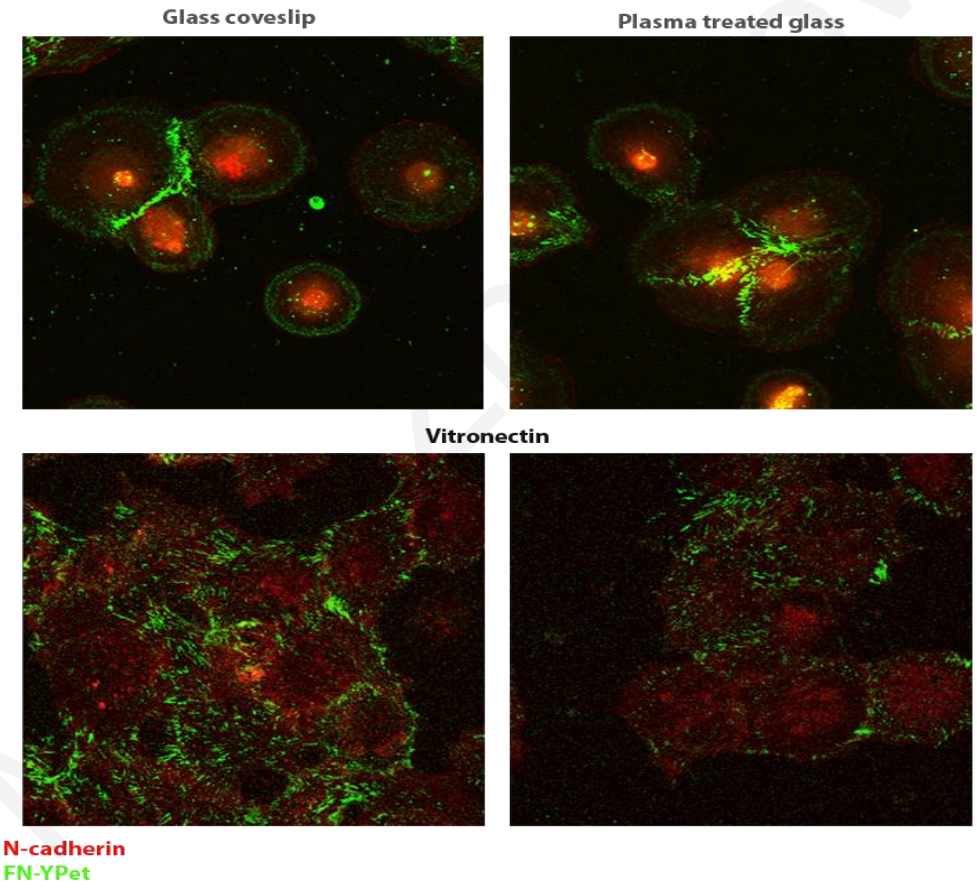

Figure 31. VN coating fails to eliminate the basal deposition of FN

Confocal images of cells transfected with N-cadherin and incubated in soluble FN-YPet for 2 hours before fixation on VN coated coverslips. Basal deposition of FN was observed.

6.6.3 Use of polyacrylamide (PA) hydrogels for the promotion of cell spreading on substrates that closely resemble the biological tissues

Since none of the above options could be used to generate a substrate that would eliminate basal deposition of FN, we went on to test if polyacrylamide (PA) hydrogels conjugated with VN are a more suitable option. PA gels are widely used to test stiffness-dependent cell responses since distinct concentrations of acrylamide and bis-acrylamide can generate PA-gels with various stiffness ranges, from 0.3 to 300 kPa (Syed et al., 2015). Therefore, these gels display mechanical properties closely resembling biological tissues. Additionally, several proteins can be conjugated to PA-gels to promote cell adhesion, where cells can spread, but cannot remodel the underlying substrate. In addition, cells cannot deposit any ligands onto acrylamide gels, ensuring that they spread exclusively through the substrate provided. Thus, using PA-gels conjugated with VN, we hypothesized that cell spreading will not be affected, and cells would not be capable of depositing and incorporating FN basally. Before moving further, we initially seeded cells on two well-characterized gel stiffnesses by members of our lab, on 30kPa and 66kPa gels, conjugated with VN for 30 minutes before fixation, to ensure that cell spreading is efficient onto a substrate of this stiffness. As shown, cell spreading on 30kPa gels was delayed compared to 66kPa gels, and thus we decided to move on with the 66kPa gel stiffness (**Figure 32A**). Moreover, we wanted to exclude the possibility that FN-YPet can be adsorbed by PA-gels resulting in a background similar to what we observed on gelatin-coated coverslips (**Figure 30B**). For this purpose, we seeded cells on 66kPa gels with media containing FN-YPet for 1 hour before fixation. As shown in **Figure 32B**, no background was observed suggesting that PA-gels cannot passively adsorb the fluorescently labeled FN. Furthermore, cells transfected with N-cadherin were seeded on 66kPa VN-conjugated gel supplemented with FN-YPet media and live imaged. Although the basal deposition of FN was drastically reduced (**Figure 32C**), we came across another significant problem. In order to monitor the initial accumulation of ligands at the cell-cell contact sites, high-resolution imaging is required. All the previous experiments showing FN accumulation at AJs were done with the use of the 63X oil immersion lens using 1au aperture to achieve the maximum possible resolution. However, the 63X oil immersion lens cannot be used on gel coverslips due to its small working distance, since the thickness of the acrylamide gel did not allow the lens to focus on the cells. Thus, for imaging gel coverslips only the 63X water immersion lens or the 40X lens can be used, resulting in lower

resolution and a drastic reduction of signal intensity, limitations that we couldn't resolve. Thus, this method was not efficient for the visualization of AJ promoted fibril formation.

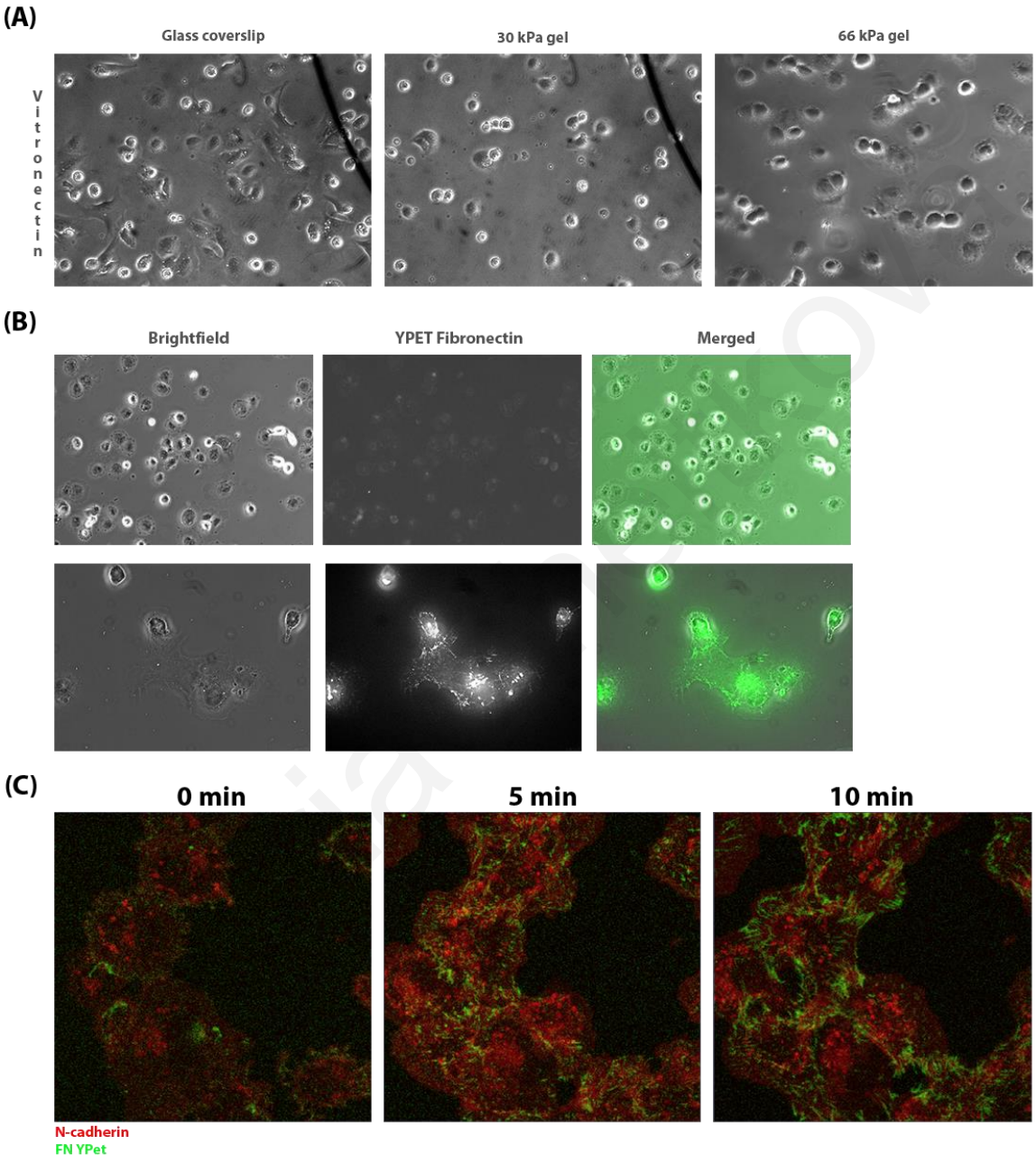

Figure 32. VN polyacrylamide gels eliminate basal FN deposition to a great extent

(A) Brightfield images of cells seeded on 30kDa and 66kDa VN-PA gels for 30 minutes showed that more soft substrates delay cell spreading compared to the 66kDa stiffness.

(B) Images of cells seeded on 66kDa VN-PA gel for 1 hour in media conditioned with FN-YPet. No background was observed.

(C) Still images from a live movie of cells transfected with N-cadherin in FN-YPet conditioned media. Elimination of FN basal deposition was observed.

6.6.4 Use of RO-3306 inhibitor leads to FA remodelling and stronger fibril formation

Given our failure to establish a substrate that could effectively be used for live imaging we decided to attempt to eliminate focal adhesions which are responsible for FN basal deposition. RO3306 is an inhibitor of CDK1/cyclin B1 and CDK1/cyclin A. Several studies showed that the reduction of CDK1 levels upon entry into the G2 phase promotes the disassembly of FAs in preparation for mitotic entry (Jones et al., 2018; Grobe et al., 2018). We hypothesized that RO3306 would suppress the ability of cells to deposit ECM basally on the glass, since the cells will not have the capacity to generate sufficient force to expose the necessary cryptic sites within the FN molecule for FN fibrillogenesis. As shown in **Figure 33**, HeLa cells were cultured for 12 hours in the presence of the inhibitor before fixation. As a negative control, a ROCK inhibitor (Y-27632) was used, since we previously showed that upon ROCK treatment FN accumulation was lost (**Figure 24B**). Immunofluorescence experiments were carried out with the use of antibodies against FN and actin. We observed that cells treated with the RO inhibitor displayed more dense and strong fibrils correlated with the cell-cell boundaries, compared to the fibrils formed in untreated cells, which were below the entire cell bodies and not localized only between cell-cell contacts (**Figure 33A**). However, when fibroblasts were treated with the RO-3306 inhibitor we observed the formation of stronger fibrils without any correlation with the cell-cell boundaries **(Figure 33B**). Since the inhibitor had a distinct and kind of opposite impact on the two different cell lines and due to time limitations, we didn't explore this approach further since we wanted to find an approach that would work both for HeLa and fibroblasts. Nevertheless, future experiments need to be carried out to further optimize and examine the effects of RO-3306 on fibrillogenesis.

(A)

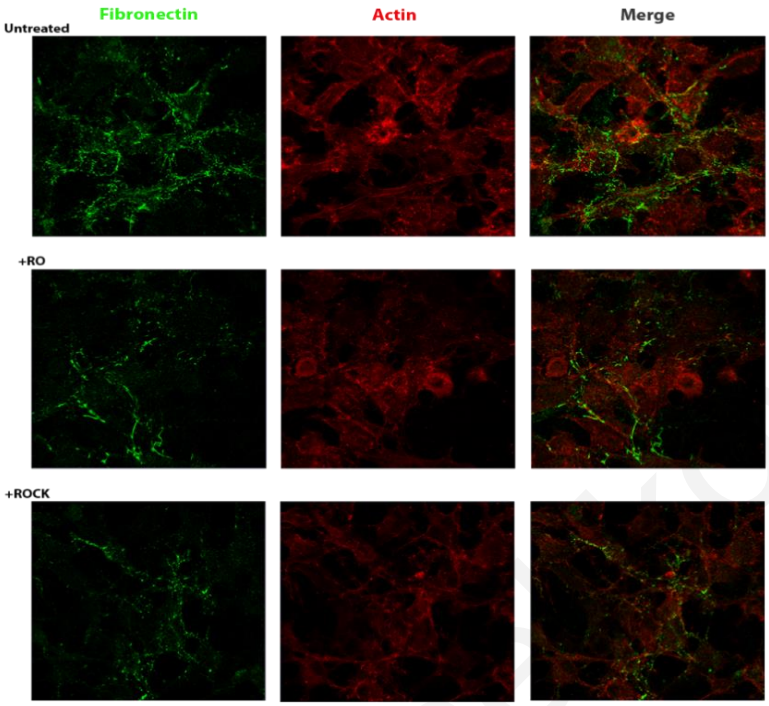

(B)

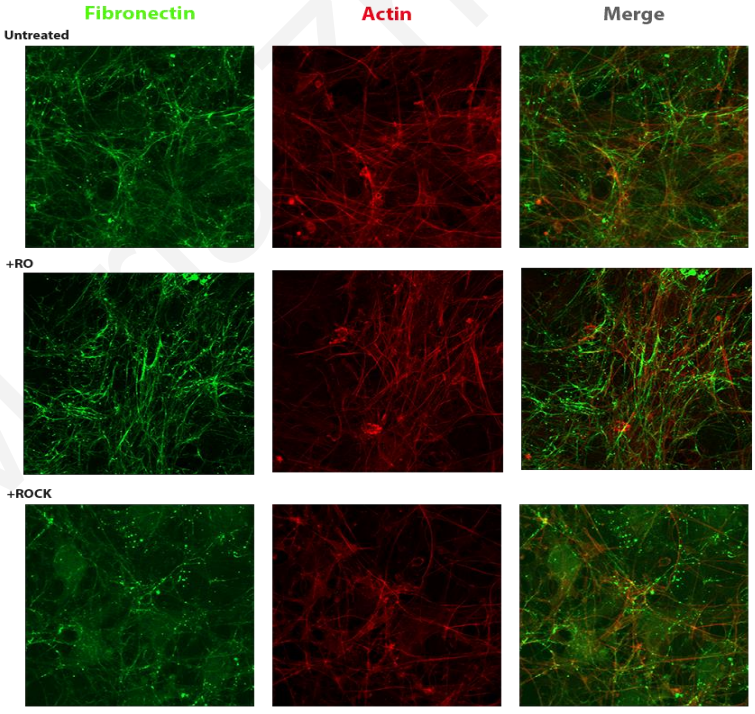

Figure 33. Use of a CDK1 inhibitor leads to stronger fibrils both in HeLa and in fibroblasts

(A) Confocal images of HeLa cells cultured for 12 hours in the presence of RO-3306 inhibitor, fixed and stained against FN and actin. As a negative control cells treated with ROCK inhibitor were used, while as a positive control untreated cells were used.

(B) Confocal images of NIH3T3 cells cultured for 12 hours in the presence of RO-3306 inhibitor, fixed and stained against FN and actin. As a negative control cells treated with ROCK inhibitor were used, while as a positive control untreated cells were used.

6.6.5 Use of concanavalin A (conA) promotes cell spreading without FA formation

We thus proceeded to explore the possibility of using a lectin and specifically concanavalin A coated substrates. Concanavalin A (conA) belongs to the lectin protein family, which are carbohydrate-binding proteins. conA is highly specific for alpha glucosides, mannosides, and biopolymers. Several studies proposed that lectins can bind to the cell surface through these carbohydrate-directed interactions, promoting cell adhesion (Guy et al., 1979; Carter et al, 1981; Hughes, 1992). Hence, we sought to investigate whether the conA substrate could promote fast cell spreading via carbohydrate-directed interactions and thus eliminate the basal deposition of FN. For that reason, we initially optimized the glass substrate for efficient conA coating. Specifically, different treatment combinations for glass coverslips were tested to promote efficient conA adsorption on the coverslips. In order to increase the hydrophilicity of glass coverslips, they were either plasma-treated or silanized. Additionally, work by Carter et al. showed that cross-linking of conA leads to faster cell spreading (Carter et al., 1981), and thus after conA incubation, coverslips were exposed to UV for 3 minutes, since UV can promote the crosslinking of proteins on the glass surface. As a control, plasma-treated FN coverslip silanized FN coverslip, and silanized crosslinked coverslip were used. Cells were seeded on each treated coverslip and images were taken every 30 minutes for a period of 2 hours (**Figure 34A**). Quantification of the ratio of spreading revealed that crosslinked, silanized conA coated coverslips were the most efficient to promote fast cell spreading resembling the spreading on FN substrate, compared to the other conditions tested (**Figure 34B**), and thus we proceeded with this method. Furthermore, in order to examine whether the observed cell spreading is achieved through the formation of FAs or not, we

seeded cells on crosslinked, silanized conA coated coverslips for 1 hour, fixed them, and stained against Paxillin and Vinculin, two known components of FAs. As a control, we used FN-coated coverslips on which cells will spread through the formation of FAs. As shown in **Figure 34C**, conA coating prevented FA formation without affecting cell spreading, compared to cells on FN substrate, where cells formed FAs. To further validate the above observation, we repeated the experiment and stained for actin to examine if stress fibers were disorganized in cells seeded on conA since no FAs were observed, which are the anchorage points of stress fibers. As expected, disorganized stress fibers were observed in cells seeded on conA (**Figure 34D**). So far, the above data showed that the conA substrate is a promising substrate that could resolve our initial limitation, the basal deposition of FN. In an effort to address this, we seeded cells transfected with N-cadherin on conA in FN-YPet media for 1 hour before fixation. As shown, cells were fully spread within 40 minutes and basal deposition of FN was completely eliminated. Importantly, the only FN accumulation observed was on the cadherin positive cell-cell contact sites, confirming our hypothesis that AJs can guide ligand binding on the cell surface (**Figure 34E**).

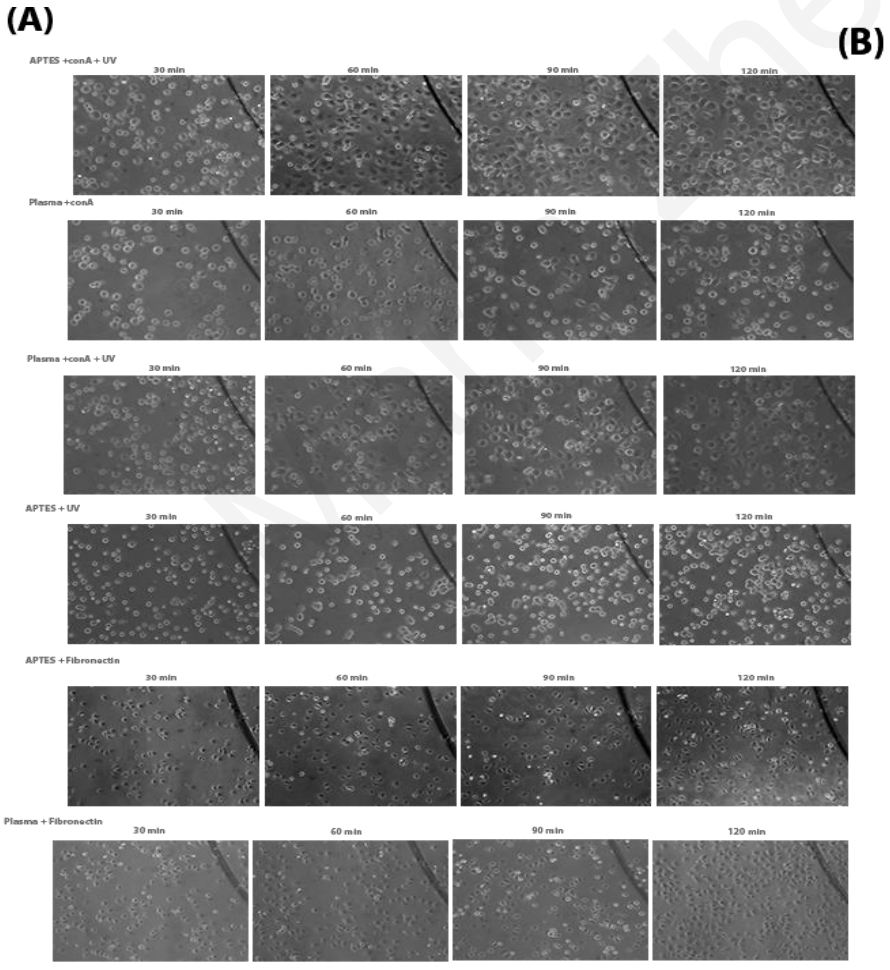

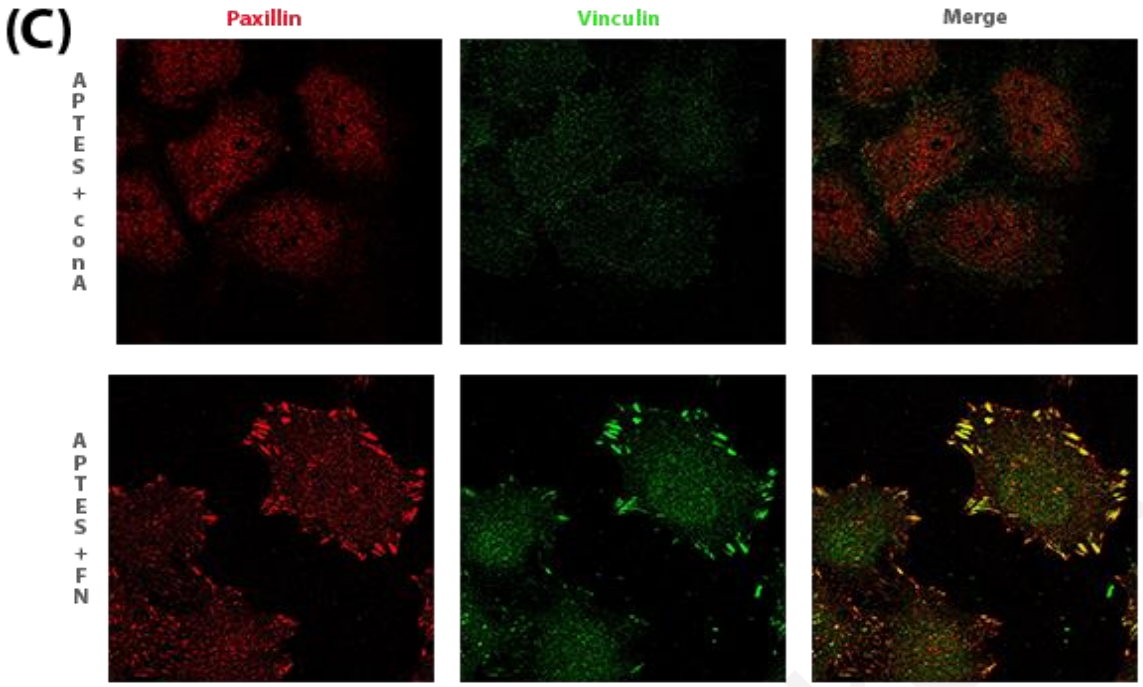
(C)
Paxillin
Vinculin
Merge
APTES + conA
APTES + FN

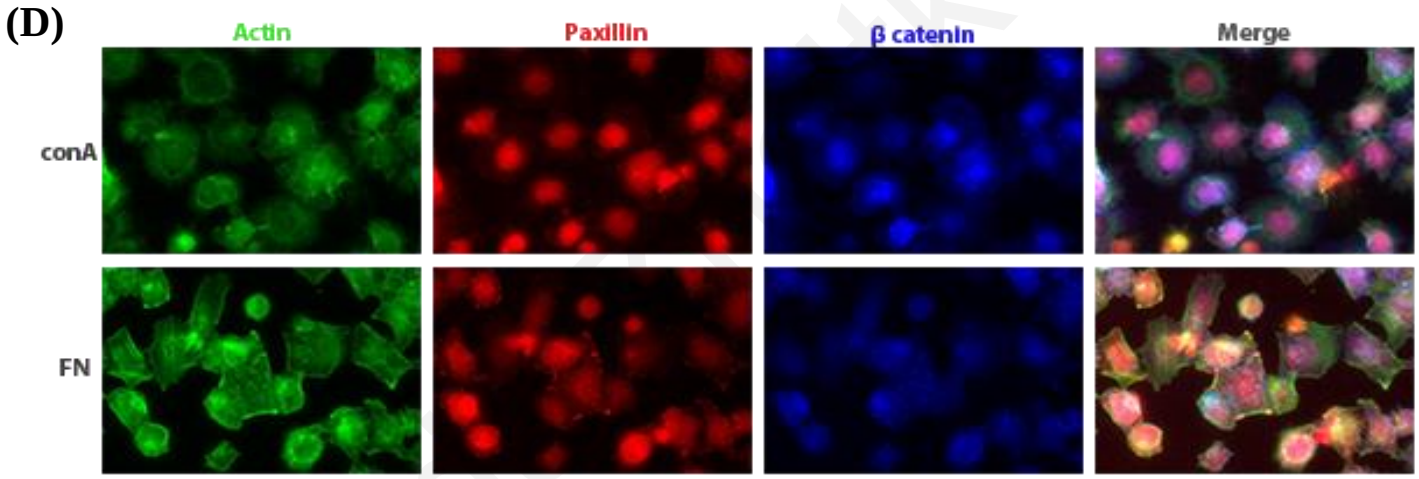
(D)
Actin
Paxillin
β catenin
Merge
conA
FN

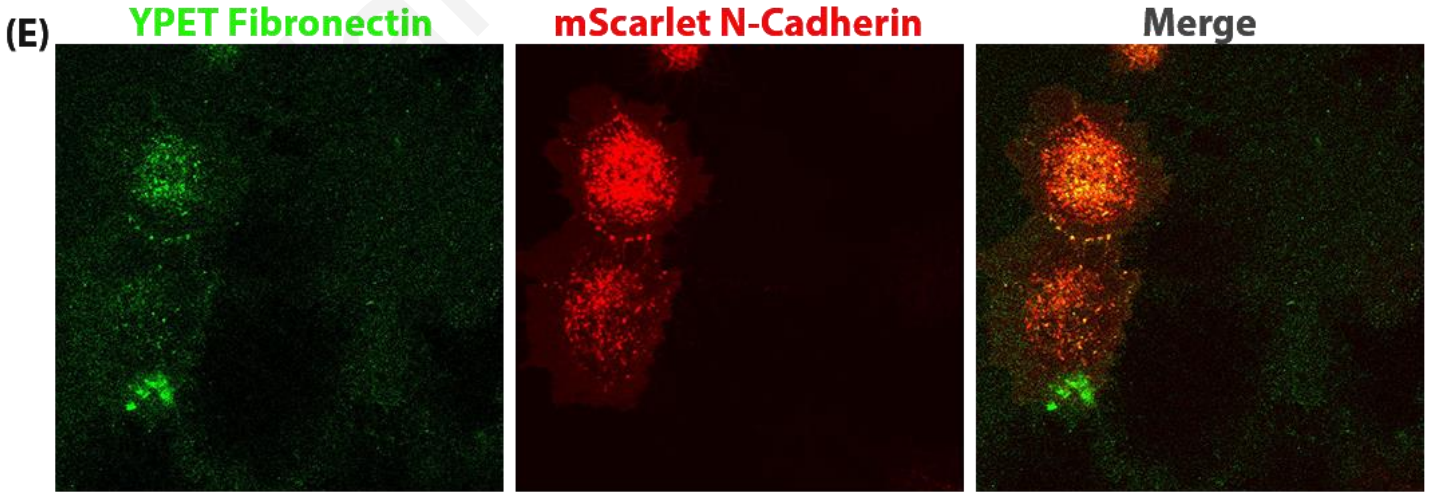
(E)
YPET Fibronectin
mScarlet N-Cadherin
Merge

Figure 34. conA coating promotes cell spreading without FA formation

(A) Brightfield images of cells seeded on coverslips treated with various combinations for maximum efficiency of conA coating on the glass.

(B) Quantification of cell spreading ratio measured in cells seeded on different conditional coverslips. P-values calculated by 2way ANOVA test. Error bars represent standard S.E.M. Crosslinked silenized coverslips promoted faster cell spreading compared to the rest.

(C) Confocal images of cells seeded on conA and FN coated coverslips, fixed and stained for Paxillin and Vinculin. Cells on conA substrates failed to form FAs, however, cell spreading was not affected.

(D) Images of cells seeded on conA and FN coated coverslips, fixed and stained for actin, Paxillin, and β-catenin. Cells seeded on conA substrates displayed disorganized stress fibers.

(E) Confocal images of cells transfected with N-cadherin and incubated with soluble FN-YPet seeded on conA coverslips. Basal deposition of FN was fully eliminated, and FN accumulation was observed at the cell-cell contact sites positive for N-cadherin.

Before moving on, given the fact that we established an FA-free system, we went on to investigate whether reduction of calcium will eliminate AJ formation, as mentioned previously, resulting in a system free from both FAs and AJs, yet a system where cells could be fully spread. For this purpose, cells were seeded on conA in the presence and absence of calcium for 1 hour, fixed, and stained against β-catenin, Paxillin, and active integrin β1 (**Figure 35A**). As a control, cells were seeded on FN coated coverslips in the presence and absence of calcium for 1 hour in order to be sure that calcium reduction will not affect FA formation (**Figure 35B**). Remarkably, calcium reduction eliminated AJ formation in cells seeded both on conA and FN, without affecting FA formation (**Figure 35A**).

In conclusion, we have established a powerful system where cells seeded on conA coated glass fail to generate sufficient force required for fibrillar assembly as single cells, thus eliminating the artificial characteristic of cells displayed when seeded on stiff substrates and therefore allowing us to monitor the accumulation and binding of ligands on the cell surface during live imaging, but

also a system where cells could be free from both FAs and AJs and can be used for investigating their roles in signaling pathways using biochemical approaches.

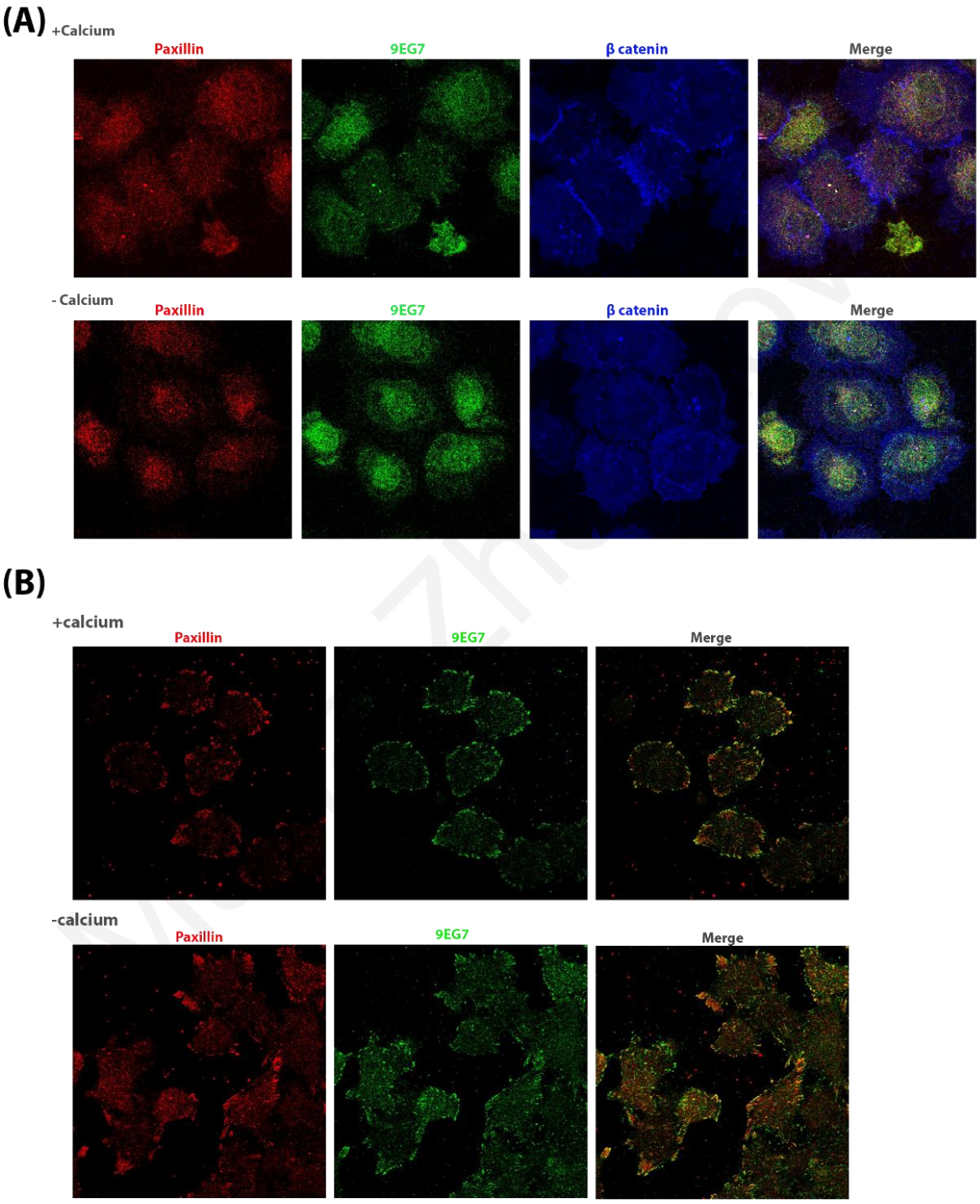

Figure 35. conA coating with calcium reduction results in a system devoid of both FA and AJ formation

(A) Confocal images of cells seeded on conA coated coverslips for 1 hour in calcium-plus and calcium-free conditions, fixed and stained against Paxillin, active integrin β1, and β-catenin. The reduction of calcium suppressed AJ formation.

(B) Confocal images of cells seeded on FN coated coverslips for 1 hour in calcium-plus and calcium-free conditions, fixed and stained against Paxillin and active integrin β1were used as a control to ensure that FA formation is not affected by calcium reduction.

6.7 Intracellular signaling is taking place via the AJ-driven active integrins at cell-cell junction sites

It is well established that upon interaction with ligands, integrins not only mediate cell attachment to the ECM, but they also stimulate numerous intracellular signaling pathways to regulate cellular functions, including spreading, migration, and apoptosis (Longhursta and Jenningsa, 1998). Several studies showed that protein phosphorylation is one of the earliest events detected in response to integrin activation. An example of such proteins is FAK, which has been shown to display elevated phosphotyrosine levels upon integrin activation, resulting in the formation of the FAK signaling complex (Burridge et al., 1992). Several studies proposed that Paxillin acts as a downstream target of FAK (Richardson et al., 1997). Therefore, upon integrin activation, phosphorylation levels of Paxillin are also increased. So far, our data showed ligand-independent activation of integrins recruited at the cell-cell contacts of both cell doublets and cells spread on a charged glass substrate, which was in agreement with unpublished data from our lab that showed ligand-independent activation of integrins at the linear AJs formed on Fc substrates (Hadjisavva et al., Cell Reports-under revision). Taking this into consideration, we went on to determine the role of those AJ-driven active integrins in intracellular signaling, since most of the information available in the literature is related to the ligand-dependent activation of integrins. For that purpose, we decided to examine the phosphorylation levels of Paxillin in cells under different conditions. In order to examine that, we plated cells under different conditions, followed by cell

lysis and immunoblotting against phospho-Pax. Specifically, lysates from cells seeded on conA, on Fibronectin as control, and cells in suspension in calcium-free and calcium-plus conditions were used for western blot analysis. Both suspended cells and cells seeded on conA will not form FAs; however, suspended cells are exerting minimum forces on each other compared to the cells seeded on conA. By removing calcium, AJ formation was eliminated in all three conditions. Blotting with an antibody against phosphorylated Paxillin on Tyr31, showed a clear reduction of pPax in calcium-free conditioned cells, suggesting that signaling is taking place after AJ-driven integrin activation (**Figure 36A**). Paxillin expression levels were also examined, and they are shown as a loading control (**Figure 36C**). Quantification of the pPaxillin to Paxillin intensity ratio confirmed the above observation (**Figure 36B**). In conclusion, these results show that AJ-driven activation of integrins leads to intracellular signaling that actually contributes to the integrin signaling output of a cell. This direct biochemical demonstration of AJ driven integrin signaling is an exciting finding raising the possibility that AJ based integrin signaling may have significant roles at early stages of embryonic development prior to basement membrane deposition.

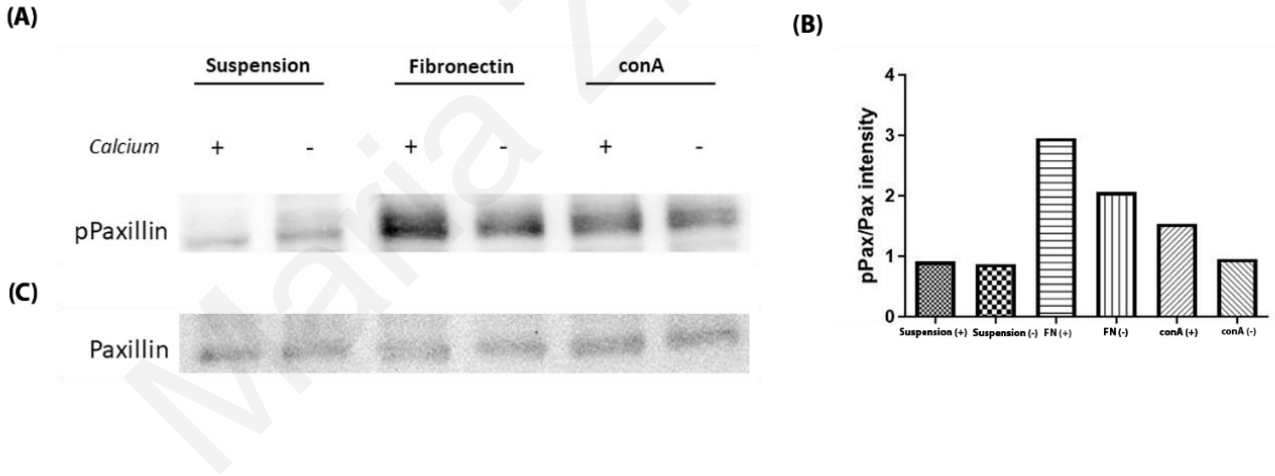

Figure 36. AJ-driven activation of integrins contributes to phosphotyrosine signaling downstream of FAK/Paxillin

Representative western blot from lysates of cells seeded on conA, on Fibronectin, and cells in suspension in calcium-free and calcium-plus conditions.

(A) Blotting of the membrane with an antibody against phosphorylated Paxillin at Tyr31, reveals a decrease in the levels of pPax of cells cultured in all three different conditions without calcium.

(B) Quantification of the pPaxillin to Paxillin mean intensity ratio from cells cultured under different conditions in calcium-free and calcium-plus media. Error bars represent S.E.M.

(C) Paxillin expression levels are not affected, indicated by the detection of a band at 68 kDa on every lane.

6.8 Live imaging reveals the selective recruitment of FN-YPet at cell-cell junctions

We then continued by examining whether AJs can spatially guide ECM ligand binding during live imaging using the optimized substrate. In an effort to address this, both NIH3T3 and HeLa cells were transfected with β-catenin and N-cadherin respectively, seeded on conA coated glass-bottom imaging dishes in serum-free FN-YPet media, and imaged live using a Zeiss LSM 910 airyscan laser confocal microscope. As shown, transfection of NIH3T3 cells did not work efficiently; nonetheless, accumulation of FN was observed immediately after the two cells come in contact (**Figure 37A**). Further analysis by quantifying the average FN intensity over time, confirmed that as time passed, more and more FN accumulated at this site, compared to the rest of the cells where no accumulation of FN was observed at all (**Figure 37B**). Similar results were obtained during the live imaging of HeLa cells. Remarkably, for the first time, we showed the formation of AJs and the subsequent accumulation of FN at those sites during live imaging (**Figure 37C**). As shown, when the two cells came in contact, small AJs were formed, represented as bright red puncta, and within minutes FN accumulated there. Notably, as AJs were remodeling and new ones were forming, FN recruitment was changing accordingly. Intensity profiles made along those AJs confirmed the localization of FN and N-cadherin at those sites. This critical observation shows that ligand accumulation at AJs is dynamic and that at initial stages of AJ formation soluble ligands become associated with AJs which at later stages develop into fibrils. These observations which could not have been made without the capacity to image the process live provide important insights on the mechanism through which AJs regulate integrin activation and spatial distribution and how this is translated in the regulation of ECM deposition and remodeling. They also demonstrate how

powerful the model system we have established is and how it could be used to address the precise input of various factors in the process. We have effectively decoupled AJ-driven integrin activation from cell ECM interactions and focal adhesion formation which otherwise mask the input of PM tension and AJs on integrin receptor spatial distribution and activation status.

In conclusion, our results using live imaging were in agreement with what we showed previously in fixed cells and at the same time provide important insights (**Figures 20,21**). These data further confirm our hypothesis that AJs can in fact spatially influence ligand recruitment and binding on the cell surface by integrin distribution and activation.

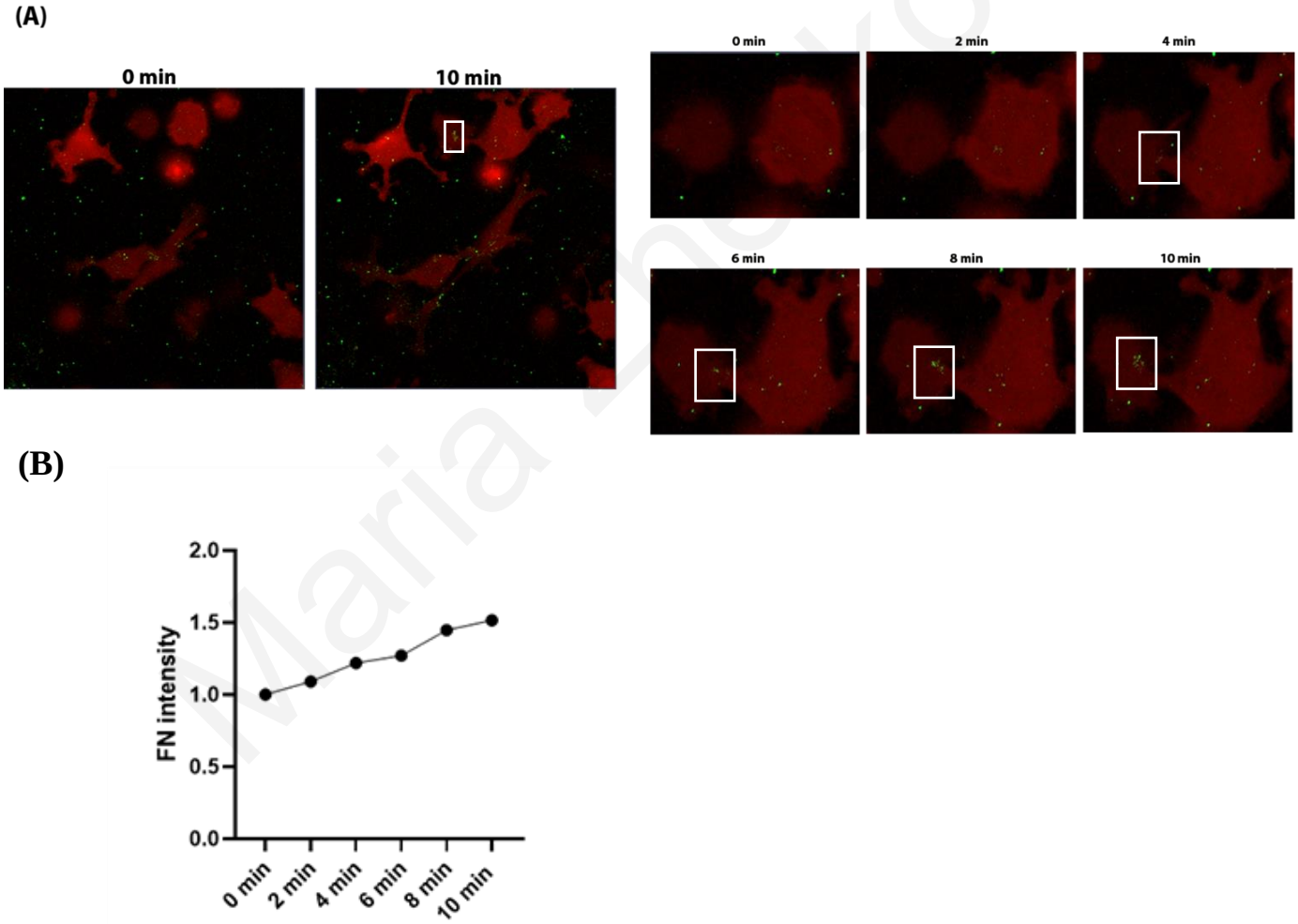

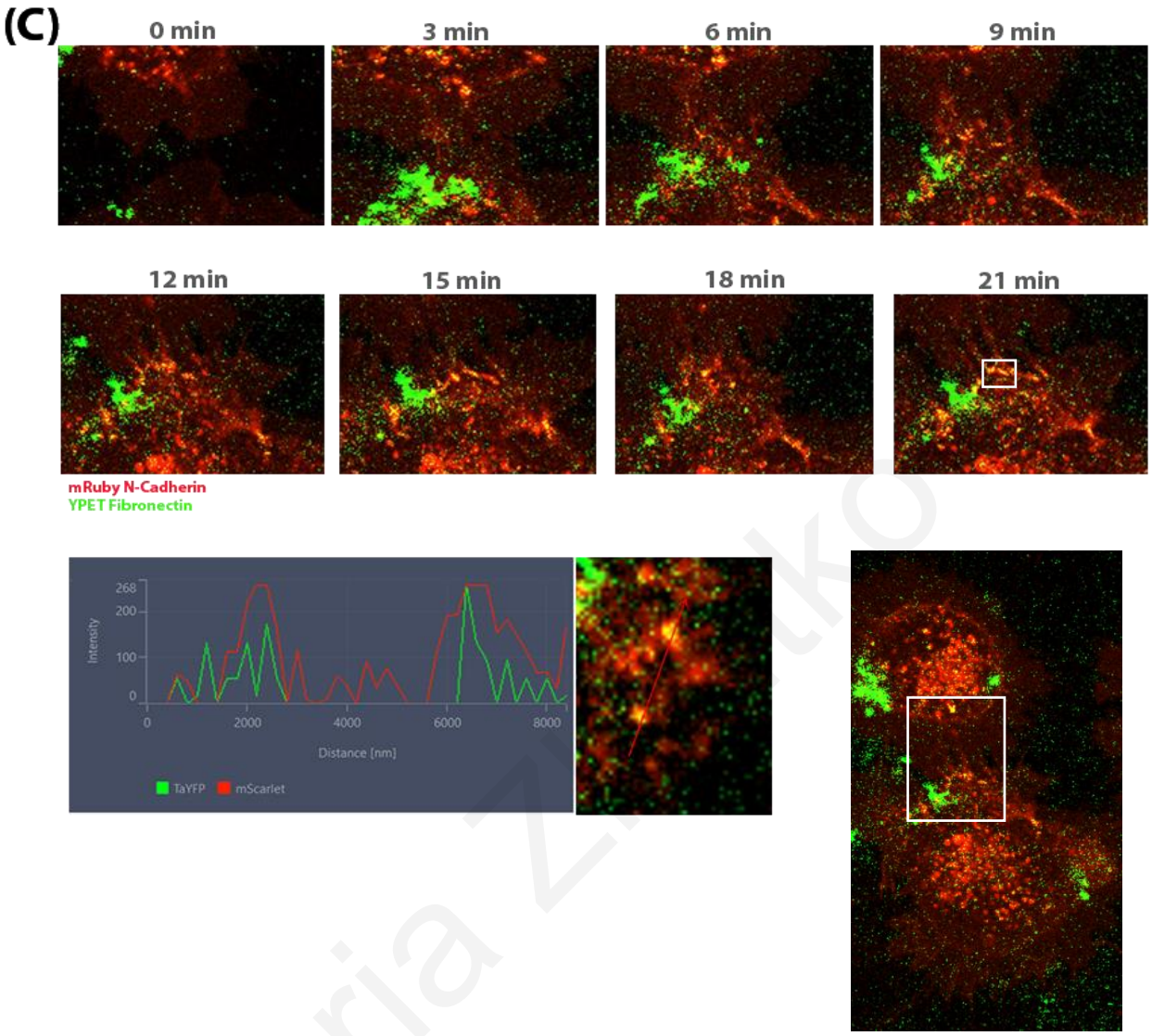

Figure 37. Selective accumulation of FN at the cadherin positive cell-cell junction sites during live imaging in NIH3T3 and HeLa cells.

(A) Still images from a live movie of NIH3T3 cells expressing β-catenin with the addition of soluble YPet-FN on a conA coated glass-bottom imaging dish. As indicated with a white box upon cell-cell contact FN accumulation was observed at this site.

(B) Graph showing the increase in FN intensity at the cell-cell contact site, indicated by the white box, over a period of 10 minutes.

(C) Still images from a live movie of HeLa cells expressing N-cadherin in FN-YPet conditioned media on a conA coated glass-bottom imaging dish. As indicated with a white box upon AJ formation recruitment of FN was observed at the newly formed AJs. Intensity profile was generated perpendicular to two AJs at cell-cell contact revealing the co-localization of FN at the cadherin positive AJs.

DISCUSSION

The extracellular matrix (ECM) is an essential structural component in all multicellular organisms, involved in a broad range of biological processes, including cell migration, tissue, and organ morphogenesis, cell growth, and survival (Rozario and DeSimone, 2009; Frantz et al., 2010). The fundamental role of the ECM is emphasized by the wide range of syndromes stemming from defective ECM components (Jarvelainen et al., 2009). Given the importance of the ECM in both embryonic development and in the adult organism, the mechanisms regulating ECM formation have been studied extensively both *in vitro* and *in vivo.*

Several lines of evidence support that integrin-generated tension is required for ECM deposition *in vitro* (Pankov et al., 2000), however, the mechanisms underlying the ECM formation on the free surfaces of multi-layered tissues *in vivo* are still unclear. The presence of integrin receptors and soluble ECM component FN in the blastocoel fluid are shown to be insufficient to initiate fibrillar assembly (Gawantka et al., 1992; Joos et al., 1995; Lee et al., 1984). Importantly, further studies revealed that free surface and lateral adhesive cell contacts are required to initiate fibrillogenesis (Winklbauer, 1998). Tissue tension and cadherin-based interactions were identified as critical factors through which ECM deposition was regulated in *Xenopus laevis* embryos, however, the mechanism through which adherens junctions influence ECM deposition was ambiguous and believed to be indirect, through the establishment of tissue-level tension (Dzamba et al., 2009). Notably, recent work from our group revealed that AJs have a profound impact on integrin distribution and activation creating spatially restricted pools of high ligand affinity integrin receptors at cell-cell junction sites (Hadjisavva et al., Cell Reports-under revision).

The main aim of this project was to investigate whether these AJ-driven pools of integrins at the cell-cell junctions can spatially guide ligand binding on the cell surface and influence ECM deposition and remodeling. In an effort to address these questions, we initially developed a protocol that allowed us to monitor FN assembly both during live imaging as well as in fixed samples. Moving on, with the use of several conformational specific integrin antibodies we examined the temporal evolution of integrin conformation at cell-cell junctions. Furthermore, using pharmacological agents and a KO cell line we investigated the impact of Talin and

contractile force on the cell-surface ligand binding and ECM deposition. Additionally, to directly address the role of AJs in ECM formation we modulated AJs using several approaches including pharmacological agents and function-blocking cadherin mutants.

In order to monitor fibrillar assembly, a protocol was developed in our lab that allowed the introduction of external fluorescently labeled FN (FN-YPet) to cells, in order to eliminate the limitations and issues that occurred when cells directly expressed fluorescently labeled FN themselves (Hadjisavva et al., Cell Reports-under revision). These limitations included the detection of FN signal coming from secretory vesicles or from the lamelum ridges of cells expressing the FN construct, masking the specific deposition of fibronectin. In contrast, by introducing external FN we ensured that the detected signal is coming from the accumulation and binding of FN molecules on the cell surface. Moving on, we showed that these FN-YPet conditioned media allows labeling of FN fibrils and used this assay to select the appropriate cell lines for our experiments based on the ability to generate FN fibrils and capacity to form strong cell cell adhesions.

Using immunofluorescence experiments we examined whether AJ-driven activation and distribution of integrins could influence ligand binding on the cell surface. Remarkably, we showed the selective accumulation of FN on the active integrin positive cell-cell junction sites in various contexts, including cells seeded on N-cadherin Fc substrate, cell doublets, and in cells seeded on glass substrates promoting non-specific cell attachment, and thus revealed that AJs can in fact spatially regulate cell surface ligand binding.

We went on and further investigated the sequence of events taking place at these cell-cell contact sites. We propose that AJ formation defines integrin β1 activation topology and subsequently guides ligand accumulation there. We examined that by taking advantage of a number of well-characterized conformational-specific antibodies against integrin β1. As described in the Introduction, integrins exhibit three distinct conformational states regarding their affinity for ligands, both bent-closed and extended-closed conformational states are ligand-free, while the extended-open conformation is ligand-bound (Xiong et al., 2001; Takagi et al., 2002). Our data, in agreement with what has been shown from work by our lab, revealed that initially only integrins with an extended closed headpiece conformation are recruited at cell-cell contacts, which have

high affinity for ligand, while accumulation of FN can, later on, leads to headpiece opening, confirming our initial hypothesis.

The fact that only integrins with an extended-closed headpiece conformation were sequestered at the cell-cell junction sites raised the question of how these high-ligand affinity receptors are stabilized in their extended conformational state in those sites. One possible explanation for this is that Talin and force contractility are involved in this process, by regulating integrin stabilization at the cell-cell contact regions. Notably, AJ-generated tension at the plasma membrane (PM) is responsible for the activation and extension of integrin receptors, which allow Talin binding and therefore interactions with actin leading to their stabilization through contractile force. To explore this possibility, we used Talin null cells and a ROCK inhibitor treatment, which revealed that ligand accumulation at cell-cell junctions is strictly dependent on Talin and actin contractility. Notably, when Talin KO cells were stained for FN, a nonspecific detection of FN signal along the cell surface with no correlation with cell-cell contact sites was observed (**Figure 23B)**. To confirm that this signal stems from the secretory FN vesicles of the cell, future experiments need to be performed with the external introduction of FN-YPet in cell doublets. Interestingly, we also showed that AJs fail to promote integrin β1 activation in Talin KO cells, where AJ-driven tension at the PM can be generated, raising the possibility that additional mechanisms may contribute to the process of integrin activation at AJs and additional work will be required to address the basis of this observation. It is clear that Talin plays a major role in stabilizing the active conformation at AJs, hence in its absence, even in the presence of tension, integrins cannot become stabilized at the active conformation. Presumably topological adaptation of the transmembrane domains takes place leading to transient activation which fails to be stabilized in the absence of interactions with actomyosin bundles that would sequester integrins and retain them at the high-tension area in the vicinity of the AJ. Thus, integrins in the active state would be free to diffuse away and enter PM regions with lower tension returning to the bent state.

Subsequently, we went on to directly address the impact of AJs in ECM deposition and remodeling by modulating AJ dynamics using several approaches. Modulation of Calcium ion concentration was the first approach we attempted, since in the absence or under low levels of calcium cadherins undergo conformational changes that result in AJ disruption. Surprisingly, the reduction of calcium led to a 4.5-fold increase in fibril intensity. This observation was unexpected given the absence of

the AJs, however, the likely explanation for this is the fact that calcium ions can bind at the MIDAS and other divalent ion binding sites and have a negative impact on integrin activation. Removal of calcium has been shown to increase ligand affinity in several integrin heterodimers including α5β1 which is the major FN receptor (Zhang and Chen, 2012). Our results suggest that this stimulation is more potent than any reduction in integrin activation stemming from loss of AJs. Therefore, in this case, calcium may act as a negative regulator of integrin activity, and by reducing its levels integrin activation was promoted. Future experiments need to be done to address the effect of calcium on FN fibrillogenesis since it has not been previously reported.

Considering the possible effects of calcium on both AJs and integrin receptors, we decided to move on with the function-blocking mutant of N-cadherin to address the direct role of AJs on fibrillar assembly. Expression of the N-cadherin ΔCP mutant, which has shown to eliminate cadherin clustering and therefore suppresses integrin activation, had a dramatic impact on FN fibril assembly in cell doublets, eliminating ligand accumulation at the cell-cell junction site. Interestingly, mutant expression in cultured fibroblasts led to a 1.5-fold reduction in the average fibril intensity, revealing that AJs have a profound impact not only on determining the ligand binding on the cell surface via the recruitment of active integrin receptors there, but also on the generation and remodeling of the complex 3D fibrillar meshwork.

Our last aim was to examine the impact of AJs on the cell-surface ligand binding during live imaging, in order to acquire more mechanistic insights into this process. However, during live imaging, we came across various problems, with the most challenging one being the basal deposition of FN by individual cells, an artifact of seeding cells on extremely stiff substrates, like glass. *In vivo,* single cells don't have the ability to form fibrils since they cannot generate the sufficient force required for exposing cryptic sites within FN molecules necessary for fibrillar assembly. However, single cells seeded on stiff substrates have the capacity to generate sufficient force via actin contractility to expose the cryptic sites and promote fibrillar formation. Therefore, the basal deposition of FN observed masks any initial accumulation of FN at the cell-cell junctions, that we wanted to investigate. For this purpose, we went on to optimize a substrate that will closely mimic the *in vivo* state and thus eliminate basal deposition of FN with the use of various approaches. We concluded that the most efficient way to achieve this was with the use of concanavalin A coated substrates, which eliminated the artificial characteristic of cells seeded on

stiff substrates and allowed us to monitor FN accumulation and binding on the cell surface during live imaging. Remarkably, our data showed that AJ formation precedes and subsequently preferentially guides FN accumulation at these sites, further confirming our initial hypothesis. Future experiments need to be done regarding the further investigation of the role of AJs on ECM deposition and remodeling during live imaging. For instance, we could express the N-cadherin ΔCP mutant in cells with high transfection efficiency and examine its effect on the formation of the 3D fibrillar matrix. Moreover, given that the use of the RO-3306 inhibitor resulted in stronger fibrils at the cell-cell boundaries (**Figure 33**), we could examine whether treating cells with the inhibitor would impact FN accumulation at cell-cell junctions during live imaging.

Given the fact that we have established a system where cells fail to form FAs, but cell spreading is not affected, and simultaneously with the reduction of calcium AJ formation can be disrupted, we went on to take advantage of this system to explore the role of AJ-driven ligand-independent active integrin receptors in intracellular signaling pathways. Taking into consideration that most of the information available on integrin signaling concerns ligand-dependent integrin activation. Our data revealed that AJ-driven activation of integrins promotes intracellular signaling, given that disruption of AJs led to a decrease in phosphorylated Paxillin levels. Interestingly, phosphorylated Paxillin levels were also reduced in cells seeded on FN in calcium-free conditions suggesting that signaling from AJ-driven active integrins contributes to the total signaling of cells interacting with ECM.

Collectively our data provided substantial evidence and revealed the profound role of AJs not only on ligand binding on the cell surface but also on the 3D architecture of the ECM. Importantly, we showed that the impact of AJs on ECM formation and remodeling goes well beyond the establishment of tissue-level tension and provided mechanistic insight into the critical integrin-cadherin cross talk.

Based on the above effects of AJs on ECM deposition and remodeling *in vitro,* future experiments will have to be performed to examine the impact of AJs on ECM formation *in vivo*. Interestingly, during the early stages of embryonic development, the establishment of cell-cell adhesion happens prior to the basement membrane formation, implying that AJs could display a major role in the regulation of integrin activation and distribution. Notably, work by Kim et al., showed that integrin β1 is restricted only to the cell-cell boundaries of the early blastocyst prior to the establishment of

apicobasal polarity in the preimplantation mouse (Kim et al., 2021). Several studies revealed the impact of AJs on ECM formation using amphibian embryos, where the first fibrils form at the cell-cell boundaries (Boucaut et al., 1985; Schwarzbauer and DeSimone, 2011), similar to what we observed in cultured cells.

ABBREVIATIONS

ABBREVIATION	MEANING
FN	Fibronectin
ECM	Extracellular Matrix
FAK	Focal Adhesion Kinase
FAs	Focal Adhesions
FXs	Focal Complexes
FBs	Fibrillar Adhesions
AJs	Adherens Junctions
EMT	Epithelial to Mesenchymal Transition
EC	Extracellular Domain
ER	Endoplasmic Reticulum
CBD	Catenin Binding Domain
JMD	Juxtamembrane Domain
Y	Tyrosine
S	Serine
PM	Plasma Membrane

BIBLIOGRAPHY

ABERLE, T., BURCHARD, W., VORWERG, W. & RADOSTA, S. 1994. Conformational Contributions of Amylose and Amylopectin to the Structural Properties of Starches from Various Sources. 46**,** 329-335.

ACHARYA, B. R., WU, S. K., LIEU, Z. Z., PARTON, R. G., GRILL, S. W., BERSHADSKY, A. D., GOMEZ, G. A. & YAP, A. S. 2017. Mammalian Diaphanous 1 Mediates a Pathway for E-cadherin to Stabilize Epithelial Barriers through Junctional Contractility. *Cell Rep,* 18**,** 2854-2867.

ADAMS, C. L., CHEN, Y. T., SMITH, S. J. & NELSON, W. J. 1998. Mechanisms of epithelial cell-cell adhesion and cell compaction revealed by high-resolution tracking of E-cadherin-green fluorescent protein. *J Cell Biol,* 142**,** 1105-19.

ARGRAVES, W. S., SUZUKI, S., ARAI, H., THOMPSON, K., PIERSCHBACHER, M. D. & RUOSLAHTI, E. 1987. Amino acid sequence of the human fibronectin receptor. *J Cell Biol,* 105**,** 1183-90.

ARJONEN, A., KAUKONEN, R. & IVASKA, J. 2011. Filopodia and adhesion in cancer cell motility. *Cell Adh Migr,* 5**,** 421-30.

AUERNHEIMER, V., LAUTSCHAM, L. A., LEIDENBERGER, M., FRIEDRICH, O., KAPPES, B., FABRY, B. & GOLDMANN, W. H. 2015. Vinculin phosphorylation at residues Y100 and Y1065 is required for cellular force transmission. *Journal of cell science,* 128**,** 3435-3443.

AVIZIENYTE, E., FINCHAM, V. J., BRUNTON, V. G. & FRAME, M. C. 2004. Src SH3/2 domain-mediated peripheral accumulation of Src and phospho-myosin is linked to deregulation of E-cadherin and the epithelial-mesenchymal transition. *Mol Biol Cell,* 15**,** 2794-803.

BACHMANN, M., KUKKURAINEN, S., HYTÖNEN, V. P. & WEHRLE-HALLER, B. 2019. Cell Adhesion by Integrins. *Physiol Rev,* 99**,** 1655-1699.

BALLESTREM, C., HINZ, B., IMHOF, B. A. & WEHRLE-HALLER, B. 2001. Marching at the front and dragging behind: differential alphaVbeta3-integrin turnover regulates focal adhesion behavior. *J Cell Biol,* 155**,** 1319-32.

BARRY, A. K., TABDILI, H., MUHAMED, I., WU, J., SHASHIKANTH, N., GOMEZ, G. A., YAP, A. S., GOTTARDI, C. J., DE ROOIJ, J., WANG, N. & LECKBAND, D. E. 2014. α-catenin cytomechanics--role in cadherin-dependent adhesion and mechanotransduction. *J Cell Sci,* 127**,** 1779-91.

BARRY, A. K., WANG, N. & LECKBAND, D. E. 2015. Local VE-cadherin mechanotransduction triggers long-ranged remodeling of endothelial monolayers. *J Cell Sci,* 128**,** 1341-51.

BAYS, J. L. & DEMALI, K. A. 2017. Vinculin in cell-cell and cell-matrix adhesions. *Cell Mol Life Sci,* 74**,** 2999-3009.

BAYS, J. L., PENG, X., TOLBERT, C. E., GUILLUY, C., ANGELL, A. E., PAN, Y., SUPERFINE, R., BURRIDGE, K. & DEMALI, K. A. 2014. Vinculin phosphorylation differentially regulates mechanotransduction at cell-cell and cell-matrix adhesions. *J Cell Biol,* 205**,** 251-63.

BERTHIAUME, F., MOGHE, P. V., TONER, M. & YARMUSH, M. L. 1996. Effect of extracellular matrix topology on cell structure, function, and physiological responsiveness: hepatocytes cultured in a sandwich configuration. *Faseb j,* 10**,** 1471-84.

BERX, G. & VAN ROY, F. 2001. The E-cadherin/catenin complex: an important gatekeeper in breast cancer tumorigenesis and malignant progression. *Breast Cancer Res,* 3**,** 289-93.

BOGGON, T. J., MURRAY, J., CHAPPUIS-FLAMENT, S., WONG, E., GUMBINER, B. M. & SHAPIRO, L. 2002. C-Cadherin Ectodomain Structure and Implications for Cell Adhesion Mechanisms. 296**,** 1308-1313.

BÖKEL, C. & BROWN, N. H. J. D. C. 2002. Integrins in development: moving on, responding to, and sticking to the extracellular matrix. 3 3**,** 311-21.

BOUCAUT, J. C., DARRIBERE, T., LI, S. D., BOULEKBACHE, H., YAMADA, K. M. & THIERY, J. P. 1985. Evidence for the role of fibronectin in amphibian gastrulation. *J Embryol Exp Morphol,* 89 Suppl**,** 211-27.

BOUCHET, B. P., GOUGH, R. E., AMMON, Y. C., VAN DE WILLIGE, D., POST, H., JACQUEMET, G., ALTELAAR, A. M., HECK, A. J., GOULT, B. T. & AKHMANOVA,

A. 2016. Talin-KANK1 interaction controls the recruitment of cortical microtubule stabilizing complexes to focal adhesions. *Elife,* 5.

BOWLER, M. A., BERSI, M. R., RYZHOVA, L. M., JERRELL, R. J., PAREKH, A. & MERRYMAN, W. D. 2018. Cadherin-11 as a regulator of valve myofibroblast mechanobiology. *American journal of physiology. Heart and circulatory physiology,* 315**,** H1614-H1626.

BREMBECK, F. H., SCHWARZ-ROMOND, T., BAKKERS, J., WILHELM, S., HAMMERSCHMIDT, M., BIRCHMEIER, W. J. G. & DEVELOPMENT 2004. Essential role of BCL9-2 in the switch between beta-catenin's adhesive and transcriptional functions. 18 18**,** 2225-30.

BROWN, M. C. & TURNER, C. E. 2004. Paxillin: adapting to change. *Physiol Rev,* 84**,** 1315-39.

BURRIDGE, K., TURNER, C. E. & ROMER, L. H. 1992. Tyrosine phosphorylation of paxillin and pp125FAK accompanies cell adhesion to extracellular matrix: a role in cytoskeletal assembly. *J Cell Biol,* 119**,** 893-903.

CALDERWOOD, D. A., FUJIOKA, Y., DE PEREDA, J. M., GARCÍA-ALVAREZ, B., NAKAMOTO, T., MARGOLIS, B., MCGLADE, C. J., LIDDINGTON, R. C. & GINSBERG, M. H. 2003. Integrin beta cytoplasmic domain interactions with phosphotyrosine-binding domains: a structural prototype for diversity in integrin signaling. *Proc Natl Acad Sci U S A,* 100**,** 2272-7.

CAMPBELL, I. D. & HUMPHRIES, M. J. 2011. Integrin structure, activation, and interactions. *Cold Spring Harb Perspect Biol,* 3.

CAPALDO, C. T. & MACARA, I. G. 2007. Depletion of E-cadherin disrupts establishment but not maintenance of cell junctions in Madin-Darby canine kidney epithelial cells. *Mol Biol Cell,* 18**,** 189-200.

CARISEY, A., TSANG, R., GREINER, A. M., NIJENHUIS, N., HEATH, N., NAZGIEWICZ, A., KEMKEMER, R., DERBY, B., SPATZ, J. & BALLESTREM, C. 2013. Vinculin regulates the recruitment and release of core focal adhesion proteins in a force-dependent manner. *Curr Biol,* 23**,** 271-81.

CARTER, W. G., RAUVALA, H. & HAKOMORI, S. I. 1981. Studies on cell adhesion and recognition. II. The kinetics of cell adhesion and cell spreading on surfaces coated with

carbohydrate-reactive proteins (glycosidases and lectins) and fibronectin. *The Journal of cell biology,* 88**,** 138-148.

CHANG, D., NALLS, M. A., HALLGRÍMSDÓTTIR, I. B., HUNKAPILLER, J., VAN DER BRUG, M., CAI, F., KERCHNER, G. A., AYALON, G., BINGOL, B., SHENG, M., HINDS, D., BEHRENS, T. W., SINGLETON, A. B., BHANGALE, T. R. & GRAHAM, R. R. 2017. A meta-analysis of genome-wide association studies identifies 17 new Parkinson's disease risk loci. *Nat Genet,* 49**,** 1511-1516.

CHARRAS, G. & YAP, A. S. 2018. Tensile Forces and Mechanotransduction at Cell-Cell Junctions. *Curr Biol,* 28**,** R445-R457.

CHARRIER, E. E., POGODA, K., LI, R., PARK, C. Y., FREDBERG, J. J. & JANMEY, P. A. 2020. A novel method to make viscoelastic polyacrylamide gels for cell culture and traction force microscopy. *APL Bioeng,* 4**,** 036104.

CHEN, X. L., NAM, J. O., JEAN, C., LAWSON, C., WALSH, C. T., GOKA, E., LIM, S. T., TOMAR, A., TANCIONI, I., URYU, S., GUAN, J. L., ACEVEDO, L. M., WEIS, S. M., CHERESH, D. A. & SCHLAEPFER, D. D. 2012. VEGF-induced vascular permeability is mediated by FAK. *Dev Cell,* 22**,** 146-57.

CHEN, Y.-T., STEWART, D. B. & NELSON, W. J. J. T. J. O. C. B. 1999. Coupling Assembly of the E-Cadherin/β-Catenin Complex to Efficient Endoplasmic Reticulum Exit and Basal-lateral Membrane Targeting of E-Cadherin in Polarized MDCK Cells. 144**,** 687 - 699.

COLIN HUGHES, R. 1992. Lectins as cell adhesion molecules. *Current Opinion in Structural Biology,* 2**,** 687-692.

CONACCI-SORRELL, M., SIMCHA, I., BEN-YEDIDIA, T., BLECHMAN, J., SAVAGNER, P. & BEN-ZE'EV, A. 2003. Autoregulation of E-cadherin expression by cadherin-cadherin interactions: the roles of beta-catenin signaling, Slug, and MAPK. *J Cell Biol,* 163**,** 847-57.

CUKIERMAN, E., PANKOV, R., STEVENS, D. R. & YAMADA, K. M. 2001. Taking cell-matrix adhesions to the third dimension. *Science,* 294**,** 1708-12.

DAVIDENKO, N., SCHUSTER, C. F., BAX, D. V., FARNDALE, R. W., HAMAIA, S., BEST, S. M. & CAMERON, R. E. 2016. Evaluation of cell binding to collagen and gelatin: a study of the effect of 2D and 3D architecture and surface chemistry. *J Mater Sci Mater Med,* 27**,** 148.

DAVIDSON, L. A., DZAMBA, B. D., KELLER, R. & DESIMONE, D. W. 2008. Live imaging of cell protrusive activity, and extracellular matrix assembly and remodeling during morphogenesis in the frog, Xenopus laevis. *Dev Dyn,* 237**,** 2684-92.

DAVIDSON, L. A., KELLER, R. E. & DESIMONE, D. W. J. D. D. 2004. Assembly and remodeling of the fibrillar fibronectin extracellular matrix during gastrulation and neurulation in Xenopus laevis. 231.

DAVIDSON, L. A., MARSDEN, M., KELLER, R. E. & DESIMONE, D. W. J. C. B. 2006. Integrin#±5²1 and Fibronectin Regulate Polarized Cell Protrusions Required for Xenopus Convergence and Extension. 16**,** 833-844.

DAVIS, M. A., IRETON, R. C. & REYNOLDS, A. B. J. T. J. O. C. B. 2003. A core function for p120-catenin in cadherin turnover. 163**,** 525 - 534.

DE ROOIJ, J., KERSTENS, A., DANUSER, G., SCHWARTZ, M. A. & WATERMAN-STORER, C. M. 2005. Integrin-dependent actomyosin contraction regulates epithelial cell scattering. *J Cell Biol,* 171**,** 153-64.

DERAMAUDT, T. B., DUJARDIN, D., HAMADI, A., NOULET, F., KOLLI, K., DE MEY, J., TAKEDA, K. & RONDÉ, P. 2011. FAK phosphorylation at Tyr-925 regulates cross-talk between focal adhesion turnover and cell protrusion. *Mol Biol Cell,* 22**,** 964-75.

DOHERTY, P. & WALSH, F. S. 1996. CAM-FGF Receptor Interactions: A Model for Axonal Growth. *Mol Cell Neurosci,* 8**,** 99-111.

DZAMBA, B. J., JAKAB, K. R., MARSDEN, M., SCHWARTZ, M. A. & DESIMONE, D. W. 2009. Cadherin adhesion, tissue tension, and noncanonical Wnt signaling regulate fibronectin matrix organization. *Dev Cell,* 16**,** 421-32.

ENGL, W., ARASI, B., YAP, L. L., THIERY, J. P. & VIASNOFF, V. 2014. Actin dynamics modulate mechanosensitive immobilization of E-cadherin at adherens junctions. *Nat Cell Biol,* 16**,** 587-94.

ERICKSON, H. P. & CARRELL, N. A. J. T. J. O. B. C. 1983. Fibronectin in extended and compact conformations. Electron microscopy and sedimentation analysis. 258 23**,** 14539-44.

ETIENNE-MANNEVILLE, S. & HALL, A. 2002. Rho GTPases in cell biology. *Nature,* 420**,** 629-35.

EZRATTY, E. J., PARTRIDGE, M. A. & GUNDERSEN, G. G. 2005. Microtubule-induced focal adhesion disassembly is mediated by dynamin and focal adhesion kinase. *Nat Cell Biol,* 7**,** 581-90.

FARRAR, C. S. & HOCKING, D. C. 2018. Assembly of fibronectin fibrils selectively attenuates platelet-derived growth factor-induced intracellular calcium release in fibroblasts. *J Biol Chem,* 293**,** 18655-18666.

FELDING-HABERMANN, B. & CHERESH, D. A. 1993. Vitronectin and its receptors. *Curr Opin Cell Biol,* 5**,** 864-8.

FERRARIS, G. M., SCHULTE, C., BUTTIGLIONE, V., DE LORENZI, V., PIONTINI, A., GALLUZZI, M., PODESTÀ, A., MADSEN, C. D. & SIDENIUS, N. 2014. The interaction between uPAR and vitronectin triggers ligand-independent adhesion signalling by integrins. *Embo j,* 33**,** 2458-72.

FRANTZ, C., STEWART, K. M. & WEAVER, V. M. 2010. The extracellular matrix at a glance. *J Cell Sci,* 123**,** 4195-200.

FUJITA, Y., KRAUSE, G., SCHEFFNER, M., ZECHNER, D., LEDDY, H. E., BEHRENS, J., SOMMER, T. & BIRCHMEIER, W. 2002. Hakai, a c-Cbl-like protein, ubiquitinates and induces endocytosis of the E-cadherin complex. *Nat Cell Biol,* 4**,** 222-31.

GALBRAITH, C. G., YAMADA, K. M. & GALBRAITH, J. A. 2007. Polymerizing actin fibers position integrins primed to probe for adhesion sites. *Science,* 315**,** 992-5.

GARCIA, M. A., NELSON, W. J. & CHAVEZ, N. 2018. Cell-Cell Junctions Organize Structural and Signaling Networks. *Cold Spring Harb Perspect Biol,* 10.

GEIGER, B., BERSHADSKY, A., PANKOV, R. & YAMADA, K. M. 2001. Transmembrane crosstalk between the extracellular matrix and the cytoskeleton. *Nature Reviews Molecular Cell Biology,* 2**,** 793-805.

GENDA, T., SAKAMOTO, M., ICHIDA, T., ASAKURA, H. & HIROHASHI, S. 2000. Loss of cell-cell contact is induced by integrin-mediated cell-substratum adhesion in highly-motile and highly-metastatic hepatocellular carcinoma cells. *Lab Invest,* 80**,** 387-94.

GEORGE, E. L., GEORGES-LABOUESSE, E. N., PATEL-KING, R. S., RAYBURN, H. & HYNES, R. O. 1993. Defects in mesoderm, neural tube and vascular development in mouse embryos lacking fibronectin. *Development,* 119**,** 1079-1091.

GIANNONE, G., JIANG, G., SUTTON, D., CRITCHLEY, D. & SHEETZ, M. 2003. Talin1 is critical for force-dependent reinforcement of initial integrin-cytoskeleton bonds but not tyrosine kinase activation. *The Journal of cell biology,* 163**,** 409-19.

GILCHRIST, C. L., LEDDY, H. A., KAYE, L., CASE, N. D., ROTHENBERG, K. E., LITTLE, D., LIEDTKE, W., HOFFMAN, B. D. & GUILAK, F. 2019. TRPV4-mediated calcium signaling in mesenchymal stem cells regulates aligned collagen matrix formation and vinculin tension. *Proc Natl Acad Sci U S A,* 116**,** 1992-1997.

GINSBERG, M. H. 2014. Integrin activation. *BMB Rep,* 47**,** 655-9.

GLORIEUX, F. H. 2008. Osteogenesis imperfecta. *Best Pract Res Clin Rheumatol,* 22**,** 85-100.

GOÑI, G. M., EPIFANO, C., BOSKOVIC, J., CAMACHO-ARTACHO, M., ZHOU, J., BRONOWSKA, A., MARTÍN, M. T., ECK, M. J., KREMER, L., GRÄTER, F., GERVASIO, F. L., PEREZ-MORENO, M. & LIETHA, D. 2014. Phosphatidylinositol 4,5-bisphosphate triggers activation of focal adhesion kinase by inducing clustering and conformational changes. *Proc Natl Acad Sci U S A,* 111**,** E3177-86.

GOTO, T., DAVIDSON, L. A., ASASHIMA, M. & KELLER, R. J. C. B. 2005. Planar Cell Polarity Genes Regulate Polarized Extracellular Matrix Deposition during Frog Gastrulation. 15**,** 787-793.

GOUGH, R. E., JONES, M. C., ZACHARCHENKO, T., LE, S., YU, M., JACQUEMET, G., MUENCH, S. P., YAN, J., HUMPHRIES, J. D., JORGENSEN, C., HUMPHRIES, M. J. & GOULT, B. T. 2021. Talin mechanosensitivity is modulated by a direct interaction with cyclin-dependent kinase-1. *J Biol Chem,* 297**,** 100837.

GREEN, J. A., BERRIER, A. L., PANKOV, R. & YAMADA, K. M. 2009. beta1 integrin cytoplasmic domain residues selectively modulate fibronectin matrix assembly and cell spreading through talin and Akt-1. *J Biol Chem,* 284**,** 8148-59.

GROBE, H., WUSTENHAGEN, A., BAARLINK, C., GROSSE, R. & GRIKSCHEIT, K. 2018. A Rac1-FMNL2 signaling module affects cell-cell contact formation independent of Cdc42 and membrane protrusions. *PLoS One,* 13**,** e0194716.

GUMBINER, B. & SIMONS, K. 1986. A functional assay for proteins involved in establishing an epithelial occluding barrier: identification of a uvomorulin-like polypeptide. *J Cell Biol,* 102**,** 457-68.

GUMBINER, B. M. 2005. Regulation of cadherin-mediated adhesion in morphogenesis. *Nat Rev Mol Cell Biol,* 6**,** 622-34.

GUO, W. H., FREY, M. T., BURNHAM, N. A. & WANG, Y. L. 2006. Substrate rigidity regulates the formation and maintenance of tissues. *Biophys J,* 90**,** 2213-20.

GUPTA, S., DUSZYC, K., VERMA, S., BUDNAR, S., LIANG, X., GOMEZ, G. A., MARCQ, P., NOORDSTRA, I. & YAP, A. S. 2021. Enhanced RhoA signalling stabilizes E-cadherin in migrating epithelial monolayers. *J Cell Sci,* 134.

GUY, D., LATNER, A. L. & TURNER, G. A. 1979. A simple lectin-mediated cell-adhesion method for investigating the cell surface. *Exp Cell Biol,* 47**,** 312-9.

HAGEL, M., GEORGE, E. L., KIM, A., TAMIMI, R. M., OPITZ, S. L., TURNER, C. E., IMAMOTO, A., THOMAS, S. M. J. M. & BIOLOGY, C. 2002. The Adaptor Protein Paxillin Is Essential for Normal Development in the Mouse and Is a Critical Transducer of Fibronectin Signaling. 22**,** 901 - 915.

HALLIDAY, N. L. & TOMASEK, J. J. J. E. C. R. 1995. Mechanical properties of the extracellular matrix influence fibronectin fibril assembly in vitro. 217 1**,** 109-17.

HANKS, S. K., RYZHOVA, L. M., SHIN, N.-Y., BRÁBEK, J. J. F. I. B. A. J. & LIBRARY, V. 2003. Focal adhesion kinase signaling activities and their implications in the control of cell survival and motility. 8**,** d982-96.

HARRIS, A. R., DAEDEN, A. & CHARRAS, G. T. 2014. Formation of adherens junctions leads to the emergence of a tissue-level tension in epithelial monolayers. *Journal of Cell Science,* 127**,** 2507-2517.

HARTSOCK, A. & NELSON, W. J. 2008. Adherens and tight junctions: structure, function and connections to the actin cytoskeleton. *Biochim Biophys Acta,* 1778**,** 660-9.

HILDEBRAND, J. D., SCHALLER, M. D. & PARSONS, J. T. 1993. Identification of sequences required for the efficient localization of the focal adhesion kinase, pp125FAK, to cellular focal adhesions. *Journal of Cell Biology,* 123**,** 993-1005.

HOTCHIN, N. A. & HALL, A. 1995. The assembly of integrin adhesion complexes requires both extracellular matrix and intracellular rho/rac GTPases. *Journal of Cell Biology,* 131**,** 1857-1865.

HOWDEN, J. D., MICHAEL, M., HIGHT-WARBURTON, W. & PARSONS, M. 2021. alpha2beta1 integrins spatially restrict Cdc42 activity to stabilise adherens junctions. *BMC Biol,* 19**,** 130.

HUBER, A. H. & WEIS, W. I. 2001. The structure of the beta-catenin/E-cadherin complex and the molecular basis of diverse ligand recognition by beta-catenin. *Cell,* 105**,** 391-402.

HUI, L., ZHANG, S., DONG, X., TIAN, D., CUI, Z. & QIU, X. 2013. Prognostic significance of twist and N-cadherin expression in NSCLC. *PLoS One,* 8**,** e62171.

HUMPHREYS, B. D., LIN, S. L., KOBAYASHI, A., HUDSON, T. E., NOWLIN, B. T., BONVENTRE, J. V., VALERIUS, M. T., MCMAHON, A. P. & DUFFIELD, J. S. 2010. Fate tracing reveals the pericyte and not epithelial origin of myofibroblasts in kidney fibrosis. *Am J Pathol,* 176**,** 85-97.

HUMPHRIES, J. D., BYRON, A. & HUMPHRIES, M. J. 2006. Integrin ligands at a glance. *J Cell Sci,* 119**,** 3901-3.

HUMPHRIES, J. D., WANG, P., STREULI, C., GEIGER, B., HUMPHRIES, M. J. & BALLESTREM, C. 2007. Vinculin controls focal adhesion formation by direct interactions with talin and actin. *J Cell Biol,* 179**,** 1043-57.

HYNES, R. O. 1990. Interactions of Fibronectins. *In:* HYNES, R. O. (ed.) *Fibronectins.* New York, NY: Springer New York.

HYNES, R. O. 2002. Integrins: bidirectional, allosteric signaling machines. *Cell,* 110**,** 673-87.

HYNES, R. O. & YAMADA, K. M. 1982. Fibronectins: multifunctional modular glycoproteins. *J Cell Biol,* 95**,** 369-77.

ILIĆ, D. K., KOVAČIČ, B., JOHKURA, K., SCHLAEPFER, D. D., TOMAŠEVIĆ, N., HAN, Q., KIM, J.-B., HOWERTON, K., BAUMBUSCH, C., OGIWARA, N., STREBLOW, D. N., NELSON, J. A., DAZIN, P., SHINO, Y., SASAKI, K. & DAMSKY, C. H. 2004. FAK promotes organization of fibronectin matrix and fibrillar adhesions. *Journal of Cell Science,* 117**,** 177-187.

ISHIYAMA, N., LEE, S. H., LIU, S., LI, G. Y., SMITH, M. J., REICHARDT, L. F. & IKURA, M. 2010. Dynamic and static interactions between p120 catenin and E-cadherin regulate the stability of cell-cell adhesion. *Cell,* 141**,** 117-28.

ISLAM, S., CAREY, T. E., WOLF, G. T., WHEELOCK, M. J. & JOHNSON, K. R. J. T. J. O. C. B. 1996. Expression of N-cadherin by human squamous carcinoma cells induces a scattered fibroblastic phenotype with disrupted cell-cell adhesion. 135**,** 1643 - 1654.

IZARD, T., EVANS, G., BORGON, R., RUSH, C. L., BRICOGNE, G. & BOIS, P. R. J. J. N. 2004. Vinculin activation by talin through helical bundle conversion. 427**,** 171-175.

JÄRVELÄINEN, H., SAINIO, A., KOULU, M., WIGHT, T. N. & PENTTINEN, R. 2009. Extracellular matrix molecules: potential targets in pharmacotherapy. *Pharmacol Rev,* 61**,** 198-223.

JIANG, Y., REN, W., WANG, W., XIA, J., GOU, L., LIU, M., WAN, Q., ZHOU, L., WENG, Y., HE, T. & ZHANG, Y. 2017. Inhibitor of β-catenin and TCF (ICAT) promotes cervical cancer growth and metastasis by disrupting E-cadherin/β-catenin complex. *Oncol Rep,* 38**,** 2597-2606.

JOHNSON, K. J., SAGE, H., BRISCOE, G. & ERICKSON, H. P. 1999. The compact conformation of fibronectin is determined by intramolecular ionic interactions. *J Biol Chem,* 274**,** 15473-9.

JOHNSON, R. P. & CRAIG, S. W. 1994. An intramolecular association between the head and tail domains of vinculin modulates talin binding. *J Biol Chem,* 269**,** 12611-9.

JOHNSON, R. P. & CRAIG, S. W. 1995. F-actin binding site masked by the intramolecular association of vinculin head and tail domains. *Nature,* 373**,** 261-4.

JONES, M. C., ASKARI, J. A., HUMPHRIES, J. D. & HUMPHRIES, M. J. 2018. Cell adhesion is regulated by CDK1 during the cell cycle. *J Cell Biol,* 217**,** 3203-3218.

JULICH, D., COBB, G., MELO, A. M., MCMILLEN, P., LAWTON, A. K., MOCHRIE, S. G., RHOADES, E. & HOLLEY, S. A. 2015. Cross-Scale Integrin Regulation Organizes ECM and Tissue Topology. *Dev Cell,* 34**,** 33-44.

JÜLICH, D., MOULD, A. P., KOPER, E. & HOLLEY, S. A. 2009. Control of extracellular matrix assembly along tissue boundaries via Integrin and Eph/Ephrin signaling. *Development,* 136**,** 2913-21.

KAISER, H. W., NESS, W., OFFERS, M., O'KEEFE, E. J. & KREYSEL, H. W. 1993. Talin: adherens junction protein is localized at the epidermal-dermal interface in skin. *J Invest Dermatol,* 101**,** 789-93.

KAVERINA, I., KRYLYSHKINA, O. & SMALL, J. V. 1999. Microtubule targeting of substrate contacts promotes their relaxation and dissociation. *J Cell Biol,* 146**,** 1033-44.

KIM, E. J. Y., SOROKIN, L. & HIIRAGI, T. 2022. ECM-integrin signalling instructs cellular position sensing to pattern the early mouse embryo. *Development,* 149.

KIM, J., LEE, J., JANG, J., YE, F., HONG, S. J., PETRICH, B. G., ULMER, T. S. & KIM, C. 2020. Topological Adaptation of Transmembrane Domains to the Force-Modulated Lipid Bilayer Is a Basis of Sensing Mechanical Force. *Curr Biol,* 30**,** 1614-1625 e5.

KIM, T. J., ZHENG, S., SUN, J., MUHAMED, I., WU, J., LEI, L., KONG, X., LECKBAND, D. E. & WANG, Y. 2015. Dynamic visualization of alpha-catenin reveals rapid, reversible conformation switching between tension states. *Curr Biol,* 25**,** 218-224.

KIRCHHOFER, D., GRZESIAK, J. & PIERSCHBACHER, M. D. 1991. Calcium as a potential physiological regulator of integrin-mediated cell adhesion. *J Biol Chem,* 266**,** 4471-7.

KLANN, J. E., REMEDIOS, K. A., KIM, S. H., METZ, P. J., LOPEZ, J., MACK, L. A., ZHENG, Y., GINSBERG, M. H., PETRICH, B. G. & CHANG, J. T. 2017. Talin Plays a Critical Role in the Maintenance of the Regulatory T Cell Pool. *J Immunol,* 198**,** 4639-4651.

KLAPHOLZ, B. & BROWN, N. H. 2017. Talin – the master of integrin adhesions. *Journal of Cell Science,* 130**,** 2435-2446.

KOENIG, A., MUELLER, C., HASEL, C., ADLER, G. & MENKE, A. 2006. Collagen type I induces disruption of E-cadherin-mediated cell-cell contacts and promotes proliferation of pancreatic carcinoma cells. *Cancer Res,* 66**,** 4662-71.

KRAGTORP, K. A. & MILLER, J. R. 2006. Regulation of somitogenesis by Ena/VASP proteins and FAK during Xenopus development. *Development,* 133**,** 685-95.

KRAMER, K. L., BARNETTE, J. E. & YOST, H. J. 2002. PKCgamma regulates syndecan-2 inside-out signaling during xenopus left-right development. *Cell,* 111**,** 981-90.

KWOK, W., LEE, S. H., CULBERSON, C., KORNESZCZUK, K. & CLEMENS, M. G. 2009. Caveolin-1 mediates endotoxin inhibition of endothelin-1-induced endothelial nitric oxide synthase activity in liver sinusoidal endothelial cells. *Am J Physiol Gastrointest Liver Physiol,* 297**,** G930-9.

LE, A. T. & STAINIER, D. Y. R. 2004. Fibronectin Regulates Epithelial Organization during Myocardial Migration in Zebrafish. *Developmental Cell,* 6**,** 371-382.

LE DUC, Q., SHI, Q., BLONK, I., SONNENBERG, A., WANG, N., LECKBAND, D. E. & DE ROOIJ, J. J. T. J. O. C. B. 2010. Vinculin potentiates E-cadherin mechanosensing and is recruited to actin-anchored sites within adherens junctions in a myosin II–dependent manner. 191**,** 891 - 891.

LECKBAND, D. E., LE DUC, Q., WANG, N. & DE ROOIJ, J. 2011. Mechanotransduction at cadherin-mediated adhesions. *Curr Opin Cell Biol,* 23**,** 523-30.

LEE, G., HYNES, R. & KIRSCHNER, M. 1984. Temporal and spatial regulation of fibronectin in early Xenopus development. *Cell,* 36**,** 729-40.

LEFORT, C. T., WOJCIECHOWSKI, K. & HOCKING, D. C. 2011. N-cadherin cell-cell adhesion complexes are regulated by fibronectin matrix assembly. *J Biol Chem,* 286**,** 3149-60.

LEGATE, K. R., TAKAHASHI, S., BONAKDAR, N., FABRY, B., BOETTIGER, D., ZENT, R. & FÄSSLER, R. 2011. Integrin adhesion and force coupling are independently regulated by localized PtdIns(4,5)2 synthesis. *Embo j,* 30**,** 4539-53.

LI, L., ZHANG, R., YANG, H., ZHANG, D., LIU, J., LI, J. & GUO, B. 2020. GDF15 knockdown suppresses cervical cancer cell migration in vitro through the TGF-β/Smad2/3/Snail1 pathway. *FEBS Open Bio,* 10**,** 2750-2760.

LI, R., MITRA, N., GRATKOWSKI, H., VILAIRE, G., LITVINOV, R., NAGASAMI, C., WEISEL, J. W., LEAR, J. D., DEGRADO, W. F. & BENNETT, J. S. 2003. Activation of Integrin αIIbβ3 by Modulation of Transmembrane Helix Associations. 300**,** 795-798.

LICKERT, H., BAUER, A., KEMLER, R. & STAPPERT, J. J. T. J. O. B. C. 2000. Casein kinase II phosphorylation of E-cadherin increases E-cadherin/beta-catenin interaction and strengthens cell-cell adhesion. 275 7**,** 5090-5.

LILIEN, J., BALSAMO, J., ARREGUI, C. & XU, G. 2002. Turn-off, drop-out: functional state switching of cadherins. *Dev Dyn,* 224**,** 18-29.

LIU, Y. 2006. Renal fibrosis: new insights into the pathogenesis and therapeutics. *Kidney Int,* 69**,** 213-7.

LOH, C. Y., CHAI, J. Y., TANG, T. F., WONG, W. F., SETHI, G., SHANMUGAM, M. K., CHONG, P. P. & LOOI, C. Y. 2019. The E-Cadherin and N-Cadherin Switch in Epithelial-to-Mesenchymal Transition: Signaling, Therapeutic Implications, and Challenges. *Cells,* 8.

LONGHURST, C. M. & JENNINGS, L. K. 1998. Integrin-mediated signal transduction. *Cell Mol Life Sci,* 54**,** 514-26.

LUO, B. H., CARMAN, C. V. & SPRINGER, T. A. 2007. Structural basis of integrin regulation and signaling. *Annu Rev Immunol,* 25**,** 619-47.

MA, G. J., FERHAN, A. R., JACKMAN, J. A. & CHO, N.-J. 2020. Conformational flexibility of fatty acid-free bovine serum albumin proteins enables superior antifouling coatings. *Communications Materials,* 1**,** 45.

MAHABELESHWAR, G. H., FENG, W., REDDY, K. B., PLOW, E. F. & BYZOVA, T. V. J. C. R. 2007. Mechanisms of Integrin–Vascular Endothelial Growth Factor Receptor Cross-Activation in Angiogenesis. 101**,** 570-580.

MAIN, A. L., HARVEY, T. S., BARON, M., BOYD, J. & CAMPBELL, I. D. 1992. The three-dimensional structure of the tenth type III module of fibronectin: an insight into RGD-mediated interactions. *Cell,* 71**,** 671-8.

MAKOGONENKO, E., TSURUPA, G., INGHAM, K. & MEDVED, L. 2002. Interaction of fibrin(ogen) with fibronectin: further characterization and localization of the fibronectin-binding site. *Biochemistry,* 41**,** 7907-13.

MAO, Y. & SCHWARZBAUER, J. E. 2005. Fibronectin fibrillogenesis, a cell-mediated matrix assembly process. *Matrix Biol,* 24**,** 389-99.

MARSDEN, M. & DESIMONE, D. W. 2003. Integrin-ECM Interactions Regulate Cadherin-Dependent Cell Adhesion and Are Required for Convergent Extension in Xenopus. *Current Biology,* 13**,** 1182-1191.

MARTINEZ-RICO, C., PINCET, F., THIERY, J. P. & DUFOUR, S. 2010. Integrins stimulate E-cadherin-mediated intercellular adhesion by regulating Src-kinase activation and actomyosin contractility. *J Cell Sci,* 123**,** 712-22.

MATLASHOV, M. E., SHCHERBAKOVA, D. M., ALVELID, J., BALOBAN, M., PENNACCHIETTI, F., SHEMETOV, A. A., TESTA, I. & VERKHUSHA, V. V. 2020. A set of monomeric near-infrared fluorescent proteins for multicolor imaging across scales. *Nat Commun,* 11**,** 239.

MCDONALD, J. A., QUADE, B. J., BROEKELMANN, T. J., LACHANCE, R., FORSMAN, K., HASEGAWA, E. & AKIYAMA, S. 1987. Fibronectin's cell-adhesive domain and an

amino-terminal matrix assembly domain participate in its assembly into fibroblast pericellular matrix. *J Biol Chem,* 262**,** 2957-67.

MENG, W. & TAKEICHI, M. 2009. Adherens junction: molecular architecture and regulation. *Cold Spring Harb Perspect Biol,* 1**,** a002899.

MIIHKINEN, M., GRONLOH, M. L. B., POPOVIC, A., VIHINEN, H., JOKITALO, E., GOULT, B. T., IVASKA, J. & JACQUEMET, G. 2021. Myosin-X and talin modulate integrin activity at filopodia tips. *Cell Rep,* 36**,** 109716.

MINIGO, G., SCHOLZEN, A., TANG, C. K., HANLEY, J. C., KALKANIDIS, M., PIETERSZ, G. A., APOSTOLOPOULOS, V. & PLEBANSKI, M. 2007. Poly-L-lysine-coated nanoparticles: a potent delivery system to enhance DNA vaccine efficacy. *Vaccine,* 25**,** 1316-27.

MITRA, S. K., HANSON, D. A. & SCHLAEPFER, D. D. 2005. Focal adhesion kinase: in command and control of cell motility. *Nat Rev Mol Cell Biol,* 6**,** 56-68.

MIYAMOTO, S., TERAMOTO, H., COSO, O. A., GUTKIND, J. S., BURBELO, P. D., AKIYAMA, S. K. & YAMADA, K. M. 1995. Integrin function: molecular hierarchies of cytoskeletal and signaling molecules. *J Cell Biol,* 131**,** 791-805.

MIYAMOTO, Y., SAKANE, F. & HASHIMOTO, K. 2015. N-cadherin-based adherens junction regulates the maintenance, proliferation, and differentiation of neural progenitor cells during development. *Cell Adh Migr,* 9**,** 183-92.

MOESE, S., SELBACH, M., BRINKMANN, V., KARLAS, A., HAIMOVICH, B., BACKERT, S. & MEYER, T. F. 2007. The Helicobacter pylori CagA protein disrupts matrix adhesion of gastric epithelial cells by dephosphorylation of vinculin. *Cell Microbiol,* 9**,** 1148-61.

MOSER, M., LEGATE, K. R., ZENT, R. & FÄSSLER, R. 2009. The Tail of Integrins, Talin, and Kindlins. 324**,** 895-899.

MOSHER, D. 2012. *Fibronectin,* Elsevier.

MOULD, A. P., ASKARI, J. A., BYRON, A., TAKADA, Y., JOWITT, T. A. & HUMPHRIES, M. J. 2016. Ligand-induced Epitope Masking: DISSOCIATION OF INTEGRIN alpha5beta1-FIBRONECTIN COMPLEXES ONLY BY MONOCLONAL ANTIBODIES WITH AN ALLOSTERIC MODE OF ACTION. *J Biol Chem,* 291**,** 20993-21007.

MUI, K. L., BAE, Y. H., GAO, L., LIU, S. L., XU, T., RADICE, G. L., CHEN, C. S. & ASSOIAN, R. K. 2015. N-Cadherin Induction by ECM Stiffness and FAK Overrides the Spreading Requirement for Proliferation of Vascular Smooth Muscle Cells. *Cell Rep,* 10**,** 1477-1486.

MUI, K. L., CHEN, C. S. & ASSOIAN, R. K. 2016. The mechanical regulation of integrin-cadherin crosstalk organizes cells, signaling and forces. *J Cell Sci,* 129**,** 1093-100.

NAM, J. S., INO, Y., SAKAMOTO, M. & HIROHASHI, S. 2002. Src family kinase inhibitor PP2 restores the E-cadherin/catenin cell adhesion system in human cancer cells and reduces cancer metastasis. *Clin Cancer Res,* 8**,** 2430-6.

NELSON, W. J. & NUSSE, R. 2004. Convergence of Wnt, beta-catenin, and cadherin pathways. *Science,* 303**,** 1483-7.

NG, M. R., BESSER, A., BRUGGE, J. S. & DANUSER, G. 2014. Mapping the dynamics of force transduction at cell-cell junctions of epithelial clusters. *Elife,* 3**,** e03282.

NISHIMURA, T. & TAKEICHI, M. 2009. Remodeling of the adherens junctions during morphogenesis. *Curr Top Dev Biol,* 89**,** 33-54.

OHASHI, T. & ERICKSON, H. P. 2009. Revisiting the mystery of fibronectin multimers: The fibronectin matrix is composed of fibronectin dimers cross-linked by non-covalent bonds. *Matrix Biology,* 28**,** 170-175.

OHASHI, T., KIEHART, D. P. & ERICKSON, H. P. J. J. O. C. S. 2002. Dual labeling of the fibronectin matrix and actin cytoskeleton with green fluorescent protein variants. 115 Pt 6**,** 1221-9.

OLIINYK, O. S., SHEMETOV, A. A., PLETNEV, S., SHCHERBAKOVA, D. M. & VERKHUSHA, V. V. 2019. Smallest near-infrared fluorescent protein evolved from cyanobacteriochrome as versatile tag for spectral multiplexing. *Nat Commun,* 10**,** 279.

OUYANG, M., LU, S., KIM, T., CHEN, C. E., SEONG, J., LECKBAND, D. E., WANG, F., REYNOLDS, A. B., SCHWARTZ, M. A. & WANG, Y. 2013. N-cadherin regulates spatially polarized signals through distinct p120ctn and beta-catenin-dependent signalling pathways. *Nat Commun,* 4**,** 1589.

PALADI, M. & TEPASS, U. 2004. Function of Rho GTPases in embryonic blood cell migration in Drosophila. *Journal of Cell Science,* 117**,** 6313-6326.

PANKOV, R., CUKIERMAN, E., KATZ, B.-Z., MATSUMOTO, K., LIN, D. C., LIN, S., HAHN, C. S. & YAMADA, K. M. J. J. O. C. B. 2000. Integrin Dynamics and Matrix Assembly:

Tensin-Dependent Translocation of#±8²1 Integrins Promotes Early Fibronectin Fibrillogenesis. 148**,** 1075-1090.

PANKOV, R. & YAMADA, K. M. 2002. Fibronectin at a glance. *J Cell Sci,* 115**,** 3861-3.

PARADZIK, M., HUMPHRIES, J. D., STOJANOVIC, N., NESTIC, D., MAJHEN, D., DEKANIC, A., SAMARZIJA, I., SEDDA, D., WEBER, I., HUMPHRIES, M. J. & AMBRIOVIC-RISTOV, A. 2020. KANK2 Links alphaVbeta5 Focal Adhesions to Microtubules and Regulates Sensitivity to Microtubule Poisons and Cell Migration. *Front Cell Dev Biol,* 8**,** 125.

PARSONS, J. T., HORWITZ, A. R. & SCHWARTZ, M. A. 2010. Cell adhesion: integrating cytoskeletal dynamics and cellular tension. *Nat Rev Mol Cell Biol,* 11**,** 633-43.

PATEL, N. S., DOBBIE, M. S., ROCHESTER, M., STEERS, G., POULSOM, R., LE MONNIER, K., CRANSTON, D. W., LI, J. L. & HARRIS, A. L. 2006. Up-regulation of endothelial delta-like 4 expression correlates with vessel maturation in bladder cancer. *Clin Cancer Res,* 12**,** 4836-44.

PETIT, V. & THIERY, J. P. 2000. Focal adhesions: structure and dynamics. *Biol Cell,* 92**,** 477-94.

PETRIDOU, N. I. & SKOURIDES, P. A. 2016. A ligand-independent integrin β1 mechanosensory complex guides spindle orientation. *Nat Commun,* 7**,** 10899.

PICKFORD, A. R., POTTS, J. R., BRIGHT, J. R., PHAN, I. & CAMPBELL, I. D. 1997. Solution structure of a type 2 module from fibronectin: implications for the structure and function of the gelatin-binding domain. *Structure,* 5**,** 359-70.

PIEDRA, J., MIRAVET, S., CASTAÑO, J., PÁLMER, H. G., HEISTERKAMP, N., GARCÍA DE HERREROS, A. & DUÑACH, M. 2003. p120 Catenin-associated Fer and Fyn tyrosine kinases regulate beta-catenin Tyr-142 phosphorylation and beta-catenin-alpha-catenin Interaction. *Mol Cell Biol,* 23**,** 2287-97.

PLAYFORD, M. P., VADALI, K., CAI, X., BURRIDGE, K. & SCHALLER, M. D. 2008. Focal adhesion kinase regulates cell-cell contact formation in epithelial cells via modulation of Rho. *Experimental cell research,* 314**,** 3187-3197.

PLESTANT, C., STRALE, P. O., SEDDIKI, R., NGUYEN, E., LADOUX, B. & MEGE, R. M. 2014. Adhesive interactions of N-cadherin limit the recruitment of microtubules to cell-cell contacts through organization of actomyosin. *J Cell Sci,* 127**,** 1660-71.

POKUTTA, S., HERRENKNECHT, K., KEMLER, R. & ENGEL, J. 1994. Conformational changes of the recombinant extracellular domain of E-cadherin upon calcium binding. *Eur J Biochem,* 223**,** 1019-26.

POKUTTA, S. & WEIS, W. I. J. M. C. 2000. Structure of the Dimerization and β-Catenin- Binding Region of α-Catenin. 5**,** 533-543.

POSTEL, R., MARGADANT, C., FISCHER, B., KREFT, M., JANSSEN, H., SECADES, P., ZAMBRUNO, G. & SONNENBERG, A. 2013. Kindlin-1 mutant zebrafish as an in vivo model system to study adhesion mechanisms in the epidermis. *J Invest Dermatol,* 133**,** 2180-90.

PULOUS, F. E., GRIMSLEY-MYERS, C. M., KANSAL, S., KOWALCZYK, A. P. & PETRICH, B. G. 2019. Talin-Dependent Integrin Activation Regulates VE-Cadherin Localization and Endothelial Cell Barrier Function. *Circ Res,* 124**,** 891-903.

QUADRI, S. K. & BHATTACHARYA, J. 2007. Resealing of endothelial junctions by focal adhesion kinase. *Am J Physiol Lung Cell Mol Physiol,* 292**,** L334-42.

QURESHI, O. S., BON, H., TWOMEY, B., HOLDSWORTH, G., FORD, K., BERGIN, M., HUANG, L., MUZYLAK, M., HEALY, L. J., HURDOWAR, V. & JOHNSON, T. S. 2017. An immunofluorescence assay for extracellular matrix components highlights the role of epithelial cells in producing a stable, fibrillar extracellular matrix. *Biol Open,* 6**,** 1423-1433.

RAMACHANDRAN, C. & SRINIVAS, S. P. 2010. Formation and disassembly of adherens and tight junctions in the corneal endothelium: regulation by actomyosin contraction. *Invest Ophthalmol Vis Sci,* 51**,** 2139-48.

RICHARDSON, A., MALIK, R. K., HILDEBRAND, J. D. & PARSONS, J. T. 1997. Inhibition of cell spreading by expression of the C-terminal domain of focal adhesion kinase (FAK) is rescued by coexpression of Src or catalytically inactive FAK: a role for paxillin tyrosine phosphorylation. *Molecular and cellular biology,* 17**,** 6906-6914.

RIMM, D. L., KOSLOV, E. R., KEBRIAEI, P., CIANCI, C. D. & MORROW, J. S. 1995. Alpha 1(E)-catenin is an actin-binding and -bundling protein mediating the attachment of F-actin to the membrane adhesion complex. *Proceedings of the National Academy of Sciences of the United States of America,* 92**,** 8813-8817.

RIO, A. D., PEREZ-JIMENEZ, R., LIU, R., ROCA-CUSACHS, P., FERNANDEZ, J. M. & SHEETZ, M. P. 2009. Stretching Single Talin Rod Molecules Activates Vinculin Binding. 323**,** 638-641.

ROSKOSKI, R., JR. 2015. Src protein-tyrosine kinase structure, mechanism, and small molecule inhibitors. *Pharmacol Res,* 94**,** 9-25.

ROTHLEIN, R., DUSTIN, M. L., MARLIN, S. D. & SPRINGER, T. A. 2011. A human intercellular adhesion molecule (ICAM-1) distinct from LFA-1. J. Immunol. 1986. 137: 1270-1274. *J Immunol,* 186**,** 5034-8.

ROWIN, M. E., WHATLEY, R. E., YEDNOCK, T. & BOHNSACK, J. F. 1998. Intracellular calcium requirements for beta1 integrin activation. *J Cell Physiol,* 175**,** 193-202.

ROZARIO, T. & DESIMONE, D. W. 2010. The extracellular matrix in development and morphogenesis: a dynamic view. *Dev Biol,* 341**,** 126-40.

SANTORO, S. A. 1986. Identification of a 160,000 dalton platelet membrane protein that mediates the initial divalent cation-dependent adhesion of platelets to collagen. *Cell,* 46**,** 913-20.

SCHALLER, M. D. 2001. Paxillin: a focal adhesion-associated adaptor protein. *Oncogene,* 20**,** 6459-72.

SCHALLER, S., GRANDEMANGE, S., SHPAKOVSKI, G. V., GOLEMIS, E. A., KEDINGER, C. & VIGNERON, M. 1999. Interactions between the full complement of human RNA polymerase II subunits. *FEBS Lett,* 461**,** 253-7.

SCHNEIDER, D. & ENGELMAN, D. M. 2004. Involvement of transmembrane domain interactions in signal transduction by alpha/beta integrins. *J Biol Chem,* 279**,** 9840-6.

SCHWARZBAUER, J. E. & DESIMONE, D. W. 2011. Fibronectins, their fibrillogenesis, and in vivo functions. *Cold Spring Harb Perspect Biol,* 3.

SCHWARZBAUER, J. E., PATEL, R. S., FONDA, D. & HYNES, R. O. 1987. Multiple sites of alternative splicing of the rat fibronectin gene transcript. *Embo j,* 6**,** 2573-80.

SCHWARZBAUER, J. E. & SECHLER, J. L. 1999. Fibronectin fibrillogenesis: a paradigm for extracellular matrix assembly. *Curr Opin Cell Biol,* 11**,** 622-7.

SECHLER , J. L., RAO , H., CUMISKEY , A. M., VEGA-COLÓN , I., SMITH , M. S., MURATA , T. & SCHWARZBAUER , J. E. 2001. A novel fibronectin binding site required for fibronectin fibril growth during matrix assembly. *Journal of Cell Biology,* 154**,** 1081-1088.

SHAHBAZI, M. N., MEGIAS, D., EPIFANO, C., AKHMANOVA, A., GUNDERSEN, G. G., FUCHS, E. & PEREZ-MORENO, M. 2013. CLASP2 interacts with p120-catenin and governs microtubule dynamics at adherens junctions. *J Cell Biol,* 203**,** 1043-61.

SHAHBAZI, M. N. & PEREZ-MORENO, M. 2014. Microtubules CLASP to Adherens Junctions in epidermal progenitor cells. *Bioarchitecture,* 4**,** 25-30.

SHAPIRO, L. & WEIS, W. I. 2009. Structure and biochemistry of cadherins and catenins. *Cold Spring Harb Perspect Biol,* 1**,** a003053.

SHEMESH, T., GEIGER, B., BERSHADSKY, A. D. & KOZLOV, M. M. 2005. Focal adhesions as mechanosensors: a physical mechanism. *Proc Natl Acad Sci U S A,* 102**,** 12383-8.

SHEN, L., WEBER, C. R. & TURNER, J. R. 2008. The tight junction protein complex undergoes rapid and continuous molecular remodeling at steady state. *J Cell Biol,* 181**,** 683-95.

SINGH, P., CARRAHER, C. & SCHWARZBAUER, J. E. 2010. Assembly of fibronectin extracellular matrix. *Annu Rev Cell Dev Biol,* 26**,** 397-419.

SOTTILE, J., SCHWARZBAUER, J., SELEGUE, J. & MOSHER, D. F. 1991. Five type I modules of fibronectin form a functional unit that binds to fibroblasts and Staphylococcus aureus. *Journal of Biological Chemistry,* 266**,** 12840-12843.

SPEZIALE, P., VISAI, L., RINDI, S. & DI POTO, A. 2008. Purification of human plasma fibronectin using immobilized gelatin and Arg affinity chromatography. *Nat Protoc,* 3**,** 525-33.

SPRINGER, T. A. & DUSTIN, M. L. 2012. Integrin inside-out signaling and the immunological synapse. *Curr Opin Cell Biol,* 24**,** 107-15.

STEHBENS, S. J., PASZEK, M., PEMBLE, H., ETTINGER, A., GIERKE, S. & WITTMANN, T. 2014. CLASPs link focal-adhesion-associated microtubule capture to localized exocytosis and adhesion site turnover. *Nat Cell Biol,* 16**,** 561-73.

SU, Y., XIA, W., LI, J., WALZ, T., HUMPHRIES, M. J., VESTWEBER, D., CABANAS, C., LU, C. & SPRINGER, T. A. 2016. Relating conformation to function in integrin alpha5beta1. *Proc Natl Acad Sci U S A,* 113**,** E3872-81.

SYED, S., KARADAGHY, A. & ZUSTIAK, S. 2015. Simple polyacrylamide-based multiwell stiffness assay for the study of stiffness-dependent cell responses. *Journal of visualized experiments: JoVE* [Online].

TAKAGI, J., PETRE, B. M., WALZ, T. & SPRINGER, T. A. 2002. Global conformational rearrangements in integrin extracellular domains in outside-in and inside-out signaling. *Cell,* 110**,** 599-11.

THARMALINGAM, S., DAULAT, A. M., ANTFLICK, J. E., AHMED, S. M., NEMETH, E. F., ANGERS, S., CONIGRAVE, A. D. & HAMPSON, D. R. 2011. Calcium-sensing receptor modulates cell adhesion and migration via integrins. *J Biol Chem,* 286**,** 40922-33.

TIEDE, S., MEYER-SCHALLER, N., KALATHUR, R. K. R., IVANEK, R., FAGIANI, E., SCHMASSMANN, P., STILLHARD, P., HÄFLIGER, S., KRAUT, N., SCHWEIFER, N., WAIZENEGGER, I. C., BILL, R. & CHRISTOFORI, G. J. O. 2018. The FAK inhibitor BI 853520 exerts anti-tumor effects in breast cancer. 7.

TIWARI, S., ASKARI, J. A., HUMPHRIES, M. J. & BULLEID, N. J. 2011. Divalent cations regulate the folding and activation status of integrins during their intracellular trafficking. *Journal of Cell Science,* 124**,** 1672-1680.

TOMINAGA, Y., MOCHIDA, A., MURAKAMI, S. & SAWAKI, S. 2008. Comparison of various revised k–ε models and LES applied to flow around a high-rise building model with 1:1:2 shape placed within the surface boundary layer. *Journal of Wind Engineering and Industrial Aerodynamics,* 96**,** 389-411.

TURNER, C. E., GLENNEY, J. R., JR. & BURRIDGE, K. 1990. Paxillin: a new vinculin-binding protein present in focal adhesions. *J Cell Biol,* 111**,** 1059-68.

TZIMA, E., IRANI-TEHRANI, M., KIOSSES, W. B., DEJANA, E., SCHULTZ, D. A., ENGELHARDT, B., CAO, G., DELISSER, H. & SCHWARTZ, M. A. 2005. A mechanosensory complex that mediates the endothelial cell response to fluid shear stress. *Nature,* 437**,** 426-31.

VICENTE-MANZANARES, M., CHOI, C. K. & HORWITZ, A. R. 2009. Integrins in cell migration--the actin connection. *J Cell Sci,* 122**,** 199-206.

WANG, J. H. 2012. Pull and push: talin activation for integrin signaling. *Cell Res,* 22**,** 1512-4.

WANG, M., REN, D., GUO, W., HUANG, S., WANG, Z., LI, Q., DU, H., SONG, L. & PENG, X. 2016. N-cadherin promotes epithelial-mesenchymal transition and cancer stem cell-like traits via ErbB signaling in prostate cancer cells. *Int J Oncol,* 48**,** 595-606.

WANG, Y., JIN, G., MIAO, H., LI, J. Y., USAMI, S. & CHIEN, S. 2006. Integrins regulate VE-cadherin and catenins: dependence of this regulation on Src, but not on Ras. *Proc Natl Acad Sci U S A,* 103**,** 1774-9.

WANG, Z., SYMONS, J. M., GOLDSTEIN, S. L., MCDONALD, A., MINER, J. H. & KREIDBERG, J. A. 1999. (Alpha)3(beta)1 integrin regulates epithelial cytoskeletal organization. *J Cell Sci,* 112 (Pt 17)**,** 2925-35.

WATANABE, T., SATO, K. & KAIBUCHI, K. 2009. Cadherin-mediated intercellular adhesion and signaling cascades involving small GTPases. *Cold Spring Harb Perspect Biol,* 1**,** a003020.

WAYNER, E. A., GARCIA-PARDO, A., HUMPHRIES, M. J., MCDONALD, J. A. & CARTER, W. G. 1989. Identification and characterization of the T lymphocyte adhesion receptor for an alternative cell attachment domain (CS-1) in plasma fibronectin. *J Cell Biol,* 109**,** 1321-30.

WEBER, G. F., BJERKE, M. A. & DESIMONE, D. W. 2011. Integrins and cadherins join forces to form adhesive networks. *J Cell Sci,* 124**,** 1183-93.

WIERZBICKA-PATYNOWSKI, I. & SCHWARZBAUER, J. E. 2003. The ins and outs of fibronectin matrix assembly. *J Cell Sci,* 116**,** 3269-76.

WINKLBAUER, R. 1998. Conditions for fibronectin fibril formation in the early Xenopus embryo. 212**,** 335-345.

WU, C. 2007. Focal adhesion: a focal point in current cell biology and molecular medicine. *Cell Adh Migr,* 1**,** 13-8.

XIANG, B., LIU, Y., ZHAO, W., ZHAO, H. & YU, H. 2019. Extracellular calcium regulates the adhesion and migration of osteoclasts via integrin α(v) β (3) /Rho A/Cytoskeleton signaling. *Cell Biol Int,* 43**,** 1125-1136.

XIAO, K., ALLISON, D. F., BUCKLEY, K. M., KOTTKE, M. D., VINCENT, P. A., FAUNDEZ, V. & KOWALCZYK, A. P. 2003. Cellular levels of p120 catenin function as a set point for cadherin expression levels in microvascular endothelial cells. *The Journal of cell biology,* 163**,** 535-545.

XIAO, T., TAKAGI, J., COLLER, B. S., WANG, J. H. & SPRINGER, T. A. 2004. Structural basis for allostery in integrins and binding to fibrinogen-mimetic therapeutics. *Nature,* 432**,** 59-67.

XIONG, J.-P., STEHLE, T., ZHANG, R., JOACHIMIAK, A., FRECH, M., GOODMAN, S. L. & ARNAOUT, M. A. 2002. Crystal Structure of the Extracellular Segment of Integrin αVβ3 in Complex with an Arg-Gly-Asp Ligand. 296**,** 151-155.

XIONG, J. P., STEHLE, T., DIEFENBACH, B., ZHANG, R., DUNKER, R., SCOTT, D. L., JOACHIMIAK, A., GOODMAN, S. L. & ARNAOUT, M. A. 2001. Crystal structure of the extracellular segment of integrin alpha Vbeta3. *Science,* 294**,** 339-45.

XU, W., ALPHA, K. M., ZEHRBACH, N. M. & TURNER, C. E. 2022. Paxillin promotes breast tumor collective cell invasion through maintenance of adherens junction integrity. *Mol Biol Cell,* 33**,** ar14.

XU, W., BARIBAULT, H. & ADAMSON, E. D. 1998. Vinculin knockout results in heart and brain defects during embryonic development. *Development,* 125**,** 327-337.

YAMADA, S. & NELSON, W. J. 2007. Synapses: sites of cell recognition, adhesion, and functional specification. *Annu Rev Biochem,* 76**,** 267-94.

YAMADA, S., POKUTTA, S., DREES, F., WEIS, W. I. & NELSON, W. J. 2005. Deconstructing the cadherin-catenin-actin complex. *Cell,* 123**,** 889-901.

YAMAMOTO, H., EHLING, M., KATO, K., KANAI, K., VAN LESSEN, M., FRYE, M., ZEUSCHNER, D., NAKAYAMA, M., VESTWEBER, D. & ADAMS, R. H. 2015. Integrin beta1 controls VE-cadherin localization and blood vessel stability. *Nat Commun,* 6**,** 6429.

YANO, H., MAZAKI, Y., KUROKAWA, K., HANKS, S. K., MATSUDA, M. & SABE, H. 2004. Roles played by a subset of integrin signaling molecules in cadherin-based cell-cell adhesion. *J Cell Biol,* 166**,** 283-95.

YAP, A. S., NIESSEN, C. M. & GUMBINER, B. M. 1998. The juxtamembrane region of the cadherin cytoplasmic tail supports lateral clustering, adhesive strengthening, and interaction with p120ctn. *J Cell Biol,* 141**,** 779-89.

YE, F., KIM, C. & GINSBERG, M. H. 2012. Reconstruction of integrin activation. *Blood,* 119**,** 26-33.

YONEDA, A., USHAKOV, D., MULTHAUPT, H. A. B. & COUCHMAN, J. R. 2007. Fibronectin Matrix Assembly Requires Distinct Contributions from Rho Kinases I and -II. 18**,** 66-75.

YONEMURA, S., WADA, Y., WATANABE, T., NAGAFUCHI, A. & SHIBATA, M. 2010. α-Catenin as a tension transducer that induces adherens junction development. *Nature Cell Biology,* 12**,** 533-542.

YU, M., LE, S., AMMON, Y. C., GOULT, B. T., AKHMANOVA, A. & YAN, J. 2019. Force-Dependent Regulation of Talin-KANK1 Complex at Focal Adhesions. *Nano Lett,* 19**,** 5982-5990.

ZAIDEL-BAR, R., BALLESTREM, C., KAM, Z. & GEIGER, B. 2003. Early molecular events in the assembly of matrix adhesions at the leading edge of migrating cells. *J Cell Sci,* 116**,** 4605-13.

ZAIDEL-BAR, R., COHEN, M., ADDADI, L. & GEIGER, B. 2004. Hierarchical assembly of cell-matrix adhesion complexes. *Biochem Soc Trans,* 32**,** 416-20.

ZAMIR, E. & GEIGER, B. 2001. Molecular complexity and dynamics of cell-matrix adhesions. *J Cell Sci,* 114**,** 3583-90.

ZHANG, K. & CHEN, J. 2012. The regulation of integrin function by divalent cations. *Cell Adh Migr,* 6**,** 20-9.

ZHANG, F., SAHA, S. & KASHINA, A. J. T. J. O. C. B. 2012. Arginylation-dependent regulation of a proteolytic product of talin is essential for cell–cell adhesion. 197**,** 819 - 836.

ZHANG, Q., MAGNUSSON, M. K. & MOSHER, D. F. 1997. Lysophosphatidic acid and microtubule-destabilizing agents stimulate fibronectin matrix assembly through Rho-dependent actin stress fiber formation and cell contraction. *Molecular biology of the cell,* 8**,** 1415-1425.

ZHONG, C., CHRZANOWSKA-WODNICKA, M., BROWN, J., SHAUB, A., BELKIN, A. M. & BURRIDGE, K. 1998. Rho-mediated contractility exposes a cryptic site in fibronectin and induces fibronectin matrix assembly. *J Cell Biol,* 141**,** 539-51.

ZIEGLER, W. H., LIDDINGTON, R. C. & CRITCHLEY, D. R. J. T. I. C. B. 2006. The structure and regulation of vinculin. 16 9**,** 453-60.